# A Clonal Analysis of Zebrafish Heart Morphogenesis and Regeneration

by

Vikas Gupta

Department of Cell Biology
Duke University

Date:_____

Approved:

_____
Kenneth D. Poss, Supervisor

_____
John Klingensmith, Chair

_____
Fan Wang

_____
Michel Bagnat

_____
Scott Soderling

Dissertation submitted in partial fulfillment of the requirements for the degree of Doctor of Philosophy in the Department of Cell Biology in the Graduate School of Duke University

2013

ABSTRACT

A Clonal Analysis of Zebrafish Heart Morphogenesis and Regeneration

by

Vikas Gupta

Department of Cell Biology
Duke University

Date:_____

Approved:

_____
Kenneth D. Poss, Supervisor

_____
John Klingensmith, Chair

_____
Fan Wang

_____
Michel Bagnat

_____
Scott Soderling

An abstract of a dissertation submitted in partial fulfillment of the requirements for the degree of Doctor of Philosophy in the Department of Cell Biology in the Graduate School of Duke University

2013

## Abstract

As vertebrate embryos grow and develop into adults, their organs must acquire mass and mature tissue architecture to maintain proper homeostasis. While juvenile growth encompasses a significant portion of life, relatively little is known about how individual cells proliferate, with respect to one another, to orchestrate this final maturation. For its simplicity and ease of genetic manipulations, the teleost zebrafish (*Danio rerio*) was used to understand how the proliferative outputs of individual cells generate an organ from embryogenesis into adulthood.

To define the proliferative outputs of individual cells, a multicolor clonal labeling approach was taken that visualized a large number of cardiomyocyte clones within the zebrafish heart. This Brainbow technique utilizes *Cre-loxP* mediated recombination to assign cells upwards of ~90 unique genetic tags. These tags are comprised of the differential expression of 3 fluorescent proteins, which combine to give rise to spectrally distinct colors that represent these genetic tags. Tagging of individual cardiomyocytes was induced early in development, when the wall of the cardiac ventricle is a single myocyte thick. Single cell cardiomyocyte clones within this layer expanded laterally in a

developmentally plastic manner into patches of variable shapes and sizes as animals grew into juveniles. As maturation continued into adulthood, a new lineage of cortical muscle appeared at the base of the ventricle and enveloped the ventricle in a wave of proliferation that fortified the wall to make it several myocytes thick. This outer cortical layer was formed from a small number (~8) of dominant cortical myocyte clones that originated from trabecular myocytes. These trabecular myocytes were found to gain access to the ventricular surface through rare breaches within the single cell thick ventricular wall, before proliferating over the surface of the ventricle.

These results demonstrated an unappreciated dynamic juvenile remodeling event that generated the adult ventricular wall. During adult zebrafish heart regeneration, the primary source of regenerating cardiomyocytes stems from this outer wall of muscle. Regenerating cardiomyocytes within this outer layer of muscle are specifically marked by the cardiac transcription factor gene *gata4*, which they continue to express as they proliferate into the wound area.

Using heart regeneration to guide investigation of juvenile cortical layer formation, we found that both processes shared similar molecular and tissue

specific responses including expression and requirement of *gata4*. Additional markers suggested that juvenile hearts were under stress and that this stress could play a role to initiate cortical morphogenesis. Indeed, experimental injury or a physiologic increase in stress to juvenile hearts caused the ectopic appearance of cortical muscle, demonstrating that injury could trigger premature morphogenesis.

These studies detail the cardiomyocyte proliferative events that shape the heart and identify molecular parallels that exist between regeneration and cortical layer formation. They show that adult zebrafish heart regeneration utilizes an injury/stress responsive program that was first used to remodel the heart during juvenile growth.

## Dedication

This work is dedicated to none other than my family:

Words cannot express the lengths to which my mother has been involved in my upbringing and wellbeing. From a young age, she has always expected the best from me academically and as an individual. She has sacrificed her time and energy to make sure that I would have the best opportunities in life to succeed and has always been supportive of the decisions that I make.

My father has only served to reinforce those same principles my mother held so dear by instilling into me the belief that no task in life should be pursued carelessly. Whether one is washing dishes or engaging in complex surgery, all tasks should be pursued with diligence and focus.

Lastly, my little brother Maneesh has been a constant companion since he was born. He was been a wonderful brother who has been supportive of my goals and is a person that I know I can count on for anything.

# Contents

# List of Figures

## List of Abbreviations

| | |
|---|---|
| 4-HT | 4-hydroxytamoxifen |
| AG | Accelerated growth |
| Amhc | Atrial myosin heavy chain |
| β-act2 | β actin 2 |
| BFP | Blue fluorescent protein |
| Bmp | Bone morphogenetic protein |
| BrdU | Bromodeoxyuridine |
| c-Kit | Cytokine receptor |
| CFP | Cyan fluorescent protein |
| Cmlc2 | Cardiac myosin light chain 2 |
| Com | Compact |
| Cor | Cortical |
| CreER | Cre recombinase conjugated to estrogen receptor |
| dpa | Days post amputation |
| dpf | Days post fertilization |
| DsRed | Red Fluorescent Protein |
| EGFP | Enhanced Green Fluorescent Protein |

| | |
|---|---|
| EK | Ekkwill |
| EMT | Epithelial-to-mesenchymal transition |
| Erbb2 | Erythroblastic leukemia viral oncogene homolog 2 |
| Fgf | Fibroblast growth factor |
| Hand | Heart and neural crest derivatives expressed |
| hpf | Hours post fertilization |
| Isl1 | Insulin gene enhancer protein |
| Ltbp3 | Latent transforming growth factor $\beta$ binding protein |
| Mef | Myocyte enhancer factor |
| Mesp | Mesoderm posterior |
| MHC | Myosin heavy chain |
| miRNA | Micro ribonucleic acid |
| NG | Normal growth |
| Nkx2.5 | Nirenberg-Kim2 transcription factor, locus 5 |
| Nppa/b | Natriuretic peptide a/b |
| PCNA | Proliferating cell nuclear antigen |
| Pitx | Paired-like homeodomain transcription factor |
| Pr | Primordial |

| | |
|---|---|
| RA | Retinoic acid |
| Raldh2 | Retinoic acid aldehyde dehydrogenase 2 |
| SA | Surface Area |
| Sca-1 | Stem cell antigen 1 |
| SEM | Standard error and the mean |
| Tbx | T-box transcription factor |
| Tcf21 | Transcription factor 21 |
| Tr | Trabecular |
| Vegf | Vascular endothelial growth factor |
| Vmhc | Ventricular myosin heavy chain |
| Wnt | Wingless and Int |
| wpf | Weeks post fertilization |
| YFP | Yellow fluorescent protein |

## Acknowledgements

I would first like to acknowledge my mentor Ken, who has been instrumental to my development as a scientist. It was very clear to me upon first meeting him, and through my subsequent interactions over the years, that Ken is an extremely dedicated scientist who wants to discover the answers to big questions. To that end, he is fearless in the adaptation of new approaches, techniques, and ideas in order to solve the complex mysteries that surround regeneration or other avenues of scientific inquiry. Yet, at the same time, he fosters an environment that allows each individual to maintain a level of creative independence that results in a synergistic effect. I cannot express how much Ken has taught me about how to go about being a successful investigator that contributes meaningfully to the scientific community, and I feel lucky to have him as my mentor.

Personally, Ken always has his door open even if he is not in the lab. Whether by phone or Internet, he will make the time to discuss any issue that you have on your mind. He ensures that all of his pupils are forging their own paths and stays involved with them scientifically and personally.

The second person that I would like to acknowledge is a previous post-doc in the lab, Kazu Kikuchi, who essentially served as my second mentor. Upon entering the lab, Kazu was the individual who would take the time to walk me through foreign protocols, teaching me the nuances that are never written down on paper. As time went on, he was more than willing to provide extensive discourse upon ideas or approaches that I had and showed me what was feasible with the tools we had. Kazu further made me a better scientist through critiquing my own data to demonstrate how I should present data in order to get my message across to an audience.

My committee members Drs. Fan Wang, John Klingensmith, Michel Bagnat, and Scott Soderling have all been very supportive throughout my PhD, providing great experimental suggestions and feedback, for which I am grateful.

I would like to thank Sam Johnson and Yasheng Gao, for all of their help with imaging. Sam, though he did not realize it, inspired the idea of double cover slipping hearts by saying "all you need to image is a cover slip."

Lastly, I would like to thank all of the Poss lab members that have contributed to the academic, yet entertaining and humorous, atmosphere of lab, especially during those many numerous weekends. Jennifer Holdway, our strict

lab mother, was a beacon of technical support. From fixing microscopes to handling all of our tiny requests, she made sure that the Poss lab ran as smoothly as a well-oiled machine. Amy Dickson for her amazing cartoon constructing abilities. Tiffany Casey, our second lab mother, for organizing and making arrangements so that others and myself could attend events without any worries, baking wonderful goodies, and providing thoughtful and caring conversations. Ravi Karra and Matt Gemberling have been wonderful collogues and collaborators, making significant contributions toward our studies of cortical muscle development. Jim Burris, Amy Eastes, and the other fish facility personal have provided fantastic animal care.

Lastly I would like to thank the graduate students of the Poss lab, Sumeet Singh, Greg Nachtrab, Matt Gemberling, and Valerie Tornini for all the advice, jokes, good times, and mutual commiseration. Thanks to everyone!

# Chapter 1. Background and Introduction

## *1.1 Early Development in Vertebrates*

Development is a process that begins at the single cell stage of life, after fertilization, with some aspects continuing to operate within a fully formed multicellular organism. In order to construct the intricate parts of a vertebrate organism, the initial single cell produced after fusion of the maternal and paternal gametes, a zygote, must undergo a number of finely controlled processes to reach proper size, shape, and patterning indicated within the genetic blueprint.

Initially, the zygote undergoes cleavage, whereby the volume of the egg cytoplasm is divided through mitosis without overall growth. Cleavage takes place within vertebrates and invertebrates with divisions typically taking place very rapidly. However, the rates differ from species to species with murine cleavage events tending towards the slowest with divisions taking place every 12 to 24 hours (Beddington and Robertson, 1999).

Cell migration and involution causes the initial formation of two layers of cells. These layers are termed the hypoblast and the epiblast based upon their

position to one another. The manner in which these two layers develop varies from fish to bird to mammals (Gilbert, 2003). However, the cells within these two layers form the three embryonic germ layers: the ectoderm, mesoderm, and endoderm. In fish, cells within the epiblast will form ectoderm, while cells within the hypoblast will form mesoderm and endoderm (Warger and Kimmel, 1990).

This differs in comparison to chick and mouse embryos, in which the epiblast will form all three germ layers, and the hypoblast forms extraembryonic tissues of the yolk sac as seen with fate mapping of epiblast cells (Shoenwolf et al., 1992; Lawson et al., 1991). A thickening of the epiblast causes the formation of the primitive streak, which defines the axes of the embryo. Endodermal precursors are the first to ingress from the streak, displacing the underlying hypoblast cells (Vakaet, 1984; Eyal-Giladi et al., 1992; Bellairs, 1986). Cells that ingress and stay between the epiblast and the endoderm form mesoderm (Psychoyos and Stern, 1996). All tissues and cell types of the organism derive from these three germ layers. The major contributions of the ectoderm include the epidermis of the skin and the nervous system. The endoderm will form the epithelial linings of digestive organs, lungs, liver, pancreas, thymus, and thyroid

gland. Mesodermal cells will form structures of the musculo-skeletal, circulatory, and reproductive systems excluding the germ cells (Gilbert, 2003).

Morphogenetic gradients and secreted cues help to specify these three layers, causing axes formation and progressive fate restriction as the primitive embryo is formed and gastrulation completes. As cell fates are further specified, the embryo transitions to the stage of organogenesis, in which cells pattern and form the functional units of the body, organs.

## *1.2 Cardiac Development and Patterning in Chicks and Higher Vertebrates*

The heart is a particularly crucial organ that enables nutrient delivery and waste removal upon each rhythmic contraction, pulsing erythrocytes through the vascular network. As a result, malformations of the heart often end in embryonic lethality or, in milder cases, congenital heart disease that requires prompt diagnosis and care.

The cells that will form the heart are derived from the mesodermal embryonic germ layer. In the earliest steps of cardiogenesis in chicks and mammals, mesodermal cells migrate through the primitive streak to form two

clusters of cells on either side of the anterior region of the streak (Redkar et al., 1995; Garcia-Martinez and Schoenwolf, 1993; Tam et al., 1997). At this stage, the earliest molecular markers for these cardiac progenitors are the transcription factors *mesp1* and *mesp2*, which are expressed transiently (Kitajima et al., 2003). Murine lineage tracing experiments of cells expressing *mesp1* have shown that virtually all cells of the heart, and cells of the main cardiac vessels, derive from this subset of mesodermal cells (Saga et al., 1999; Saga et al., 2000).

The specification of these cardiac progenitors, as they continue to migrate anteriorly, involves signaling through the Bmp, Fgf, and Wnt pathways. Bmp secreted from the endoderm causes Fgf8 production and release from endoderm situated beneath mesoderm, directing it down the cardiac fate pathway (Alsan and Schultheiss, 2002). Wnt production from the neural tube will oppose cardiac specification and direct mesoderm toward a hemangiogenic fate; however, the anterior endoderm prevents this with Dickkopf and Crescent, secreted proteins that block Wnts from interacting with their receptors (Schneider and Mercola, 2001; Tzahor and Lassar, 2001; Marvin et al., 2001).

The bilateral heart primordia lengthen across the midline to form the cardiac crescent, which fuses to form the primitive heart tube. Continued Bmp

and Fgf signaling, in the absence of Wnt signaling, causes the induction of Nkx2.5 within the cardiac crescent, a crucial transcription factor for cardiac specification (Schultheiss et al., 1995; Andrée et al., 1998; Sugi and Lough, 1994; Lints et al., 1993; Komuro and Izumo, 1993). Nkx2.5 is still one of earliest molecular markers of cells destined to form the heart (Harvey, 1996). The Nkx2.5 homologue in *Drosophila melanogaster*, Tinman, demonstrates its importance in invertebrates as Tinman mutants lack all heart primordia (Azpiazu and Frasch, 1993; Bodmer, 1993). The Nkx2.5 knockout phenotype is not as severe in mice as in flies, possibly due to functional redundancy with other cardiogenic genes (Srivastava and Olson, 2000; Fu et al., 1998).

Nkx2.5 activates the synthesis of other transcription factors of the Mef2 and Gata families that are instrumental in the continued lineage specification of mesoderm into cardiac tissue (Gajewski et al., 1998; Durocher et al., 1997). Members of the Gata and Nkx families engage in positive feedback loops to reinforce each other's expression (Schwartz and Olson, 1999). These transcription factors, in concert, activate the expression of cardiac muscle proteins that will be necessary for rhythmic contractile function. This can be first appreciated while

the two clusters of cardiac progenitors are fusing to form the primitive heart tube.

After formation of the primitive heart tube, growth does not solely occur within the tube itself. There is a further addition of myocytes to both the arterial and venous pole of the heart, with these cells emanating from a second heart field (Buckingham et al., 2005). This process was first observed in 1973 by electron microscopy, in which it appeared as if pharyngeal mesoderm adjacent to the heart tube was undergoing a myocardial transition during murine heart development (Viragh and Chalice, 1973).

A decade ago, two groups used a combination of vital dye lineage tracing, epitope expression, viral infection, and ablation of heart fields to show that pharyngeal mesodermal cells act as a source for elongation of the outflow tract in chick embryos (Waldo et al., 2001; Mjaatvedt et al., 2001). This was further shown to be the case in mammals by virtue of an enhancer trap in which *Fgf10* marked pharyngeal mesodermal cells contributing to the arterial pole of the heart (Kelly et al., 2001).

The identification of this 2$^{nd}$ contribution of cells to the developing heart was reinforced by the expression pattern of the LIM homeodomain transcription

factor *isl1*. Murine genetic lineage tracing revealed that *isl1* labeled pharyngeal mesodermal cells gave rise to both poles of the heart (Cai et al., 2003). Additionally, a retrospective clonal analysis was performed that utilized a defective *β-galactosidase* reporter targeted to the cardiac *alpha-actin* locus, which upon a rare and random recombination event would restore reporter activity. This analysis lent further support to this model of two cardiac fields by describing three classes of clones: two corresponding to each field and a third class that had overlap between both fields, suggesting that each field initially arose from a common progenitor (Meilhac et al., 2004).

For proper cardiac shape and function, the heart must loop and each of the cardiac chambers must form through septation. Some of the most important molecular players in the looping process are the Hand transcription factors and Pitx2. Both Hand1 and Hand2 are synthesized throughout the early heart tube; however, *hand2* expression localizes to the right and *hand1* to the left as the heart undergoes looping. Knocking down the expression of both transcription factors results in failed looping (Srivastava et al., 1995; Biben and Harvey 1997).

*pitx2* is expressed on the left side of the heart tube, an expression pattern that is conserved throughout all vertebrates and persists throughout cardiac

looping. While having multiple roles during development, its function during cardiac patterning is best demonstrated with experiments showing that ectopic expression on the right side of the heart results in the reversal of heart orientation (Essner et al., 2000; Logan et al., 1998; Ryan et al., 1998; Campione et al., 1999; Yoshioka et al., 1998).

Partitioning of the heart tube into separate atria and ventricles further develops cardiac asymmetry. This occurs shortly after looping, in which endocardial cushions form on both sides of the heart. Cushion morphogenesis takes place via EMT, in which cells from the endocardium detach and enter into an expanded extracellular matrix that separates the myocardium from the endocardium (Markwald et al., 1997). They meet in the midline to form the septum intermedium with left and right atroventricular channels. This septum serves as point of attachment for the atrial and interventriular septum that divides the heart into the left and right sides.

As the septa of the heart begin to form, the heart develops finger like processes, known as trabeculae, from the compact layer of the heart. These trabeculae are fibers of myocytes that have a large exposed surface area. In chicks, a space forms between the 2-3 cell thick compact muscle and the

endocardium, into which myocytes expand to form trabeculae (Sedmera et al., 2000). Cell proliferation from the compact layer continues to drive this event as compact myocytes proliferate at higher rates relative to trabecular myocytes (van den Berg et al., 2009). It is thought that this method of growth allows nourishment of cardiomyocytes by diffusion from the blood, which permits large-scale proliferation.

Organisms that have higher-pressure circulatory systems do not maintain these trabeculations; instead, they possess a ventricle that is primarily composed of a thick compact layer. Currently, it is thought that these trabeculations undergo compaction, in which they compress together to add to the overall thickness of the ventricular wall. Evidence for this comes from the chick embryo in which it appeared as though basal portions of the trabecula helped to increase the overall thickness of the compact layer (Rychterova, 1971). Further support for this compaction process comes from the pathological phenotype of non-compaction, in which the ventricle remains highly trabeculated with a thin compact layer after birth. Such malformations suggest that trabecular myocytes need to be added to the compact layer for proper thickness of the ventricular wall. These non-compaction phenotypes can be seen with disruptions of RA

signaling (Kastner et al., 1994). Lastly, single marker clonal analysis visualized clonal wedges forming from the external portion of the chick and mouse ventricular wall that tapered toward the lumen, lending additional credence to the idea of compaction, though not definitive (Mikawa et al., 1992; Meilhac et al., 2003). While the compact layer grows in thickness, coronary arteries develop within the ventricular wall to supply nutrients to tightly juxtaposed compact myocytes (Rychter and Ostadal, 1971; Vrancken Peeters et al., 1997).

Myocytes transition from hyperplasia to hypertrophy shortly after birth with increases in cell size accounting for the majority of new myocardial mass (Clubb and Bishop, 1984; Pasumarthi and Field, 2002). Greater load upon the heart, due to whole organism growth, stimulates this physiologic hypertophic process to meet increased circulatory demands (Hill and Olson, 2008).

While hypertrophy is known to play a major role in postnatal cardiac growth, there have been recent studies providing evidence that proliferation of cardiomyocytes occurs at a very low rate in humans and in mice (Senyo et al., 2013; Kajstura et al., 2010; Bergmann et al., 2009). In one of these studies, the authors utilized the atmospheric increase in radiocarbon $^{14}C$ during Cold War nuclear bomb tests as a natural pulse chase. By measuring the genomic

concentration of $^{14}C$ within human cardiomyocytes, they found that cardiomyocytes were younger than the individual. Modeling of this data found that ~45% of the myocytes within a human heart turned over during the lifespan of an individual (Bergmann et al., 2009). However, this study cannot distinguish between the proliferation of myocytes themselves or a contribution from a progenitor source. Using genetic recombination and non-radioactive DNA labeling of cardiomyocytes, another group found that murine cardiomyocytes also have a low rate of postnatal proliferation that they determined to originate from cardiomyocytes themselves (Senyo et al., 2013). These studies support the notion that mammalian cardiomyocytes have a very low rate of basal proliferation that makes a small contribution to postnatal growth, with hypertrophy comprising the primary means of added myocardial mass.

## *1.3 The Zebrafish as a Model of Heart Development*

Zebrafish (*Danio rerio*) is a species of freshwater fish that is a popular vertebrate model organism to study development. Eggs are fertilized outside of the body, and the embryo is transparent. This eases visualization of developmental processes and permits embryological manipulations (Kimmel et

al., 1995). Additionally, the zebrafish is amenable to genetic approaches in the form of genetic screens, transgenesis, and morpholino mediated gene knockdowns, allowing the discovery and characterization of important gene products that regulate development (Patton and Zon, 2011; Stuart et al., 1988; Ekker, 2000).

Teleosts such as zebrafish do not have a separate pulmonary circulatory system as higher vertebrates. Instead, venous blood returning to the heart is delivered to the gills that then flows directly back to the extremities. As such, the zebrafish heart is comprised of a single atrium and ventricle connected to a structure called the bulbous arteriosus, which functions as the outflow tract.

The development of the heart begins after fertilization, while cleavage is exponentially increasing the number of cells. At 2.5 hours post fertilization, cardiac progenitors are found within the ventrolateral margin on either side of the dorsal midline. These cardiac progenitors cells can contribute to either the ventricle or atrium at this stage. Fate mapping experiments revealed that these lineages separate shortly after another hour of development into chamber specific progenitors of either ventricular or atrial myocytes (Stainier et al. 1993). The signaling pathways that control specification of myocytes are very similar to

those in higher vertebrates and include Ffg8, Bmp, and Nodal (Reifers et al., 2000; Reiter et al., 2001). Fgf8, in particular, is necessary for induction of Nkx2.5. Reduction in the function of Nkx2.5, in addition to Hand2, display severe deficiencies in the number of cardiomyocytes, demonstrating a conserved importance of these cardiac genes (Yelon et al., 2000; Reiter et al., 1999).

As gastrulation begins, differentiation continues with the expression of *cmlc2* within all of the cardiomyocytes and chamber specific expression of *vmhc* in the ventricle and *amhc* in the atrium (Yelon et al., 1999; Berdugo et al., 2003). As in other species, these two progenitor populations fuse at the midline to form the primitive heart tube, with the first contractions visible at 22 hpf.

In the following 26 hours of morphogenesis, the heart tube loops and forms two chambers with walls of single cardiomyocyte thickness. These two chambers are separated by a constriction that will eventually develop into the atroventricular canal. During this time, like higher vertebrates, a second heart field contributes cells to the outflow region of the heart. *ltbp3* expression marks this field of cells that contributes ventricular myocardium around the outflow pole in addition to cells of different lineages in the outflow tract itself (Zhou et al., 2011). By 48 hpf, myocyte proliferation within the two chambered heart is

detectable with further addition by differentiation thought to have ceased (de Prater et al., 2009; Auman et al., 2007; Hami et al., 2011; Lazic and Scott, 2011).

The zebrafish ventricle undergoes trabeculation around 3 dpf, a process that is dependent upon Erbb2. A recent study suggested that trabeculae form through directional delamination of proliferating myocytes from the single myocyte thick chamber wall (Liu et al., 2010). Both chambers remain highly trabeculated during growth into adulthood, a common feature of low-pressure circulatory systems (Sedmera et al., 2000).

While hypertrophy accounts for the majority of postnatal cardiac growth in mammals and other higher vertebrates, hyperplastic growth of the fish heart provides a substantial contribution to myocardial mass as young fish grow to adulthood, with a low baseline level of proliferation seen within adult animals (Wills et al., 2008; Poss et al., 2002).

## *1.4 Cardiac Regeneration and the Zebrafish*

Heart disease encompasses a wide variety of pathological insults to the heart that can be genetically acquired or develop over time as a result of environmental factors combined with genetic predisposition. In particular, heart

failure, in which the heart is unable to properly perfuse all cells of the body, is a burgeoning health problem. The American Heart Association estimates that 5.8 million Americans have clinically symptomatic heart failure; even more patients are thought to have asymptomatic reduced ventricular function (AHA Statistics Committee, 2010). Failure of the heart is primarily due to myocyte loss. This loss can occur insidiously over time as a result of chronic hypertensive overload or chronic ischemia (Whelan et al., 2010). Rapid loss is well known and described in the lay press that results from a thrombotic occlusion of a coronary vessel, an event known as myocardial infarction. Such an event can lead to the loss of 25% of the myocardium, and invokes a fibrotic response in humans that results in collagen deposition and scar formation (Murry et al., 2006).

As such, there has been major interest within the scientific and medical communities to develop and employ methods that would allow restoration of lost cardiomyocytes (Laflamme and Murry, 2011). These efforts have been focused primarily upon the identification and utilization of various types of stem cells, transdifferentiation/reprograming of other cardiac cell types, or stimulating resident cardiomyocytes to proliferate.

Bone marrow cells, and mesenchymal stem cells, were initially reported to have adopted a myocyte fate after injection into the myocardium of infarcted mice, with an observed improvement in cardiac function (Orlic et al., 2001; Toma et al., 2002). However, further experimentation found that these cells were not contributing to the formation of new cardiomyocytes. Instead, improved ventricular function appeared to derive from a paracrine effect, in which injected mesenchymal stem cells, and likely bone marrow cells, were secreting factors and cytokines that were the probable basis of improvement (Mirotsou et al., 2007).

Many groups have described markers of cardiac stem cells or progenitors that reside within the heart. These include cell surface markers c-Kit and Sca-1 in addition to the transcription factor Isl1. Reports of these marked cardiomyocyte stem cell populations involve their isolation, characterization, propagation *in vitro*, and in some cases, injection into infarcted myocardium (Bearzi et al, 2007; Beltrami et al, 2003; Laugwitz et al, 2005; Matsuura et al, 2004; Oh et al, 2003). Further evidence for a population of cardiac progenitor cells is suggested in a study that used Cre-*loxP* technology to label a fixed portion of cardiomyocytes. While this proportion did not change through normal ageing, the authors found

a decrease in the proportion of labeled cells throughout the heart after myocardial infarction, suggesting contribution from another source (Hsieh et al., 2007). In a follow-up study, the proportion of pre-labeled cardiomyocytes further decreased upon the addition of c-Kit$^{+}$ stem cells, but not mesenchymal stem cells (Loffredo et al., 2011). However, in a more recent study utilizing a new technique to examine cell proliferation, the same group found that a contribution by stem cells is unlikely during normal ageing and myocardial infarction. New myocytes are formed; however, these originate from pre-existing cardiomyocytes (Senyo et al., 2013).

In addition to cardiomyocytes, other cell types within the heart have been the focus of other researchers, who are using different approaches to differentiate them into muscle cells. The epicardium, a thin mesothelial sheet of cells that surrounds the heart, proliferates extensively after infarction, though, does not give rise to new muscle (Zhou et al., 2011). However, if the epicardium is "primed" with the peptide Thymosin β4 prior to infarction, *wt1* genetically tagged epicardial cells were found to turn into cardiomyocytes at low frequencies (Smart et al., 2011). This type of transdifferentiation event, of epicardial cells into cardiomyocytes, was thought to happen normally during

murine heart development that used *tbx18* and *wt1* to mark epicardial cells (Cai et al., 2008; Zhou et al., 2008). However, a common caveat with genetic lineage tracing is the specificity of the regulatory sequences that are used to label a particular population of cells. *tbx18* was found to express not only within epicardial cells, but at low levels within the cardiomyocytes themselves. This indicated that the observed transdifferentiation event was likely labeling induced from *tbx18* expression within myocytes and not a true transdifferentiation event (Christoffels et al., 2009). In the zebrafish, both *wt1* and *tbx18* were found to express within myocyte populations. Lineage tracing through development and regeneration with *tcf21*, a marker found to be specific to epicardial cells, did not identify any epicardial contributions to cardiomyocytes (Kikuchi et al., 2011b). As such, more research is still needed to evaluate the therapeutic potential of the epicardium.

The revolution of cell reprograming by the retroviral introduction of transcription factors has led scientists to investigate combinations of factors that can change one cell type into another. Screening for candidate transcription factors, one group identified three cardiac transcription factors, Gata4, Mef2c, and Tbx5 that were able to convert murine fibroblasts into cardiomyocytes *in*

*vitro* (Ieda et al., 2010). Induced expression of these factors or combined with Hand2, *in vivo*, resulted in a ~10-15% reprogramming rate of murine fibroblasts into cardiomyocytes with improved cardiac function (Qian et al., 2012; Song et al., 2012). Another group performed a similar reprograming screen using miRNAs and were also able to convert fibroblasts to cardiomyocytes *in vivo* (Jayawardena et al., 2012). These results suggest that reprogramming efforts could contain real therapeutic potential to generate new, adult cardiomyocytes.

Stimulating mammalian cardiomyocytes to reenter the cell cycle has been met with some success. Signaling molecules such as Periostin, Fgf1, and Nrg1 have all been shown to spur endogenous myocytes, within the ventricle, to proliferate (Kuhn et al., 2007; Engel et al., 2006; Bersell et al., 2009). However, the percentage of endogenous differentiated myocytes that undergo cell division in response to these factors is not robust, ~1.7% for Nrg1 (Bersell et al., 2009). These factors await clinical confirmation; yet, they offer another promising avenue for heart regeneration.

A high natural cardiomyocyte proliferative response is not completely devoid in mammals. Neonatal mice cardiomyocytes possess a transient ability to respond to cardiac injury. Ventricular resection of a 1 day old murine neonatal

apex results in the increased proliferation of differentiated cardiomyocytes, resulting in regeneration; a response that disappears by 7 days of age (Porrello et al., 2011). The ability of a neonatal mouse to transiently regenerate in this manner, shortly after birth, coincides with the transition from hyperplastic to hypertrophic growth (Clubb and Bishop, 1984; Pasumarthi and Field, 2002). This shows that injury prior to this transition results in a proliferate response that cannot be significantly reengaged once the transition to hypertrophic growth occurs.

The proliferation of differentiated cardiomyocytes, regardless of age and after injury, appears to be the greatest in lower vertebrates such as the newt and the teleost zebrafish. Initially, experiments in which the ventricular apex of the newt heart was resected found primarily scar formation with a minority of proliferating cardiomyocytes (Oberpriller and Oberpriller, 1974). However, if the resection surgery is moved closer to the base of the heart, myocyte proliferation is seen with scarless regeneration 10 weeks after injury (Witman et al., 2011).

With the added tool of genetics, zebrafish have provided a wealth of knowledge concerning the process of natural heart regeneration. Removal of ~20% of the adult zebrafish ventricular apex results in the formation of a fibrin

clot that is replaced with rapidly proliferating cardiomyocytes over a period of 30 to 60 days with little to no collagen deposition (Poss et al., 2002). Cryocauterization and genetic ablation further probed the regenerative capacity of the zebrafish, in which full regeneration was observed after cyroinjury to ~25% of the ventricle or ablation of ~60% of cardiomyocytes (Chablais et al., 2011; González-Rosa et al., 2011; Schnabel et al., 2011; Wang et al., 2011).

The origin of new zebrafish myocytes has been an area of intense research. Using regulatory sequences for *cmlc2* to express Cre recombinase, and genetically mark all cardiomyocytes, it was shown that new cardiomyocytes are formed from differentiated cardiomyocytes (Kikuchi et al., 2010; Jopling et al., 2010). Further refinement of this finding stemmed from regulatory sequences of the cardiogenic transcription factor Gata4. After resection injury to the zebrafish heart, *gata4* is expressed, at 7 dpa, within the compact layer of the ventricular wall. Through reporter analysis and lineage tracing, it was found that the primary contribution to the regenerate originated from these compact cardiomyocytes that proliferate into the wound to reform the ventricular apex (Kikuchi et al., 2010).

While we are beginning to comprehend the molecular aspects that regulate both cardiac development and regeneration, there is a relative lack of knowledge concerning the cellular proliferative dynamics that coordinate morphogenesis of the heart at a single cell level. I used the zebrafish as a model to understand how many single cell clones proliferate, from embryogenesis into adulthood, to generate the mature zebrafish heart. Utilizing a multicolor labeling technique, that can assign upwards of ~90 different colors to individual cells, I focused upon understanding how single cell clones proliferated to create the zebrafish compact layer. Since this layer serves as the primary source for regenerating myocytes after amputation based regeneration, understanding its development can give insights into the process of regeneration. Through these experiments, a number of observations were made that demonstrated how the compact layer forms in a clonally dominant fashion during juvenile growth and how regeneration recapitulates this process.

# Chapter 2. Materials and Methods

## *2.1 Zebrafish*

Wild-type or transgenic zebrafish of the EK/AB background were used for all experiments. Water temperature was maintained at 26 C for animals after 1 wpf and animal density was maintained at 8-9 fish per 3 liters for standard growth and regeneration experiments. For accelerated growth experiments, 5 fish were placed in a 10 liter tank. All transgenic strains were analyzed as hemizygotes. Ventricular resection surgeries were performed via anesthetizing adult zebrafish in either tricaine or 2-phenoxyethanol. The chest cavity was open with a small incision until the ventricular apex could be seen. Approximately 20% of the apex was resected using a pair of surgical scissors. The wound was blotted with a dry kim wipe to stimulate clotting. The fish was placed in a recovery tank, where a pipet was used to gently blow water over the gills until the fish began to swim (Poss et al., 2002).

For pierce injuries, a 30 dpf juvenile fish was anesthetized with 2-phenoxyethanol. The heart was carefully exposed and pierced with a 5 micron diameter tungsten needle until a jet of blood could be seen pumping from the

heart. The juvenile was placed into a recovery tank until it began to undergo normal swimming behaviors.

Transgenic strains used for the following studies were *cmlc2*:CreER (Tg(*cmlc2*:CreER)$^{pd10}$), *cmlc2:CreER* (*Tg(cmlc2:CreER)$^{pd13}$*) (used with *β-act2:BSg4DN*), *gata5*:RnG (Tg(*gata5*:*loxP*- mCherry- STOP-*loxP*-nucEGFP)$^{pd40}$), *cmlc2*:EGFP (Tg(*cmlc2*:EGFP)$^{f1}$), *cmlc2*:nRFP (Tg(*cmlc2*:nucDsRed2)$^{f2}$), *β-actin*:mGFP (Tg(*β-actin*:HRAS-EGFP)$^{vu119}$) *hsp70:Cre* (*Tg(hsp70l:Cre)$^{zdf13}$*), *gata4*:EGFP (Tg(*gata4*:EGFP)$^{ae1}$), *gata4:ERCreER* (*Tg(gata4:ERCreER)$^{pd39}$*), *tcf21*:DsRed2 (Tg(*tcf21*:DsRed2)$^{pd37}$), *bactin2:loxp-mCherry-STOP-loxp-DTA* (*Tg(bactin2:loxP-mCherry-STOP-loxP-DTA176)$^{pd36}$*and *tcf21*:nucEGFP (Tg(*tcf21*:nucEGFP)$^{pd41}$) (Kikuchi et al., 2010; Burns et al., 2005; Cooper et al., 2005; Wang et al., 2011; Heicklen-Klein and Evans, 2004).

## *2.2 Transgenic Strains Generation*

### 2.2.1 *priZm*

The Brainbow 1.0L plasmid (Addgene plasmid 18721) was digested with NheI and partially digested with NotI to obtain the entire cassette, and

subcloned downstream of the 9.8 kb zebrafish *β-actin2* promoter from the *β-act2*:RSG construct (Kikuchi et al., 2010). The resulting plasmid was linearized by I-SceI digestion and injected into one-cell zebrafish embryos. RFP is the initial reporter cassette and default expression state from this construct. Two paired sites, *lox2272* and *loxP*, exist in the construct, which enable Cre-recombinase-mediated switching to expression of either CFP or YFP.

Thirty founder lines were isolated and two lines were used in the following studies that were (Tg(*β-act2*:Brainbow1.0L)$^{pd49}$) and (Tg(*β-act2*:Brainbow1.0L)$^{pd50}$), called *priZm* and *priZm2*, respectively . The zebrafish *β-actin2* promoter does not drive expression in epicardial or endocardial cells, facilitating clear visualization of priZm cardiomyocytes.

### 2.2.2 *β-act2*:BSg4DN

The *β-act2:RSG* plasmid was digested with XhoI to remove the DsRed cassette and was replaced with TagBFP. Further modification was achieved by replacing EGFP with a linker sequence encompassing a PmeI site. A dominant negative coding sequence for *gata4* (*sr-gata4*) was PCR amplified from a plasmid (kindly provided by Todd Evans) with mCherry2a cloned in frame and in front

of *sr-gata4* for bi-cistronic expression. The mCherry-2a-*sr-gata4* was placed into the modified *β-act2:RSG* plasmid using the PmeI site. This construct was co-injected into one-cell-stage wild-type embryos with I-SceI. Three founders were isolated and propagated from the injected embryos. One transgenic line was chosen for the following studies (Tg(*β-actin2*:*loxP*-mTagBFP-STOP-*loxP*-mCherry-2a-*sr-gata4*)$^{pd62}$) and is called *β-act2*:BSg4DN.

## *2.3 Imaging*

For whole mount imaging, hearts were extracted at the indicated time points and fixed in 4% paraformaldehyde. After rinsing, the atrium was removed and the ventricle was placed on a coverslip in Fluoromount G. Another coverslip was used to compress the ventricle, allowing imaging of both ventricular surfaces. For surface images of whole-mounted ventricles, the z-position was adjusted until only surface muscle was visible. For confocal slices through whole-mounted hearts, the z-position was adjusted through the ventricle until trabecular muscle could be visualized. For histological analysis, 50 or 10 μm cryosections were mounted with Fluoromount G.

Images from all *priZm* samples were acquired using a Leica SP5 AOBS microscope equipped with X20 (0.7 NA) and X40 (1.25 NA) objectives. Antibodies were not used to enhance fluorescence. 458 nm, 515nm and 561nm lasers were used to excite CFP, YFP and RFP, respectively. Each channel was acquired sequentially and imported into ImageJ, where channels were overlaid. Uniform adjustments to brightness and contrast were made with the aide of Adobe Photoshop and stitched together. To quantify the surface area occupied by a given clone, it was traced in square microns using ImageJ software. To calculate the surface area occupied with respect the rest of the heart, a percentage was obtained by dividing its measured area by the total surface area of both sides of the ventricle.

Confocal images from other transgenic lines fluorescing TagBFP, EGFP, or stained with Alexa Flour 633, were excited with 405 nm, 488 nm, and 633 nm lasers, respectively. Channels were acquired sequentially, and processed in a similar fashion to *priZm* images.

*In situ* hybridization images were acquired with Leica DM6000 compound microscope equipped with a X10, X20, X40 lens and a Retiga-EXi camera (Q-IMAGING).

## *2.4 Histological Methods*

All histological procedures were carried out upon 10-12 μm cryosections of 4% paraformaldehyde fixed hearts. *In situ* hybridization was performed using digoxygenin-labeled cRNA probes with the aid of an InSituPro robot using probes for *raldh2*, *nppa*, and *nppb* (Poss et al., 2002; Kikuchi et al., 2011). To assess collagen and fibrin deposition Acid Fuchsin-Orange G staining was performed as described previously (Poss et al., 2002).

Immunofluorescence was carried out by incubating slides with primary antibody for 3 h at 37C and secondary for 1 h at 37C (Poss et al., 2002). For Mef2 and PCNA staining, an antigen retrieval step was performed using heated citrate buffer (Kikuchi et al., 2011). Primary antibodies used were anti-Mef2 (rabbit; Santa Cruz Biotechnology), anti-PCNA (mouse; Sigma), anti-Myosin heavy chain (F59, mouse; Developmental Studies Hybridoma Bank), and anti-DsRed (rabbit; Invitrogen). Secondary antibodies (Invitrogen) used were Alexa Fluor 633 goat anti-mouse IgG (H+L), Alexa Fluor 594 goat anti-rabbit IgG (H+L), and Alex Flour 488 goat anti-mouse IgG (H+L).

## *2.5 4-HT Labeling*

For 4-HT labeling of *cmlc2*:CreER; *priZm* embryos, 2 dpf embryos were placed in egg water with 4-HT added to a final concentration of 4 μM, from a 1 mM stock made in 100% ethanol. Embryos were treated for 6 h, rinsed once, and placed in fresh egg water. For labeling of 30 dpf juveniles, animals were incubated in 1 μM 4-HT in aquarium water for 3 h. To specifically label trabecular muscle at 30 dpf, animals were incubated in 0.25 mM 4-HT for 1 h. Adults of this strain were placed into 80 ml of aquarium water and underwent a 1 μM 4-HT dose for 3 h.

For 4-HT induced recombination of *β-act2*:BSg4DN; *cmlc2*:CreER juvenile fish at 5 wpf, 4 fish were placed within 40 ml of aquarium water with 4-HT added to a final concentration of 5 μM. Juvenile fish were incubated overnight, rinsed with clean aquarium water and were allowed to return to circulating water. For all adult 4-HT treatments using *β-act2*:BSg4DN; *cmlc2*:CreER, the same protocol was used except that 3 fish were placed within 80 ml of aquarium water.

To induce ablation within in juvenile *cmlc2:CreER; bactin2:loxp-mCherry-STOP-loxp-DTA*, we treated animals with 0.5 or 1 μM 4-HT for 16 hours at 4 fish

per 40 ml of aquarium water. Adult cardiomyocyte ablation injuries were performed as described previously (Wang et al., 2011).

For specifically labeling cortical muscle within *gata4*:ERCreER; *priZm2* animals, three 6 wpf juveniles were placed within 40 ml of aquarium water and underwent a 6 hr 5 μM dose. Adults were labeled with the same dose in 80 ml of aquarium water and incubated overnight.

## *2.6 Quantification*

To count the number of ventricular cardiomyocytes at 3 dpf, *cmlc2*:nucDsRed2; *cmlc2*:EGFP double transgenic animals were raised to 3 dpf, fixed, sectioned at 30 μm, and stained with an antibody to DsRed2. Confocal stacks of the entire heart from each embryo were taken, and the number of myocytes within the ventricular wall was determined from three-dimensional projections generated using Imaris to count the number of $DsRed2^+$ nuclei within the ventricle.

To quantify proliferation indices, sections were stained with Mef2 and PCNA. The numbers of $Mef2^+$ and $Mef2^+/PCNA^+$ cells were manually counted

with the aid of ImageJ software for three different sections and averaged (Kikuchi et al., 2011a).

# Chapter 3. Clonal Analysis Reveals a Dominant and Dynamic Pattern of Cardiac Morphogenesis

This chapter was originally published in:

**Gupta, V.,** and Poss, K.D. (2012). Clonally dominant cardiomyocytes direct heart morphogenesis. *Nature* 484, 479-484.

Vikas Gupta is the lead author and performed all experiments.

## *3.1 Summary*

As vertebrate embryos develop to adulthood, their organs undergo marked changes in size and tissue architecture. The heart acquires muscle mass and matures structurally to fulfill increasing circulatory needs, a process that is incompletely understood. Here we used multicolor clonal analysis to define the contributions of individual cardiomyocytes as the zebrafish heart undergoes morphogenesis from a primitive embryonic structure into its complex adult form. We find that the single-cardiomyocyte-thick wall of the juvenile ventricle forms by lateral expansion of several dozen cardiomyocytes into muscle patches of variable sizes and shapes. As juvenile zebrafish mature into adults, this structure becomes fully enveloped by a new lineage of cortical muscle. Adult cortical muscle originates from a small number of cardiomyocytes—an average of approximately eight per animal—that display clonal dominance reminiscent of stem cell populations. Cortical cardiomyocytes initially emerge from internal myofibres that in rare events breach the juvenile ventricular wall, and then expand over the surface. Our results illuminate the dynamic proliferative behaviors that generate adult cardiac structure, revealing clonal dominance as a key mechanism that shapes a vertebrate organ.

## 3.2 Introduction

Vertebrate organ development is an intricate process that begins in the early embryo and continues until the functional capacity of the organ meets adult requirements. Relatively little is known about the cellular mechanisms of organ morphogenesis after birth or hatching. This can be explained in part by the challenges of analyzing dynamic cellular behaviors in complex tissues.

New technologies can shed light on the cellular mechanisms that drive organ morphogenesis. Recently, a system was developed that allowed the designation of ~90 color labels to murine neurons (Livet et al., 2007). With this technology, termed Brainbow, it was possible to visualize adjacent neurons and their connections in the brain with high resolution. The ability to assign many colors to different cells in a population can also be applied to investigating cell proliferation and lineage decisions.

The heart is a set of chambers comprised predominantly of the contractile units, cardiomyocytes. Genetic fate mapping has been performed to determine how separate lineages contribute to developing cardiac structures in mice and zebrafish (Zhou et al., 2011; Kikuchi et al., 2011b; Cai et al., 2003; Zhou et al., 2008; Meilhac et al., 2004). Additionally, single-marker clonal analysis has traced the activity of individual cells during embryonic heart patterning (Keegan et al.,

2004; Stainier et al., 1993; Mikawa et al., 1992; Meilhac et al., 2003). These studies have enhanced our understanding of cardiogenic mechanisms in early embryos. Nevertheless, a large gap in our knowledge remains in comprehending how the size, shape and structure of an adult heart are finalized through the individual and population behaviors of many cardiac cells.

In this study, we used multicolor clonal analysis to map the proliferative histories of many individual cardiomyocytes as the zebrafish cardiac ventricle transitions from a simple tube of single cardiomyocyte thickness into a complex adult structure. Our experiments yielded several unexpected discoveries relevant to the number, nature and mechanisms of cardiomyocyte contributions during heart morphogenesis.

## *3.3 Results*

### 3.3.1 Multicolor Labeling of Cardiomyocytes

To study cell clones in zebrafish, we adapted the Brainbow 1.0L construct for combinatorial expression of three spectrally different fluorescent reporter proteins (Livet et al., 2007). Multiple copy integration of this transgene at a single

genetic locus is a common outcome of transgenesis. Thus, combinatorial Cre-recombinase-mediated excision events at paired lox recognition sites can generate many possible permanent colors (Fig. 1). We generated several transgenic lines containing a *β-actin-2*-promoter-driven multicolor construct, and assessed them in combination with a strain harboring a tamoxifen-inducible, cardiomyocyte-restricted Cre recombinase, *cmlc2*:CreER (Kikuchi et al., 2010). We identified one line, Tg(*β-act2*:Brainbow1.0L)$^{pd49}$ (referred to subsequently as *priZm*), showing limited mosaic recombination only in the presence of 4-HT (Fig. 2).

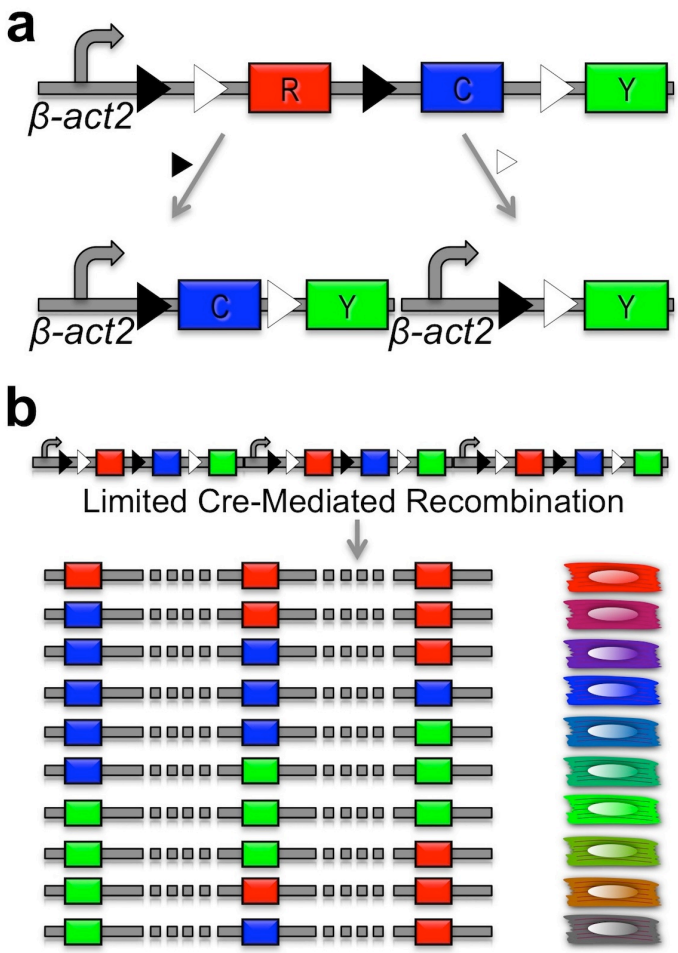


**Figure 1: Multicolor clonal labeling strategy.**

**a,** Recombination at paired *lox2272* (black triangles) or *loxP* (white triangles) sites leads to expression of cyan fluorescent protein (CFP) or yellow fluorescent protein (YFP), respectively. **b,** Limited Cre-mediated recombination of tandem cassette insertions results in combinatorial expression of fluorescent proteins.

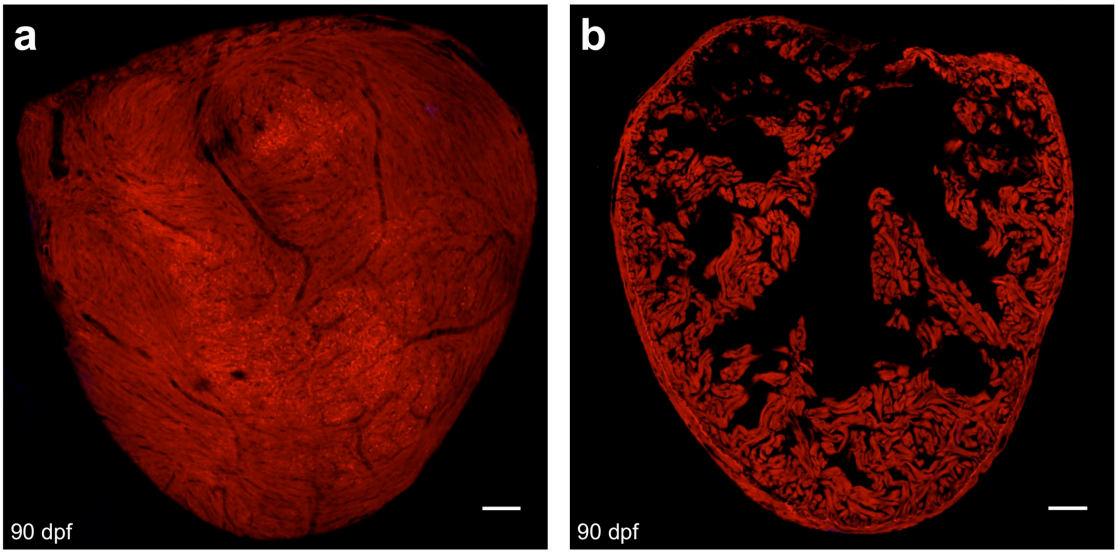


**Figure 2: Recombination and color generation require 4-HT treatment.**

**a, b,** Whole-mount surface image (**a**) and section image (**b**) of *cmlc2:CreER; priZm* ventricles at 90 dpf. Animals were treated with vehicle at 2 dpf and display no spurious recombination. Scale bars, 50 μm.

The size and structure of the zebrafish heart is conducive to clonal analysis of cardiomyocytes. The 2–3 dpf zebrafish heart is looped, has a wall of single-cardiomyocyte thickness, and consists of 250–300 muscle cells; by our measurements, 115 of these are contained within the ventricular wall (Fig. 3). Cardiomyocyte proliferation is detectable at 2 dpf and is thought to account for most or all subsequent cardiogenesis (Zhou et al., 2011; de Prater et al., 2009; Auman et al., 2007; Hami et al., 2011; Lazic and Scott, 2011). To trace the fates of individual embryonic cardiomyocytes, we briefly incubated 2dpf *cmlc2:CreER*; *priZm* embryos in 4-HT and raised them to different ages (Fig. 4a).

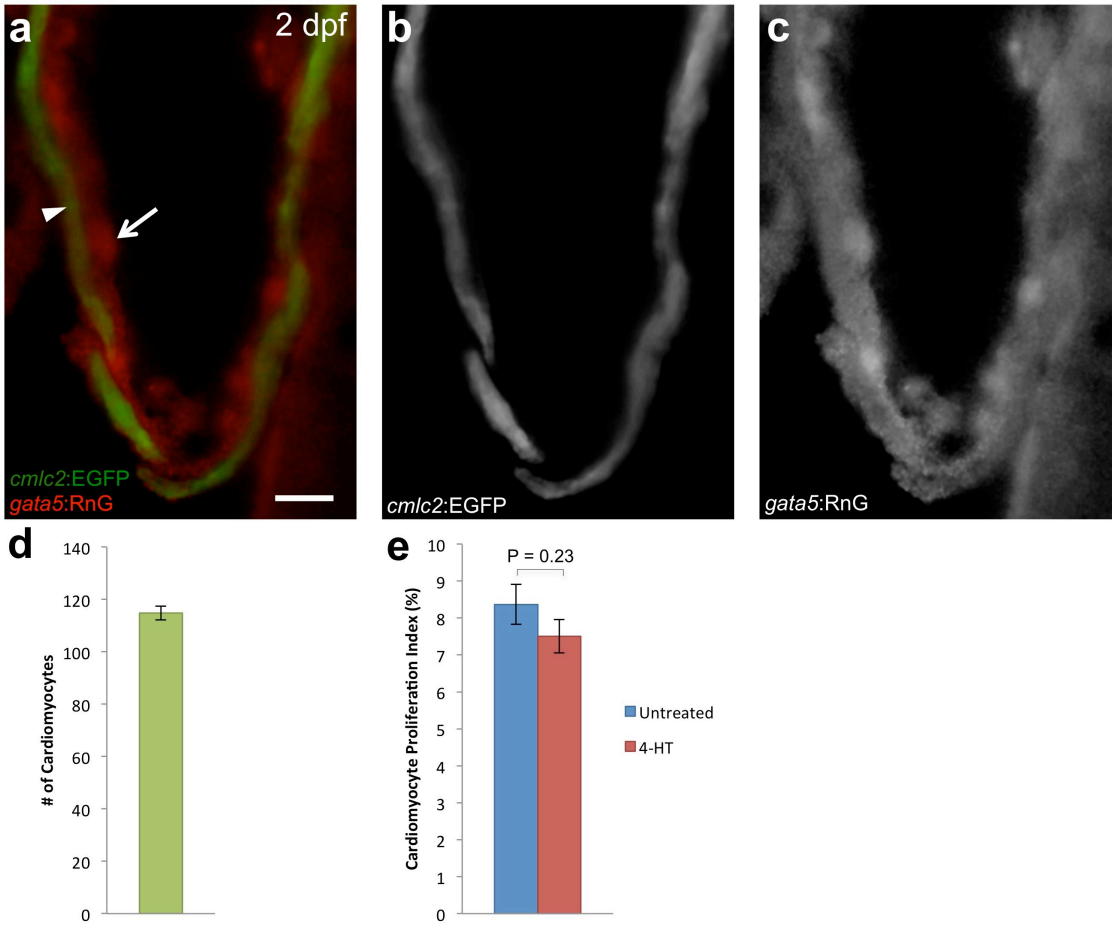


**Figure 3: Structure, cardiomyocyte number, and proliferation in the embryonic zebrafish ventricle.**

**a-c,** Section through a 2 dpf *cmlc2:EGFP; gata5:RnG* ventricle. At this stage, the myocardium (arrowhead; green in **a**) is of single cell thickness. Cardiac muscle surrounds an inner layer of endocardium (arrow; red in **a**). **d,** Quantification of cardiomyocytes in the ventricular wall at 3 dpf. Mean ± s.e.m., n = 5 embryos. **e,** Standard 4-HT labeling treatment had no detectable effects on embryonic cardiomyocyte proliferation. Mean ± s.e.m., n = 5 (untreated) and 6 (4-HT) embryos. Student's t-test. Scale bar, 50 μm.

We first assessed cardiac fluorescence at 10 dpf, a stage comparable in organismal size to 2 dpf. Our optimized 4-HT regimen generated >20 unique colors in cardiomyocytes, as viewed at 10 dpf and subsequent stages. RFP is the initial reporter cassette and default expression marker, and 4-HT treatment induced recombination (non-red colors) in ~50% of ventricular cardiomyocytes. Importantly, different colors were consistently assigned to adjacent cardiomyocytes on the surface of the 10 dpf ventricular wall (Fig. 4b, c), a prerequisite for multicolor clonal analysis.

The zebrafish ventricle is recognized to contain two types of cardiac muscle (Hu et al., 2001). These include a peripheral wall of compact muscle, and inner myofibres organized into trabeculae that initiate formation at 3 dpf (Liu et al., 2010). Histological examination of 10 dpf hearts revealed three notable observations. First, the ventricular wall remained at single cardiomyocyte thickness, as at 2 dpf. Second, trabecular myocytes connected to the wall were most often clonally unrelated to adjoining wall myocytes (58 of 63 observations, n = 55 ventricles; Fig. 4d, e). This observation supported a mechanism for trabecularization proposed recently based on different lines of evidence, in which myocytes delaminate from the ventricular wall, seed elsewhere in the

chamber, and initiate trabecular growth from a second site (Liu et al., 2010). Third, we saw that the trabecular myofibres themselves were comprised of cardiomyocytes arising from different clonal origins within the 2 dpf wall (Fig. 4e).

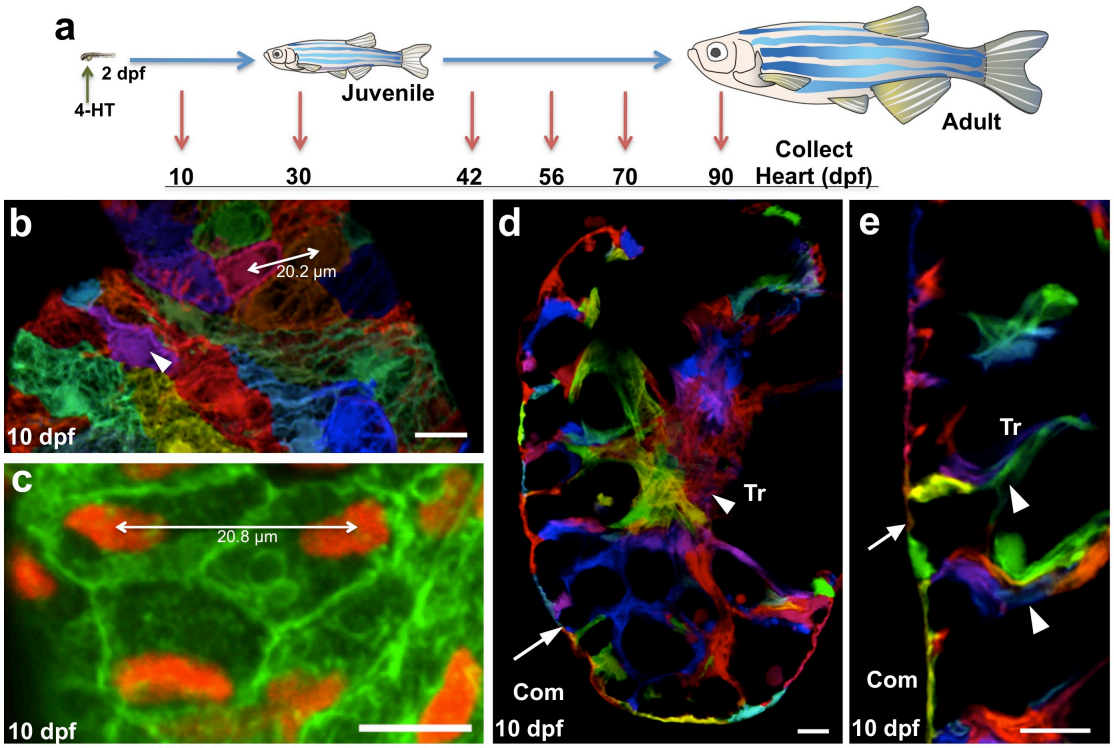


**Figure 4: Single cardiomyocytes comprise the majority of 10 dpf color clones.**

**a,** Cartoon of lineage tracing experiments. **b,** Surface myocardial image of a 10 dpf *cmlc2:CreER; priZm* ventricle, labeled at 2 dpf. Single cardiomyocytes are predominantly labeled with unique colors (arrowhead). Internuclear distance between adjacent myocardial cells is 20.2 μm. **c,** Surface myocardial image of a 10 dpf *cmlc2:nucDsRed2; β-actin:mGFP* embryo, with an internuclear distance of 20.8 μm. **d, e,** 10 dpf ventricular confocal slice, indicating trabecular cardiomyocytes connected with clonally unrelated cardiomyocytes at the wall (**d**, **e**, arrow) and within trabeculae (**e**, arrowheads). Scale bars, 10 μm.

### 3.3.2 Juvenile Ventricular Wall Formation

We next examined the ventricles of juvenile zebrafish at 30 dpf, at which time major organismal and cardiac growth have occurred since cardiomyocyte labeling with 4-HT. By whole-mount imaging of surface myocardium, we readily identified multicellular, single color regions of myocardium, indicating that progeny of embryonic cardiomyocytes generally remained connected with one another after division (Fig. 5a–c). Although less common (9.8% of clones), we also observed instances suggesting complete separation of a cardiomyocyte from its clonal partners (Fig. 5d).

We expected some uniformity to the clonal patches comprising the ventricular wall, with cardiomyocyte clones of similar shape and size. By contrast, ventricles from different animals displayed unique patterns of surface color clones, and the shapes of clones within each ventricle were highly diverse (Fig. 6a-c). Clone size also varied. Some clones showed evidence of many cell divisions, whereas others contained a single cardiomyocyte (Fig. 6d). Histological analysis showed retention of a wall of single-cardiomyocyte thickness, indicating that the expansion of wall clones was limited to lateral directions along the surface. They also revealed that substantial expansion of trabecular myocardium had occurred since 10 dpf (Fig. 6e).

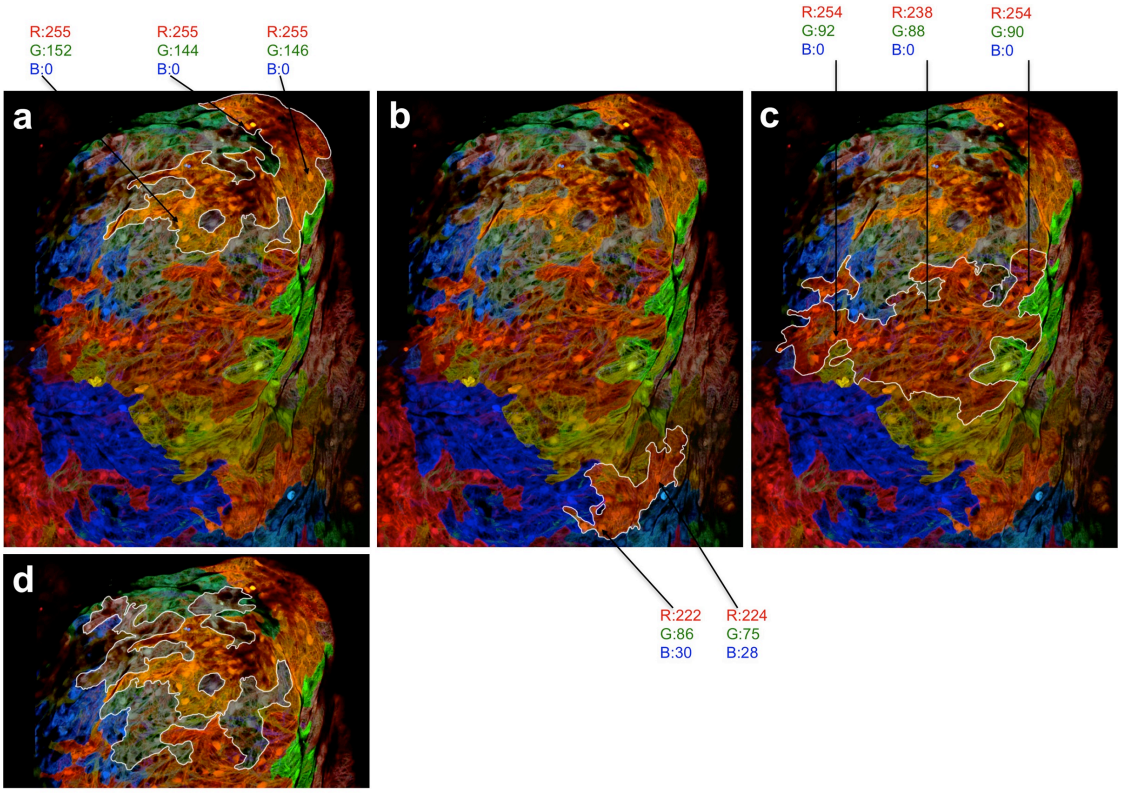


**Figure 5: Clonal color signatures and clone separation.**

**a-c,** Three orange clones of a 30 dpf ventricle were traced, and different regions throughout each clone were assigned Red/Green/Blue (RGB) values using Adobe Photoshop (black arrows). Note that the 3 different clones traced in **a**, **b**, and **c** have distinct RGB values, but the values are consistent within each clone. Values were assessed from nuclei, which obscure fluorescence from underlying trabecular better than cytosolic regions. **d,** The components of a gray clone that has been separated by a proliferating orange clone are traced, events that occurred in 9.8% of clones.

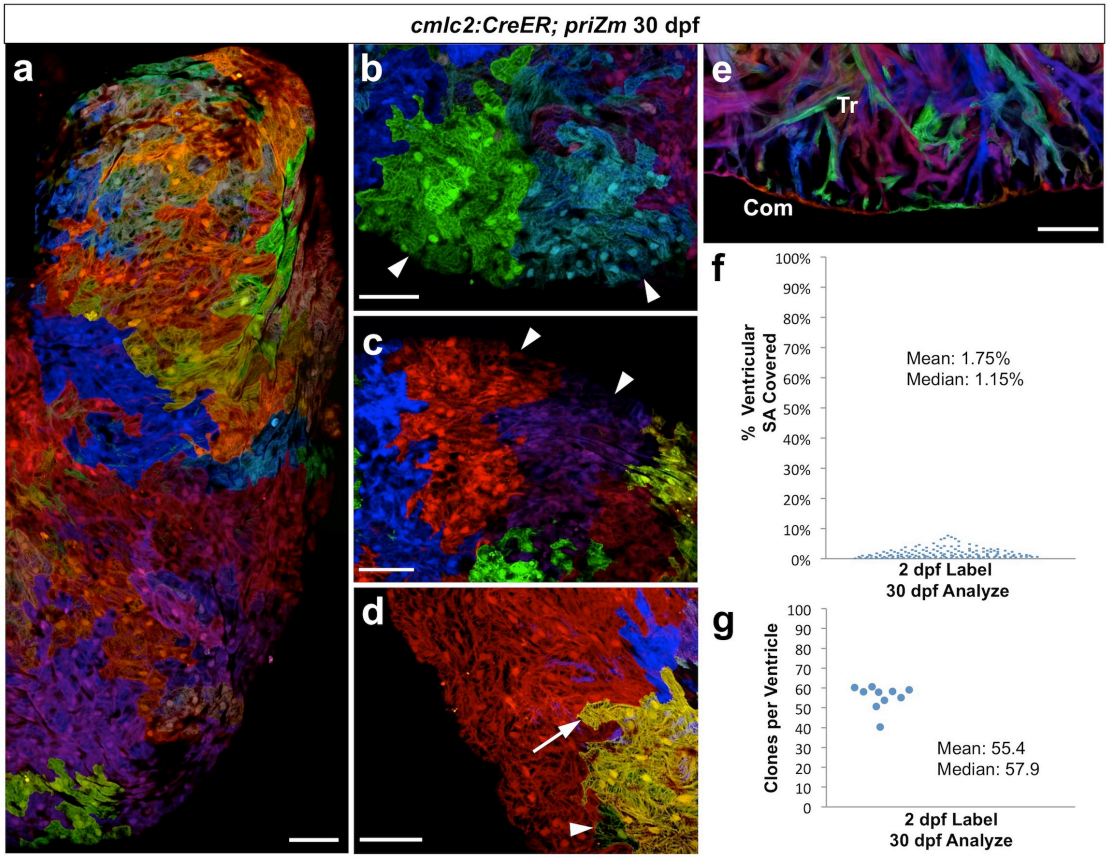


**Figure 6: Several dozen embryonic cardiomyocytes build the juvenile ventricular wall.**

**a,** Surface myocardium of half of a 30 dpf ventricular side, displaying clonal patches of varied shapes and sizes. **b, c,** Cardiomyocyte clones near the apex or chamber midpoint forming wedge/stripe shapes (arrowheads). **d,** Single-cell clone (green, arrowhead) positioned near a large clone (yellow, arrow). **e,** 30 dpf ventricular confocal slice, depicting a wall of single cardiomyocyte thickness surrounding trabecular muscle. **f,** Percentage surface area occupied by 30 dpf clones (146 clones, 5 ventricles). **g,** Surface clones per ventricle (n = 10). Scale bars, 50 μm.

To estimate the number of embryonic cardiomyocytes that create the juvenile ventricular wall, we calculated the surface areas occupied by individual clones and divided each by the total ventricular surface area. Most clones (99/146; n = 5) each occupied less than 2% of the ventricular surface area, whereas a small number (15/146) of larger clones each represented ~4–8% of the surface (Fig. 6f). Extrapolating for unrecombined myocardium, we determined that the 30 dpf ventricular surface was represented by 55.4 ± 1.9 color clones (n = 10; mean ± standard error of the mean; Fig. 6g). Thus, our data indicate that the juvenile zebrafish ventricular wall is built by lateral expansion of ~55 embryonic cardiomyocytes. These cardiogenic events create a patchwork of diverse clonal shapes and sizes that varies from animal to animal, indicating that the juvenile cardiac form can be acquired with considerable developmental plasticity.

### 3.3.3 Emergence of a New Adult Muscle Lineage

Zebrafish are typically recognized as adults at 3 months post-fertilization. We examined ventricles of 6-, 8- and 10-week-old animals that had undergone cardiomyocyte labeling at 2 dpf. At 6 weeks post-fertilization (wpf), most clonal patches comprising the surface myocardium appeared similar to those of 30 dpf

ventricles. Additionally, we detected a population of clonally related cardiomyocytes layered upon these patches near the chamber base (Fig. 7a, b). By 8 wpf, large single-color swaths containing several hundreds of such cardiomyocytes extended from the ventricular base, wrapping around both sides of the chamber and often reaching its midpoint (Fig. 7d–f). At 10 wpf, we began to see evidence of these surface clones converging with each other. These external cardiomyocytes were typically more rod-shaped with more distinct striation than underlying cardiomyocytes (Fig. 8).

We examined histological sections and confocal slices through ventricles from 6–10 wpf animals, which confirmed that a new layer of ventricular muscle had emerged externally to the wall of single cardiomyocyte thickness present at earlier stages (Fig. 7c, g). As indicated by whole-mount imaging, this external layer typically displayed substantial regions of clonally related cardiomyocytes. We will refer subsequently to the inner wall muscle as the 'primordial layer', as it retains the same single-cardiomyocyte thickness and characteristics of the embryonic ventricle throughout subsequent life stages. We will refer to the late-emerging, outermost muscle of the ventricular wall as the 'cortical layer'. Thus,

by multicolor clonal analysis, we revealed two developmentally distinct and previously unrecognized forms of ventricular wall myocardium.

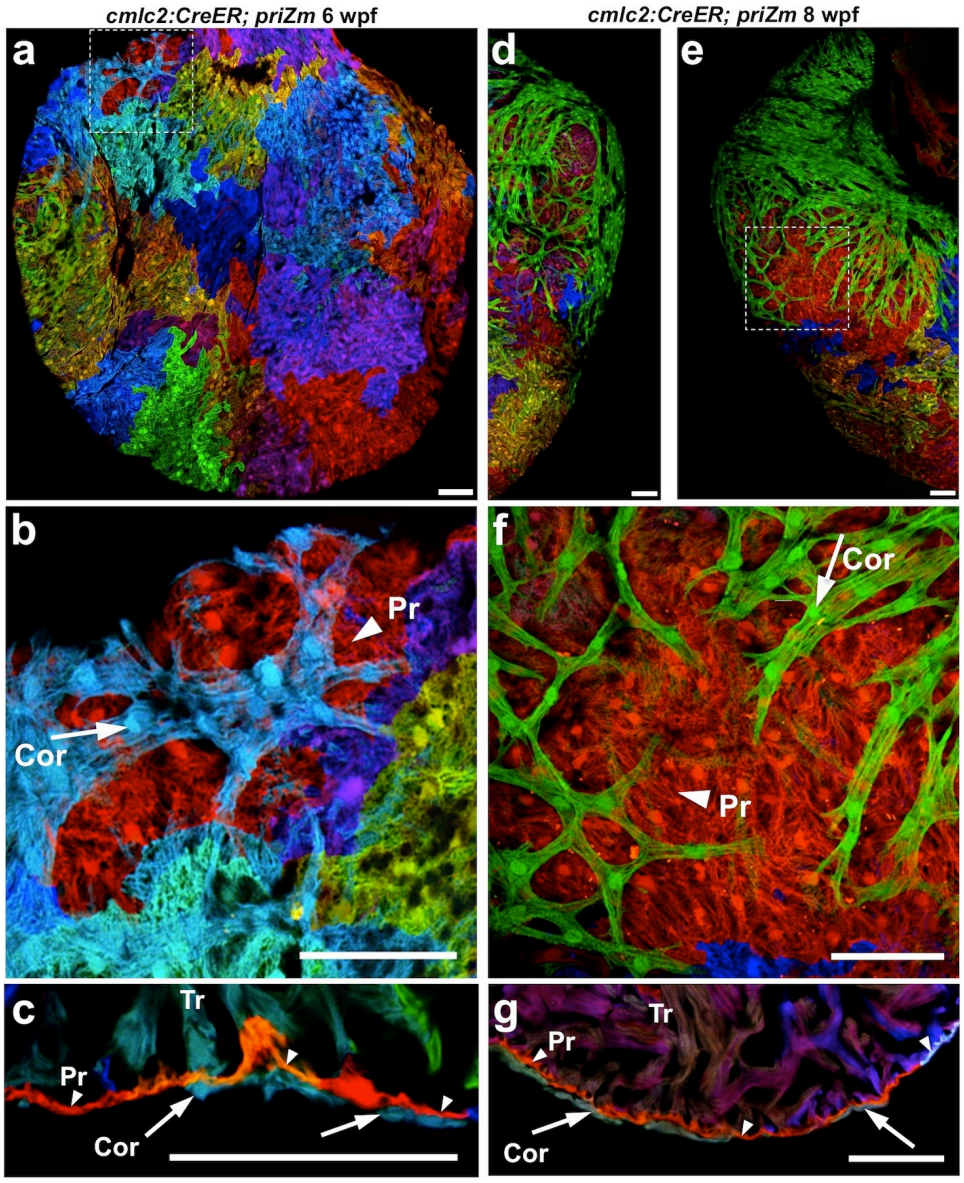


**Figure 7: Emergence of new muscle lineage at base of heart.**

**a–c,** 6 wpf ventricular surface (**a**, **b**) and confocal slice (**c**), indicating cortical (arrow), primordial (arrowhead) and trabecular muscle. **d–g**, 8 wpf ventricular surface indicating a large green basal clone (**d–f**), and section indicating 3 muscle types (**g**). Dashed boxes in **a** and **e** are shown in higher magnification in **b** and **f**, respectively. Scale bars, 50 μm.

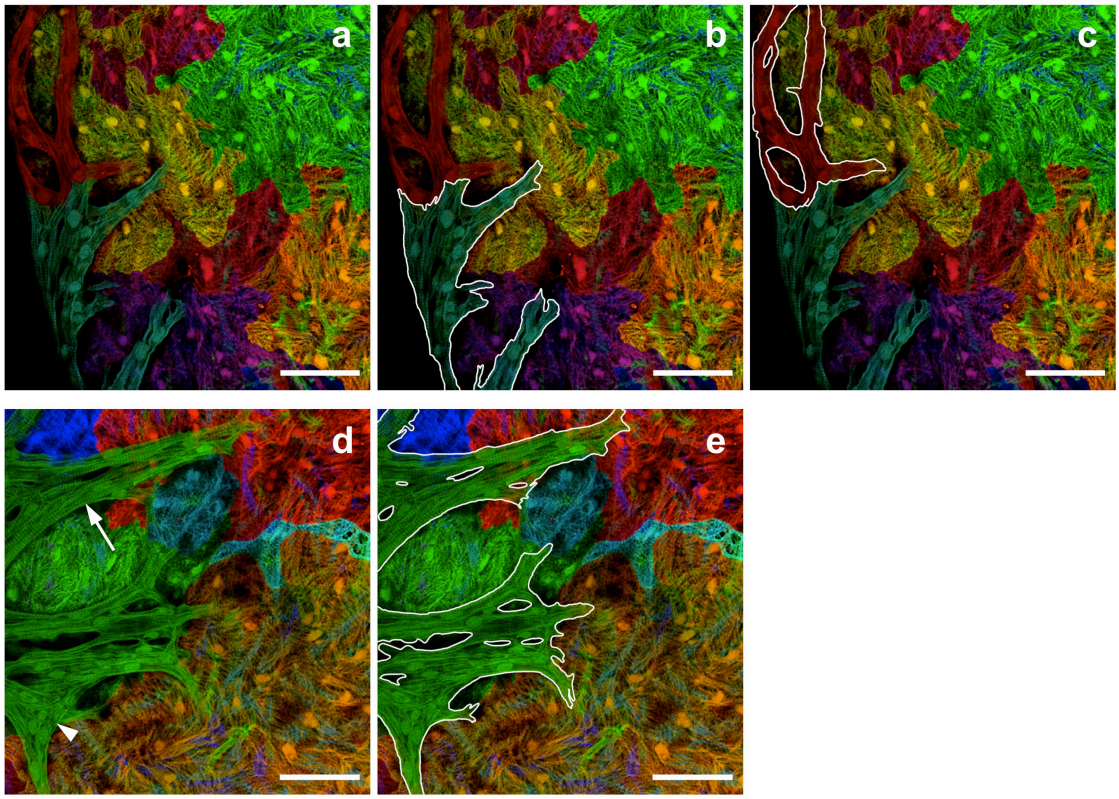


**Figure 8: Cortical cardiomyocyte clones at 10 weeks post fertilization.**

**a-c,** High magnification view of 10 wpf surface myocardium, in which two distinct cortical clones (cyan and red) are in contact. Each clone is separately traced in **b** and **c**. **d, e,** High magnification view of a single green cortical clone that contains cardiomyocytes with clear striations (arrow) or with less organized structure (arrowhead). The clone is traced in **e**. Scale bar, 50 μm.

### 3.3.4 Dominant Clones Build Adult Wall Muscle

We next examined ventricles from mature, 90 dpf zebrafish that had undergone cardiomyocyte labeling at 2 dpf. At this stage, the entire surface of the ventricle in each animal was covered by cortical cardiomyocytes (Fig. 9a and Fig. 10). Similar to the clonal representation of the primordial layer at earlier stages, cortical clone patterns appeared different in each animal. However, a common theme for each ventricle was the presence of one or two large cortical clones at the base of the heart extending across the ventricular surface towards the apex. We infer from our time-point analysis that these areas of cortex formed by a base-to-apex wave of expansion over the primordial layer. A number of smaller surface clones were apparent at other locations. Clones converged by weaving or fitting with some overlay into each other, and were penetrated by coronary vessels (Fig. 11).

Histological analysis of adult ventricular tissue indicated that the primordial layer remained at single-cardiomyocyte thickness and was comprised of multiple color clones. This appearance contrasted with the overlying cortical myocardium, which was predominantly single color and could be several cells thick (Fig. 9b). We calculated the areas of surface clones from whole-mount images of ventricles that displayed basal clones of a recombined color. Ten of

twenty ventricles met this criterion, each of which had a large cortical clone covering 30–60% of the total ventricular surface (Fig. 9c). An average of 7.8 ± 1.2 clones contributed the entire cortical muscle of each ventricle (n = 10; Fig. 9d), a number several times lower than the clonal surface representation of the much smaller juvenile ventricle. Thus, a rare group of approximately eight clonally dominant cardiomyocytes in the embryonic ventricle ultimately contribute to building the adult cortical myocardium.

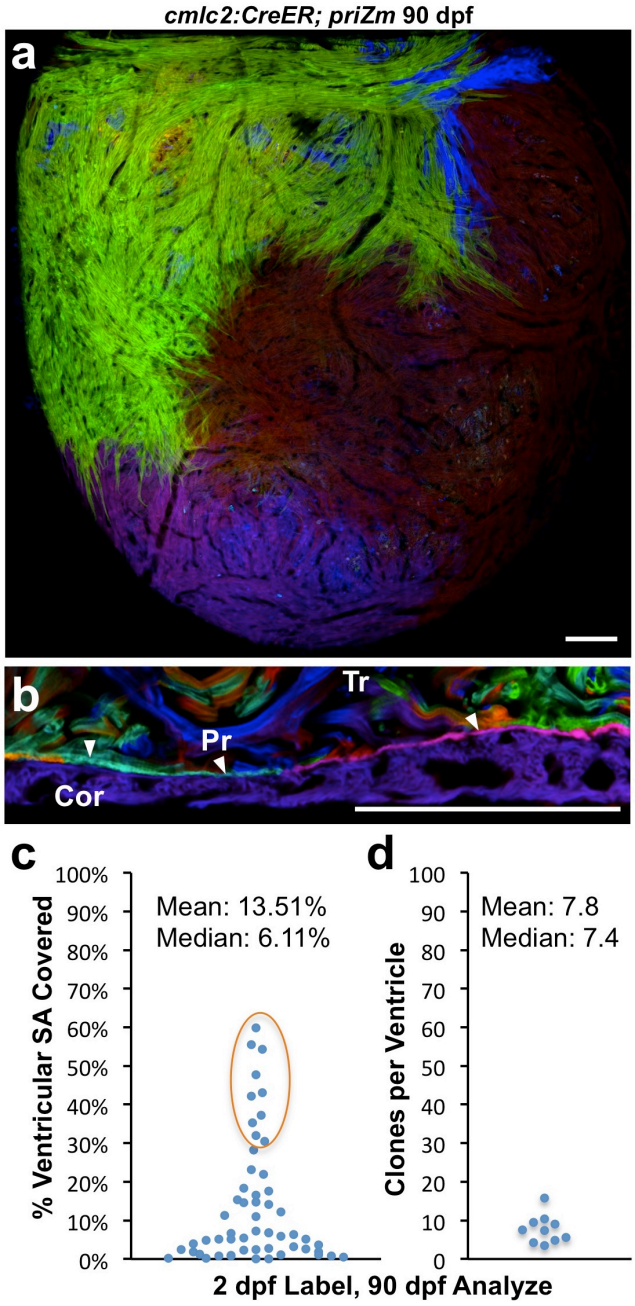


**Figure 9: Clonally dominant cortical cardiomyocytes.**

**a,** 90 dpf ventricular surface, showing only a few large cortical clones. **b,** 90 dpf ventricular section. **c,** Percentage surface area occupied by 90 dpf clones (56 clones, 10 ventricles); basal clones representing each ventricle are circled. **d,** Surface clones per ventricle (n = 10). Scale bars, 50 μm.

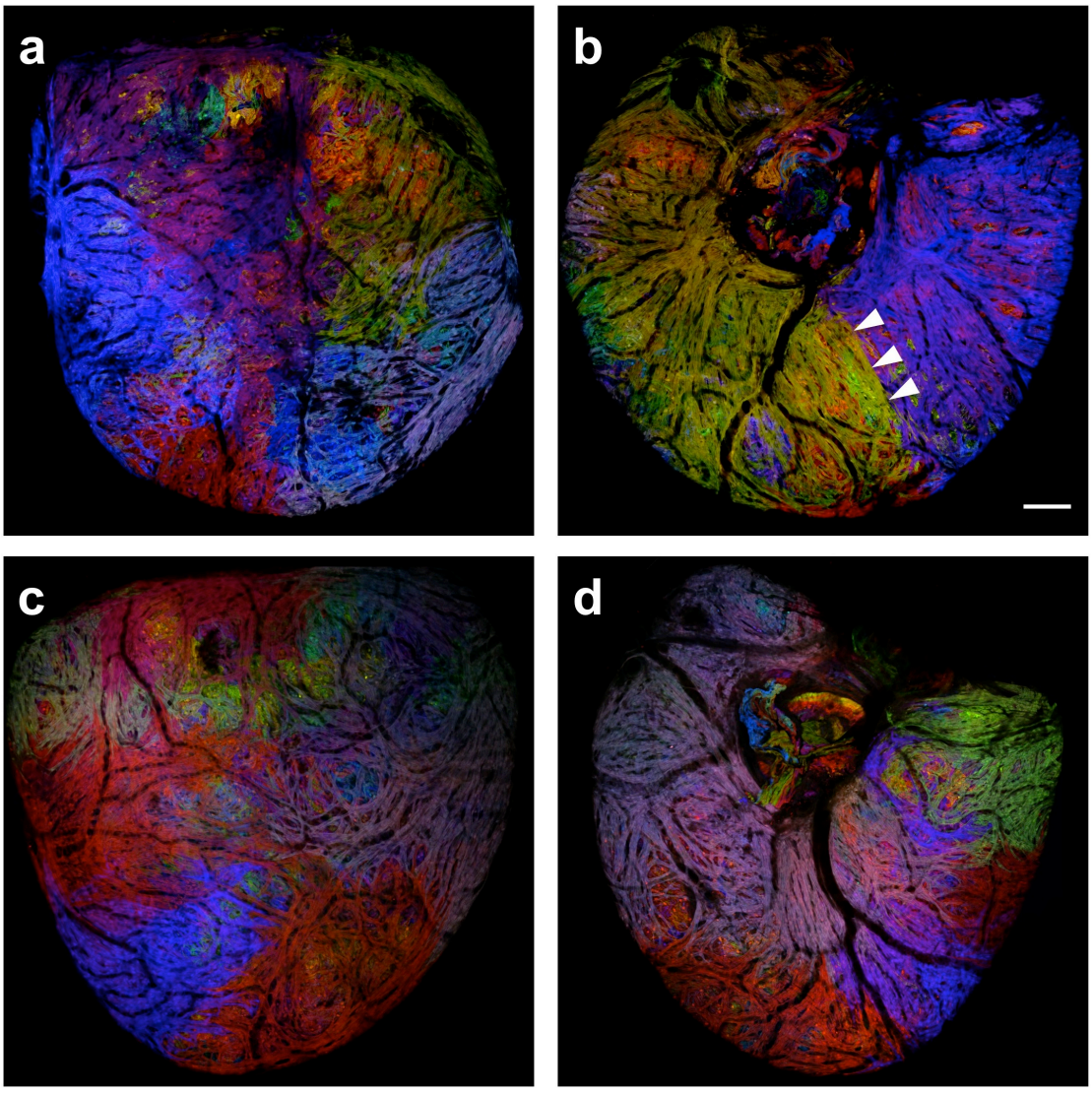


**Figure 10: Additional examples of adult ventricles, labeled at 2 dpf.**

**a-d,** Whole-mount images of 90 dpf *cmlc2:CreER; priZm* ventricles from animals that received 4-HT treatment at 2 dpf. Images in **a** and **b** are the front and back of the same ventricle, enabling visualization of full clonal extension. Arrowheads in **b** indicate a smooth boundary between clones running from base to apex. This was a rare event among our samples. Images in **c** and **d** are the front and back of a second ventricle. Scale bar, 100 μm.

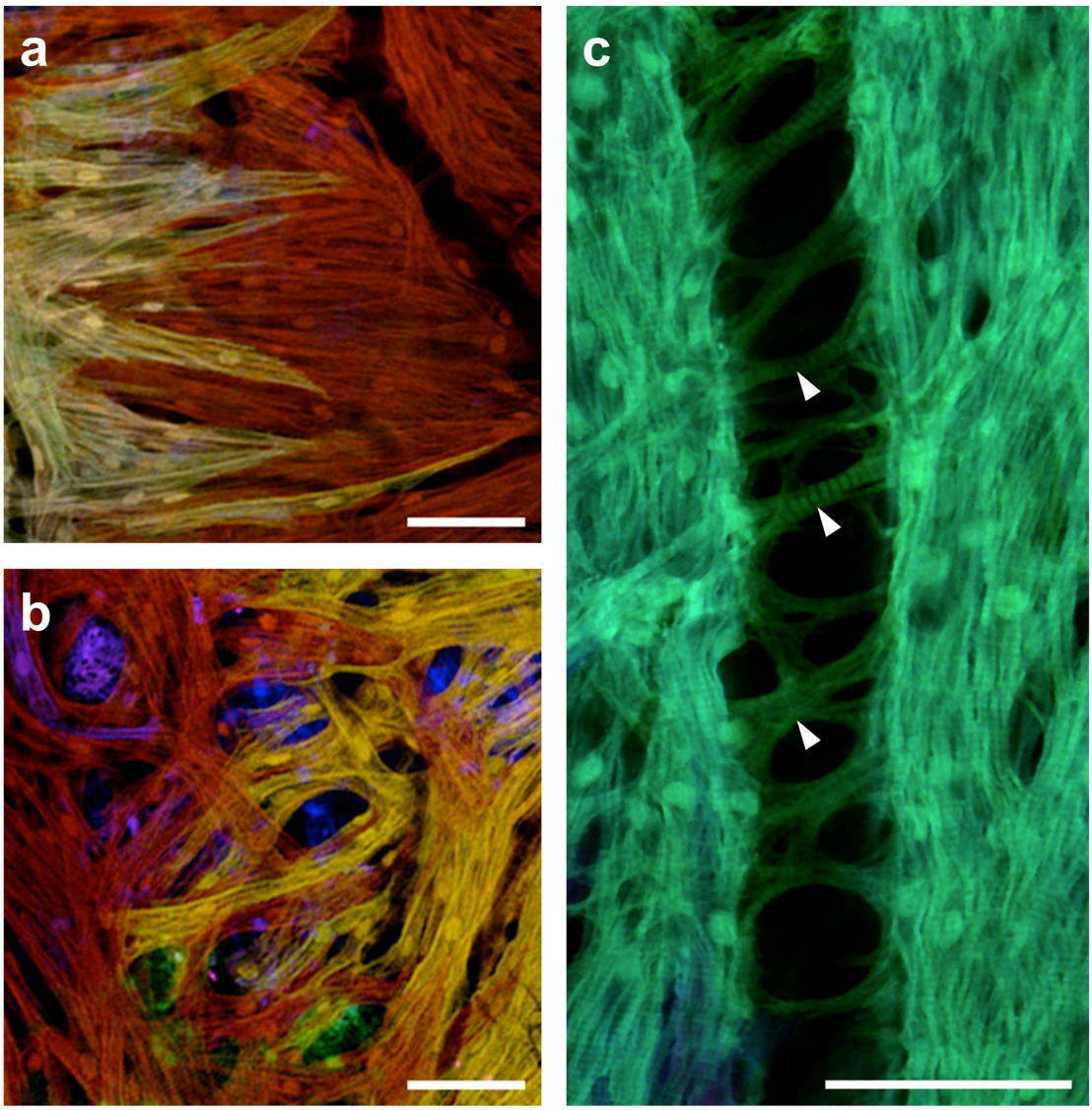


**Figure 11: Surface interactions of cortical cardiomyocyte clones.**

**a,** High magnification view of a gray-tinted clone of cortical cardiomyocytes that appears to fit like a puzzle piece with a neighboring region of red cortical myocytes. **b,** A weaving interaction between a yellow clone of cortical myocytes and red myocytes. Indigo and green primordial layer cardiomyocytes are visible beneath. **c,** A vessel tract (arrowheads) is visible in a large green clone of cortical cardiomyocytes, with some myocytes extending over the structure. Scale bars, 50 μm.

### 3.3.5 Muscle Lineage Regeneration after Injury

Zebrafish possess a robust capacity for heart regeneration throughout life, based on the ability to activate the proliferation of spared cardiomyocytes after injury (Poss et al., 2002; Kikuchi et al., 2010; Wang et al., 2011; Jopling et al 2010). We examined the regenerative potentials of primordial and cortical muscle by amputating ventricular apices from 90 dpf *cmlc2*:CreER; *priZm* animals that had been labeled at 2 dpf. At 14 days post-amputation (dpa), we detected growth of adjacent cortical muscle clones in lateral and radial directions into the wound area (Fig. 12a, b), but the primordial layer lagged behind the amputation site. By 30 dpa, as the wall was reconstructed with clonal patches of cortical cardiomyocytes, clones of single-cardiomyocyte thickness contiguous with the primordial layer first became detectable in the regenerate (Fig. 12c). By 60 dpa, the primordial layer was largely restored as a complete structure positioned between cortical and trabecular muscle (Fig. 12d). Thus, regenerating primordial muscle undergoes restricted lateral expansion as during morphogenesis, whereas cortical muscle regeneration is less constrained and assumes the primary component of the new wall. Interestingly, these events occur in a temporally reversed manner compared to initial morphogenesis, with cortical muscle regenerating before the underlying primordial layer.

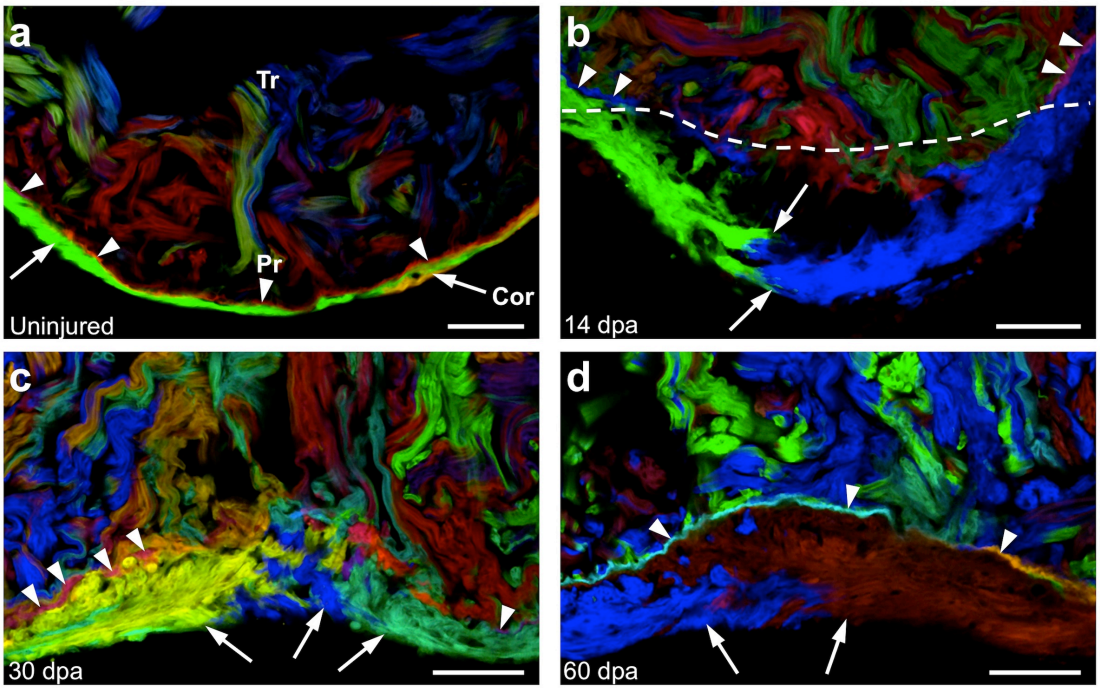


**Figure 12: Regeneration of cortical and primordial muscle after injury.**

**a,** Section of an uninjured ventricular apex, indicating the primordial (arrowheads) and cortical (arrows) layers. **b**, Regenerating ventricular apex at 14 days after resection. Cortical muscle clones converge within the injury site, whereas the primordial layer lags behind. Dashed line indicates amputation plane. **c,** 30 dpa ventricular apex, indicating multiple cortical clones and an incomplete primordial layer. **d,** Regenerated ventricular apex at 60 dpa, containing cortical muscle overlying a mostly contiguous layer of primordial muscle. n = 6 animals for each time point. Scale bars, 50 μm.

### 3.3.6 Origins of Dominant Cardiomyocyte Clones

To determine when cortical cardiomyocytes originate during heart morphogenesis, we initiated color labeling at 30 dpf, after formation of the juvenile structure but 1–2 weeks before the emergence of cortical muscle. Notably, large clonal patches were present on the surface of 90 dpf ventricles that had been incubated briefly with 4-HT at 30 dpf (Fig. 13a, e, d), with the largest clones present at the chamber base. We quantified the size and number of clones in ventricles with basal clones of recombined colors (11 of 20 animals). Our data indicated that adult cortical myocardium arises in patches of diverse sizes from an average of 8.6 ± 0.7 labeled 30 dpf cardiomyocytes (Fig. 13b, c), a number similar to that observed after labeling at 2 dpf.

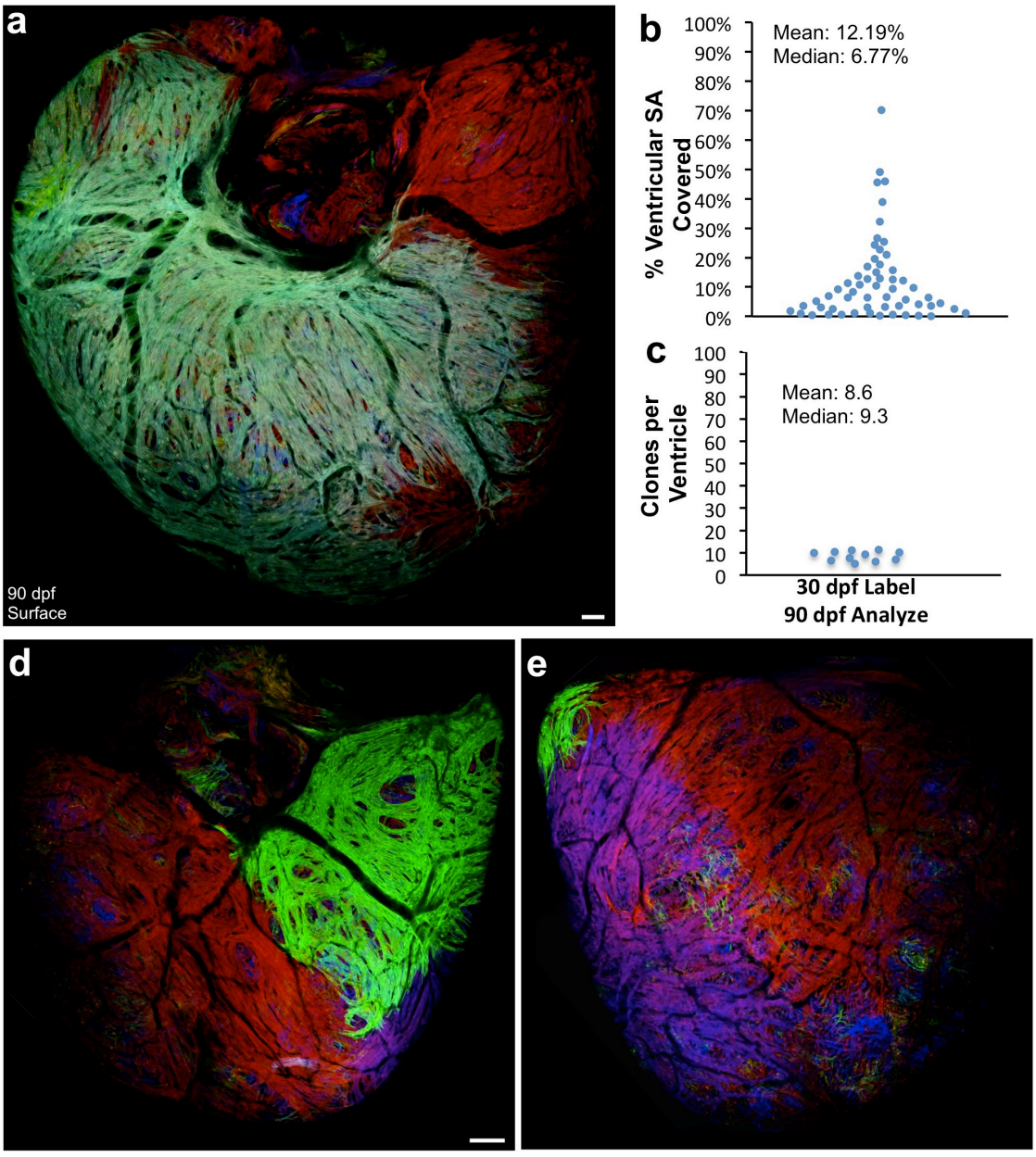


**Figure 13: Later, 30 dpf labeling displays similar clonal dominance.**

**a,** 90 dpf ventricular surface, after 30 dpf 4-HT labeling. **b,** Percentage surface area occupied by 90 dpf clones (58 clones, 11 ventricles). **c,** Surface clones per ventricle (n = 11) **d, e,** Additional example of ventral and dorsal surface of same ventricle from animals that underwent 4-HT labeling at 30 dpf, showing large cortical clones. Scale bars, 50 μm (**a**); 100 μm (**d** and **e**).

In some ventricles assessed 4 weeks after labeling (8 wpf), we observed trabecular muscle of the same color near the emergent cortical clone (Fig. 14a, b). To confirm this association, we examined sections of 6–7 wpf ventricles (labeled at 2 dpf), and consistently found nearby trabecular muscle of the same color as the small, basal cortical clone (13 of 13 ventricles). We also could identify cases from these examples in which trabecular and cortical muscle of one color connected through an apparent breach in the primordial layer (Fig. 15). These observations suggested a clonal relationship between trabecular and cortical cardiomyocytes in the maturing zebrafish ventricle.

We noticed lower color recombination in the primordial layer (~15%) than in the trabecular and cortical muscle lineages (~61%) at 8 wpf (Fig. 5a–d). Taking advantage of this differential labeling efficiency, we titrated 4-HT and identified a low dose that induced sparse recombination at 30 dpf in trabeculae and no obvious recombination in primordial muscle. Importantly, even with very limited labeling, cortical clones of a recombined color were still discernable in 3 of 24 ventricles at 8 wpf (Fig. 5e, f), a finding that reaffirmed a trabecular source for the cortical lineage. As with other samples mentioned above, images of confocal slices from these ventricles could identify single color clones containing

both cortical and trabecular muscle, connecting through an apparent breach in primordial muscle of unrecombined color (Fig. 5f–i).

Together, our findings indicate a dynamic mechanism that generates a final ventricular muscle lineage and completes adult cardiac morphogenesis. Trabecular cardiomyocytes penetrate the primordial layer in rare, spatially segregated events at the juvenile stage, seed the ventricular surface, and undergo expansion to create the cortical myocardium.

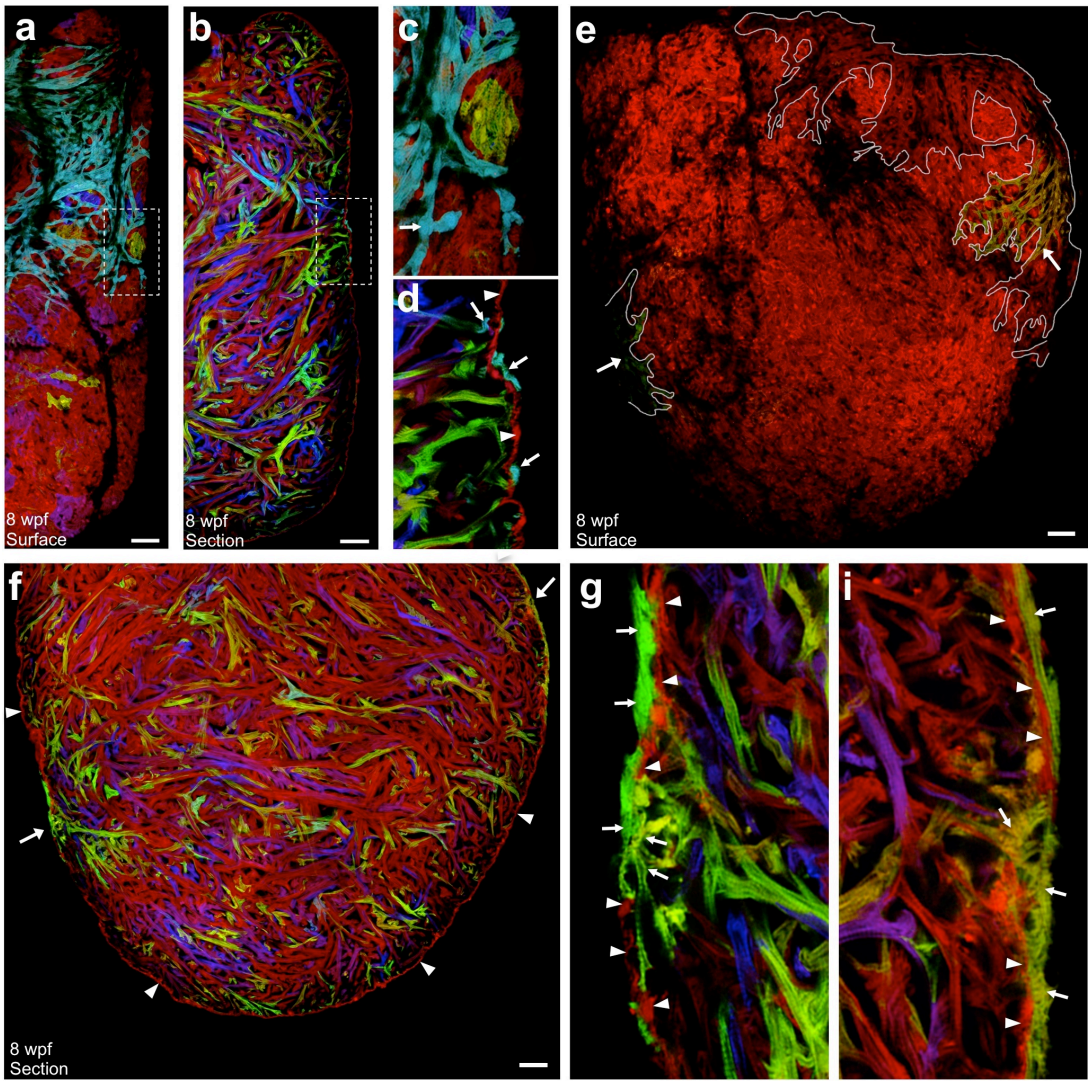


**Figure 14: Origins of clonally dominant cardiomyocytes.**

**a–d,** 8 wpf ventricular surface (**a**, **c**) and confocal slice (**b**, **d**), after 30 dpf 4-HT labeling. Cyan cortical muscle (arrows; **c**, **d**) overlies primordial muscle (arrowheads) that is largely red/unlabeled, and cyan trabeculae (arrow; **d**) Dashed boxes in **d** and **e** are shown at higher magnification in **f** and **g**, respectively. **e–i,** 8 wpf ventricular surface (**e**) and confocal slices (**f–i**) after limited 4-HT labeling, showing no obvious primordial muscle labeling (arrowheads; **f–i**). Arrows indicate green (**e**, **f** (left); **g**) and hazel (**e**, **f** (right); **i**) cortical/trabecular clones. All cortical muscle in h is outlined in white. Scale bars, 50 μm.

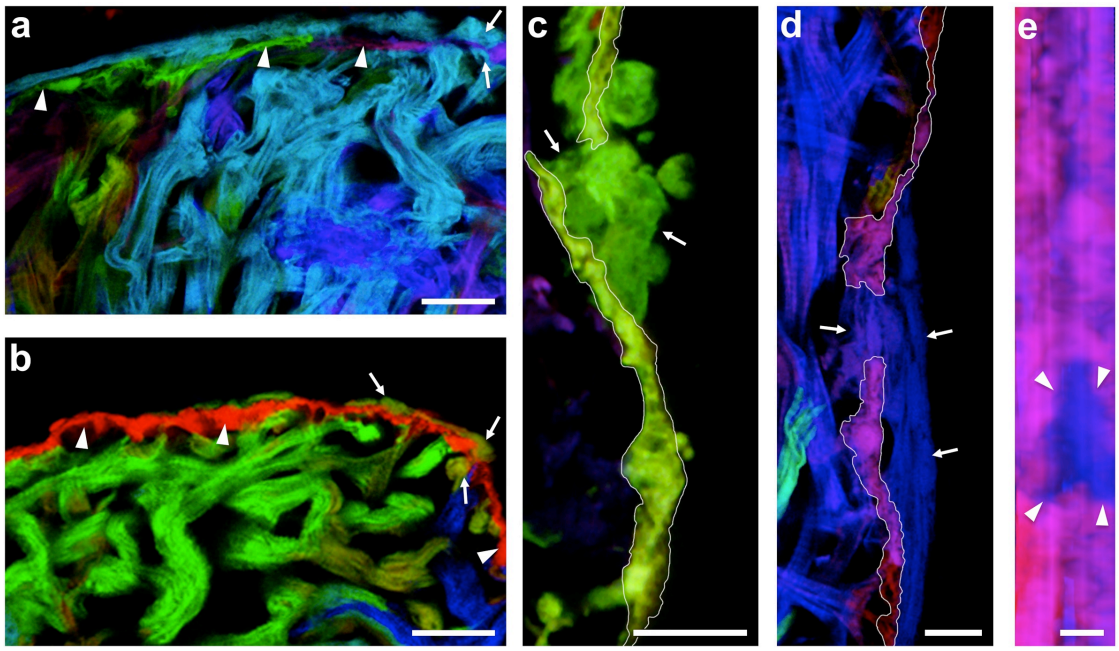


**Figure 15: Evidence that clones containing trabecular and cortical cardiomyocytes connect through a breach in the primordial layer.**

**a-d,** Four examples of 6-7 wpf *cmlc2:CreER; priZm* ventricles from animals that had been labeled at 2 dpf. Images were captured from areas near the base of the ventricle, where cortical muscle typically appears first. Primordial muscle is green and magenta (**a**) from left to right (arrowheads). Cortical muscle is cyan, as is the adjacent trabecular muscle (arrows). The primordial layer is all red (**b**) in this section (arrowheads). Cortical and trabecular muscle share the same two colors (green and hazel), and an area on the right of the image connects hazel muscle on each side (arrows).). Yellow primordial muscle (**c**) is outlined in white, showing a gap breached by a green clone (arrows). The pink and red primordial layer is outlined in white (**d**), interrupted by a blue clone spanning trabecular and cortical muscle (arrows). **e,** 3D Imaris reconstruction of the confocal stack of images in d, rotated to display a view from the periphery to the lumen to the heart. The primordial layer has a gap filled by the emergent blue clone (arrowheads). Scale bars, 20 μm (**a** and **b**); 10 μm (**c**-**e**).

## *3.4 Discussion*

Multicolor clonal analysis enables the simultaneous fate mapping of many similar cells within a developing organ. We used this technology to reveal unsuspected cellular mechanisms guiding heart morphogenesis in zebrafish. We found that three ventricular myocardial lineages are present in the adult form: primordial, trabecular and cortical muscle, created in this order from each other. Our data indicate that the innermost trabecular lineage is initiated predominantly by delamination from the embryonic primordial layer and migration, as proposed in an earlier study (Liu et al., 2010). Next, the outermost cortical layer is created as juveniles mature to adults, emerging wholly or in part via an 'insideout' mechanism from trabeculae. Here, one or more particularly expansive juvenile cardiomyocytes access the ventricular surface at each of only approximately eight sites per animal.

Zebrafish share several aspects of cardiac development with higher vertebrates, and the multicolor clonal analysis results we report here indicate some basic commonalities with results of single-marker clonal analysis performed previously in early mouse and chick embryos. For instance, cardiomyocytes were also observed in coherent clonal populations during cardiac growth in these systems, after an early phase of dispersion (Mikawa et

al., 1992; Meilhac et al., 2003). Most unexpected is that the zebrafish ventricle maintains a primordial layer of single-cardiomyocyte thickness without noticeable cell division in the z-plane, and that wall thickening instead occurs after seeding of a separate cortical lineage by dominant clones. It will be interesting to determine the evolutionary distribution of aspects of this uncovered morphogenetic mechanism within other bony fish and among other classes of vertebrates like mammals.

The origins and diversity of clonal patterns of cortical muscle we report are more consistent with a stochastic model of source cell selection than a hierarchical or predetermined model. Additionally, the observation of clonal dominance in cardiomyocytes is reminiscent of stem cell compartments that drift towards clonality during homeostatic tissue maintenance, events that have been explained by stochastic models (Snippert et al., 2010; Klein et al., 2010; Lopez-Garcia et al., 2010; Doupé, et al., 2010). We suspect that molecular and/or physiological cues enable the emergence and proliferative capacity of cortical cardiomyocytes, ostensibly with a preferential influence at the ventricular base. It is likely that clonal dominance behavior is a recurring mechanistic strategy to help shape vertebrate organs.

# Chapter 4. An Injury-Responsive Gata4 Program Shapes the Zebrafish Cardiac Ventricle

**Gupta, V.,** Gemberling, M., Karra, R., Evans, T., and Poss, K.D. (In Review).

Vikas Gupta and Matt Gemberling are co-first authors. Vikas Gupta performed all multicolor clonal experiments, reporter expression analysis, pierce injuries, juvenile Gata4 inhibition analysis, and *in situ* hybridizations. Matt Gemberling created and validated *β-act2:BSg4DN* transgenic line, performing survival analysis and adult regeneration experiments. Ravi Kara analyzed *nppa*/*nppb* expression patterns and helped with *in situ* hybridizations.

## 4.1 Summary

Defining the cellular programs and responses that govern growing juvenile tissues can be informative for understanding mechanisms of adult regeneration. During zebrafish heart regeneration, the transcription factor gene *gata4* is induced in compact or cortical myocytes that form the primary contribution to the regenerate (Kikuchi et al., 2010; Poss et al., 2002). This layer of ventricular muscle forms in a dynamic cellular fashion during juvenile growth in which a small number of internal cardiomyocytes breach the ventricular wall and expand upon its surface to encase and fortify the heart (Gupta and Poss, 2012). Here, we examined how the cortical layer is formed using a combination of expression studies, multicolor clonal analysis, and inducible transgenic misexpression. Emergent juvenile cortical cardiomyocytes induce expression of *gata4*, in a similar pattern seen after injury and during adult heart regeneration, before proliferating to build the adult cortical layer. Clonal lineage tracing indicated that gata4+ cardiomyocytes make heterogeneous contributions to wall morphogenesis, whereas they have little or no proliferation bias during regeneration. Experimental microinjuries or placement of animals under conditions of rapid organismal growth stimulated production of ectopic *gata4*$^{+}$ cortical muscle, implicating biomechanical stress in new morphogenesis of this

tissue. Induced transgenic inhibition revealed requirements for Gata4 in morphogenesis of the cortical layer and normal cardiac function in juveniles, and again in adults for regeneration of resected cortical muscle. Our experiments uncover an injury-responsive program that fortifies the juvenile ventricular wall and prevents heart failure, one that is reiterated in adults to promote regeneration after cardiac damage.

## *4.2 Introduction*

Fish and salamanders have an impressive ability to regenerate lost or damaged tissues, including limbs, fins, spinal cord, brain, heart, retina, lens, jaws, and intestinal portions (Becker et al., 1997; Brockes and Kumar, 2005; Johnson and Weston, 1995; Poss et al., 2002; Tanaka, 2003; Vihtelic and Hyde, 2000). A common character of regeneration is the re-activation of programs that helped create that tissue during embryonic development (Alvarado, 2000; Poss, 2010). For example, transcription factor expression and signaling gradients that pattern the embryonic salamander limb are reutilized to help regenerate an amputated adult limb (Nacu and Tanaka, 2011).

However, recent studies have suggested that some genes might be solely dedicated to the process of regeneration (Garza-Garcia et al., 2010; Whitehead et al., 2005). Such genes could be important in juvenile tissues, where organismal growth and organogenesis continue to be active, are similar in scale, complexity, and physiology to their adult counterparts. The cellular programs and microenvironments of growing juvenile tissues could be informative for understanding mechanisms of adult regeneration. Supporting this notion, Pax7, a transcription factor gene that marks all skeletal muscle satellite cells, is required for neonatal muscle regeneration. However, Pax7 becomes dispensable for regeneration as animals progress through juvenile and adult phases (Lepper et al., 2009). This suggests that other gene programs are active during juvenile and adult phases that mediate the regenerative response.

The capacity to regenerate heart muscle is present during early postnatal life in mice and likely other mammals, but is much lower in adults (Porrello et al., 2011; Senyo et al., 2013). By contrast, zebrafish maintain a high potential for heart regeneration into adult life (Poss et al., 2002). Following resection of the apex of the zebrafish ventricle, existing cardiomyocytes assume the primary source of new muscle. A key subpopulation of cardiomyocytes near the injury

site, within the ventricular wall, activates regulatory sequences of *gata4*, a transcription factor gene important for embryonic heart development, and proliferates to reestablish a contiguous wall of muscle (Kikuchi et al., 2010).

Many studies over the past 20 years have identified cellular and molecular events that control embryonic heart development and function in zebrafish (Glickman and Yelon, 2002; Liu and Stainier, 2012), whereas juvenile heart development has been sparingly investigated. Recent findings have shed light on the cellular mechanisms by which the juvenile zebrafish heart matures. In growing zebrafish, the wall of the cardiac ventricle remains as a single cardiomyocyte-thick primordial layer for the first several weeks of life, surrounding a meshwork of inner trabecular muscle. Then, as juvenile animals mature, the ventricle acquires an additional, multilayered cortical component that encapsulates the heart to finalize the adult cardiac architecture. Multicolor clonal analysis demonstrated that this cortical muscle is created in its entirety from an unexpectedly small number (~8) of cardiomyocytes. These cardiomyocytes emerge from inner trabecular muscle and penetrate the overlying primordial layer in rare breaching events, before proliferating upon the ventricular surface (Gupta and Poss, 2012).

Here, we examined cardiac morphogenesis in growing juvenile zebrafish to gain greater insight into the process of adult heart regeneration. We found that gata4 regulatory sequences are specifically induced in juvenile cardiomyocytes that emerge and build adult cortical muscle. Injury, the stimulus for regeneration, was able to induce the early, ectopic formation of cortical muscle in juveniles, whereas wall breaching events and myogenic contributions to the cortical layer were boosted during conditions of increased biomechanical stress. Inhibition of Gata4 within cardiomyocytes had severe effects in juvenile animals, disrupting maturation of the ventricular wall and causing heart failure, as well as preventing myocardial regeneration in adults. Our results indicate that regeneration at the adult stage recapitulates a Gata4-dependent response that drives juvenile heart morphogenesis, events that can be triggered by cardiac stress or injury.

## *4.3 Results*

### 4.3.1 *gata4* Expression is Activated in New Cortical Cardiomyocytes of the Juvenile Ventricle

To compare cardiac regeneration and juvenile heart morphogenesis, we first examined cardiac fluorescence in the *gata4:EGFP* reporter strain. *gata4:EGFP* is normally undetectable in the adult zebrafish ventricle, but its expression is activated after apical resection in spared cortical cardiomyocytes within the ventricular wall. Cardiomyocytes that activate gata4 regulatory sequences retain this expression signature as they proliferate and replace lost cortical muscle (Kikuchi et al., 2010). We did not detect *gata4:EGFP* in primordial or trabecular cardiomyocytes in 5 weeks post-fertilization (wpf) juvenile zebrafish ventricles (Fig. 16a). By contrast, at 6 wpf, the onset of cortical layer formation, *gata4:EGFP* expression was evident in a small population of cortical cardiomyocytes at the base of the ventricle near the outflow tract (Figures Fig. 16b, 16d, and 16e). This basal location mirrored the initial site of cortical myocyte emergence that was previously identified by multicolor lineage tracing (Fig. 7). By 8 wpf, *gata4:EGFP* expression was present in a larger region of cortical cardiomyocytes spanning to the chamber midpoint. Myocytes closer to the apex displayed a gradually

stronger *EGFP* signal, indicating higher levels of gata4 expression (Fig. 16c and 16f). Thus, *gata4* regulatory sequences are activated in emergent cortical muscle, resembling their activity during adult heart regeneration.

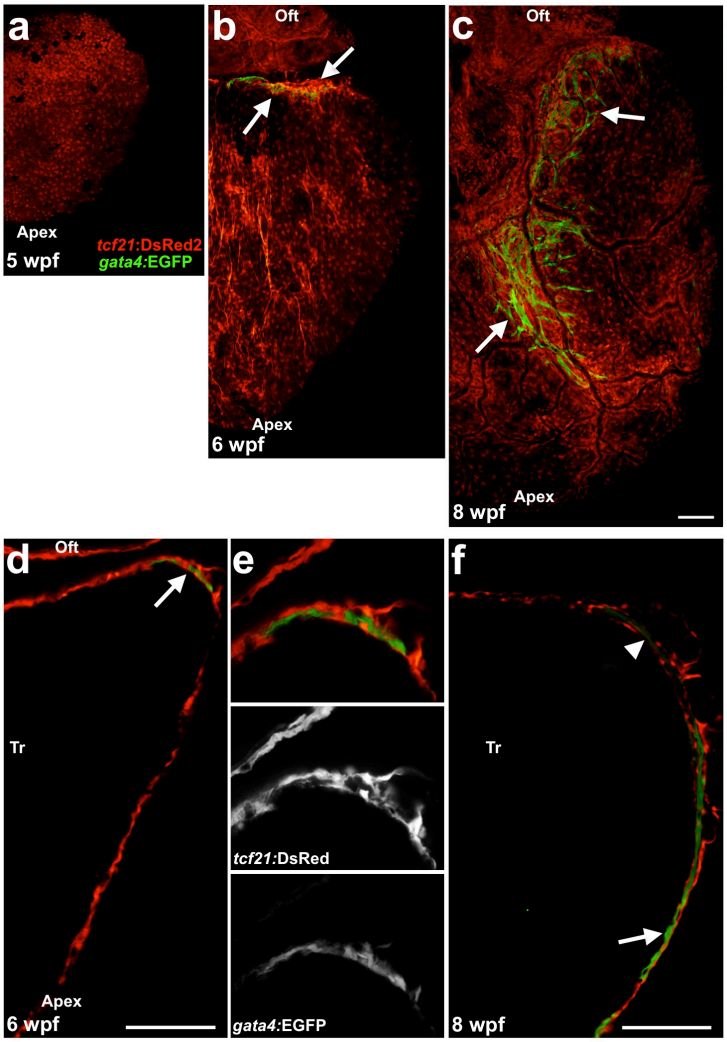


**Figure 16: *gata4* marks emerging cortical myocytes.**

**a-c,** Images of 5 (**a**), 6 (**b**), and 8 (**c**) weeks post-fertilization (wpf) ventricular surfaces, assessed *for tcf21:DsRed2*$^{+}$ epicardial cells (red) and *gata4:EGFP*$^{+}$ cardiomyocytes (green). At 6 wpf, a cluster of *gata4:EGFP*$^{+}$ surface myocytes is visible at the base of the heart in an area of dense epicardial cells (arrows in (**b**)). By 8 wpf, *gata4*$^{+}$ cortical myocytes are detected at the ventricular midpoint. **d, e,** Tissue section indicating *gata4*$^{+}$ myocytes and epicardial cells at 6 wpf. **f,** Section of 8 wpf ventricle indicating cortical *gata4:EGFP* expression that is strongest in cardiomyocytes closer to the apex (arrow), and weaker in basal myocytes (arrowhead) (n = 8-12). Scale bars, 100 μm.

### 4.3.2 Clonal Analysis of *gata4*$^{+}$ Cardiomyocytes during Cortical Morphogenesis and Regeneration

To directly test whether gata4+ cardiomyocytes that emerge at the 6 wpf ventricular base are the source of the adult cortical layer, we performed a clonal lineage trace of these cells. *gata4:ERCreER* transgenic zebrafish, employing the same regulatory sequence as *gata4:EGFP* animals (Kikuchi et al., 2010), were crossed to different priZm multicolor lineage-tracing lines. One line was identified that enabled recombination only in the presence of 4-HT, *Tg(β-act2:Brainbow1.0L)*$^{pd50}$ (referred to here as *priZm2*). To label *gata4*$^{+}$ cardiomyocytes at the ventricular base, we pulsed 6 wpf *gata4:ERCreER; priZm2* animals with 4-HT (Fig. 17a). Ventricles were analyzed in 90 dpf adults, and 9 of 32 ventricular surfaces contained labeled (non-red) clones of cortical muscle, often spanning to the apical portion (Fig. 17b, c). No labeling of trabecular muscle was detected. These fate-mapping results indicate that *gata4*$^{+}$ cardiomyocytes at the base of the 6 wpf ventricle proliferate to create the adult cortical layer, a process that involves cardiomyocyte migration or displacement toward the apex.

Notably, upon imaging and quantification of all colored clones in these ventricular halves, we identified a clear proliferation bias within cortical clones (Fig. 17b, c). Even though labeling occurred in established cortical

cardiomyocytes, this labeled population still had many clones that covered over 20% of one side of the ventricular surface (Fig. 17d), along with much smaller clones. Thus, emergent cardiomyocytes that induce *gata4* regulatory sequences have a proliferation bias as they build the cortical layer, with some cells making considerably larger contributions than others.

To examine whether similar proliferation dynamics are displayed in *gata4*$^{+}$ cardiomyocytes during adult heart regeneration, we resected ventricular apices of adult *gata4:ERCreER; priZm2* zebrafish and gave animals a 4-HT pulse at 5 dpa (Fig. 18a). 4-HT-treated ventricles displayed no recombination in the absence of injury (Fig. 18b). Upon assessing ventricles at 30 dpa, we observed many small clones in the regenerates and no evidence of a proliferation hierarchy (Fig. 18c, d). Within most sections through the regenerates, over 15 distinct colors could be readily observed.

To address the possibility that 4-HT-induced recombination continued into early stages of regeneration, we performed analogous experiments using a pan-cardiomyocyte labeling strategy. When recombination was initiated 5 days prior to injury in *cmlc2:CreER; priZm* animals, 18-30 distinct colors were observed in serial sections of 60 dpa regenerates (Fig. 19). Thus, unlike initial cortical

morphogenesis, cortical muscle regenerates through the activity of many *gata4*$^{+}$ cardiomyocytes, each of which makes a similar clonal contribution. This difference possibly reflects a contrast between cardiomyogenesis directed in a base-to-apex wave during wall creation, versus more regionalized muscle regeneration stimulated by local resection injury.

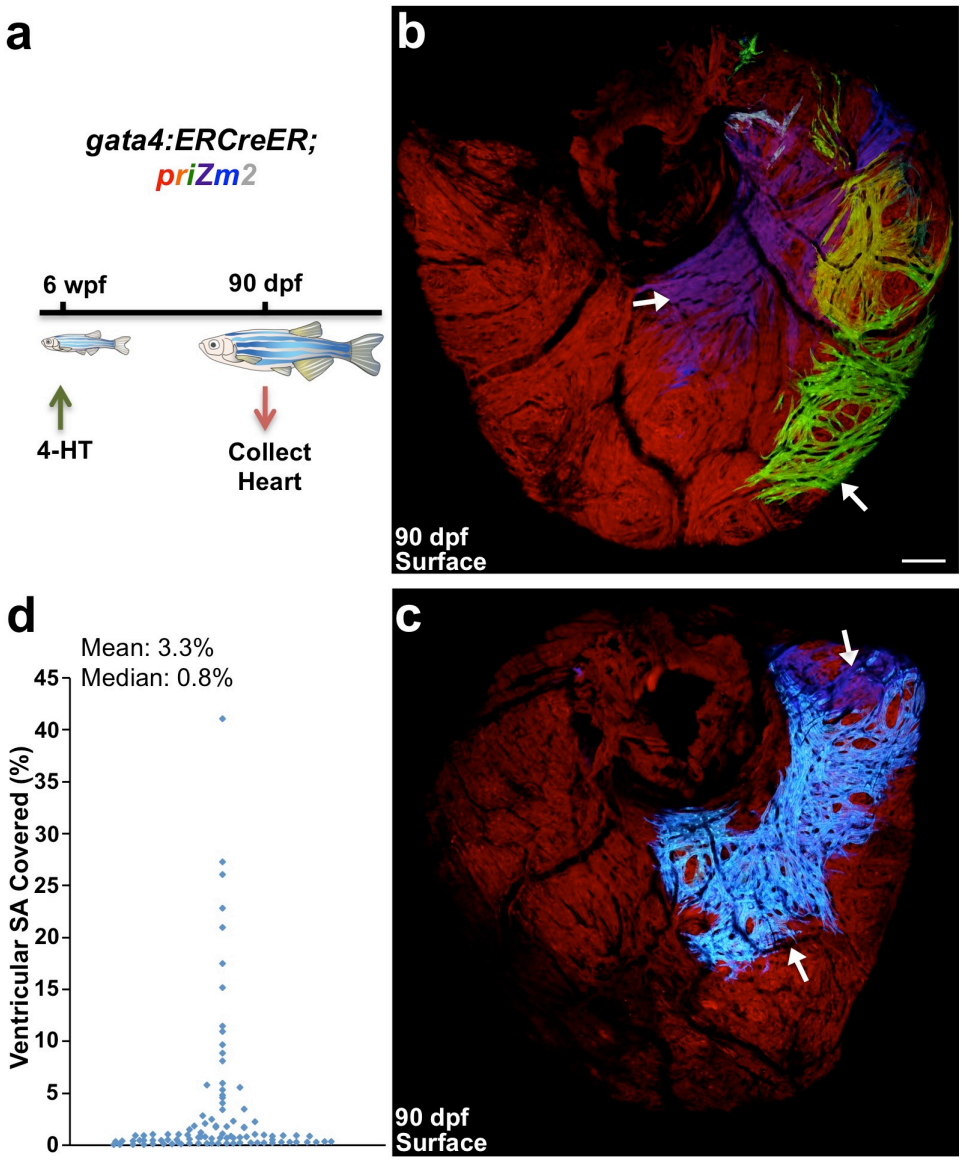


**Figure 17: Juvenile *gata4*⁺ myocytes lineage trace to adult cortical muscle and proliferate in a biased manner.**

**a,** Cartoon of lineage-tracing experiments to determine clonal dynamics in established *gata4*⁺ cortical cardiomyocytes. *gata4:ERCreER; priZm2* animals are pulsed with 4-HT at 6 wpf, and ventricles are analyzed at 90 dpf. **b, c,** Surface muscle from two ventricles in these experiments with arrows indicating large clones. **d,** Percentage surface area (SA) occupied by each clone, (96 total counted clones from 9 ventricular halves). Scale bars, 100 μm.

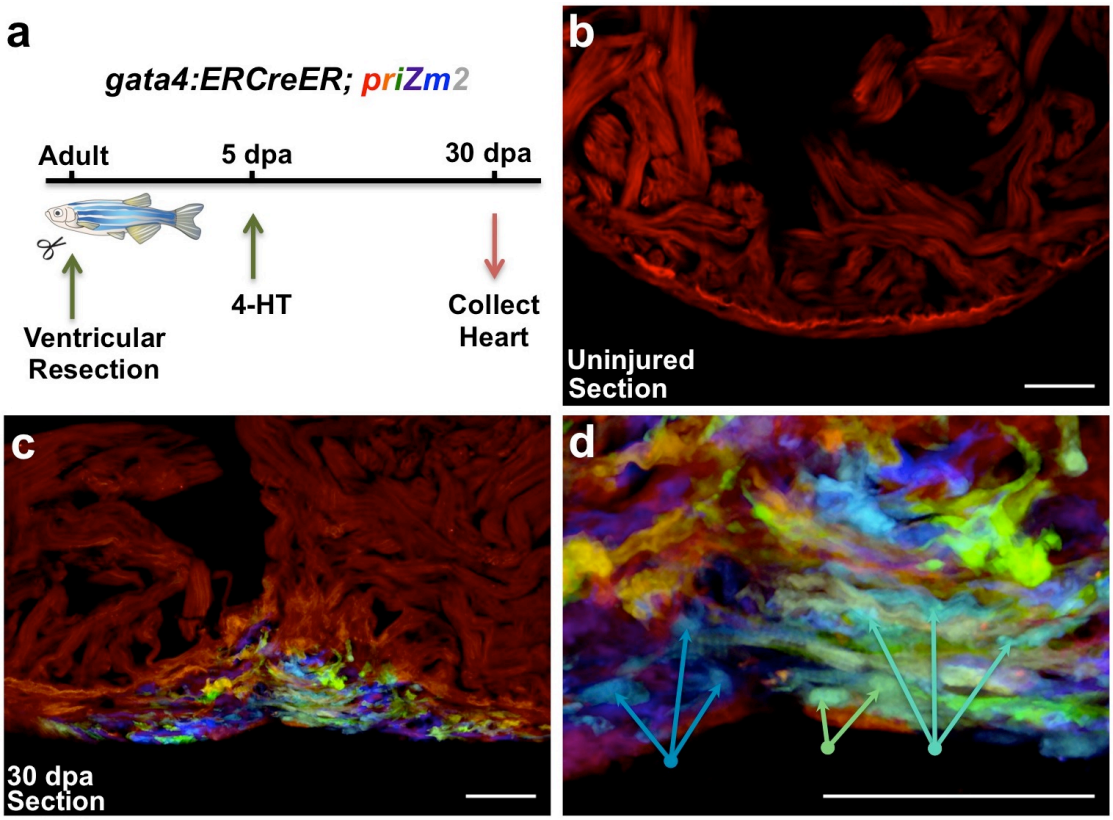


**Figure 18: Cardiomyocytes lose proliferation bias during regeneration.**

**a,** Cartoon of lineage-tracing experiments to determine clonal dynamics in regenerating *gata4*$^{+}$ cardiomyocytes. **b,** Section through a ventricle from an uninjured animal 10 days after 4-HT treatment, indicating no recombination in the absence of injury. **c,** Section through a ventricular apex at 30 dpa, visualizing multiple colored cardiomyocyte clones exclusively in regenerated muscle. Over 15 colors can be distinguished in this 10-micron section of the regenerate. A maximum projection image from confocal slices is shown (n = 6). **d,** Higher magnification view of regenerate shown in (**c**). Arrows indicate 3 differently colored multicellular clones. Scale bars, 50 μm.

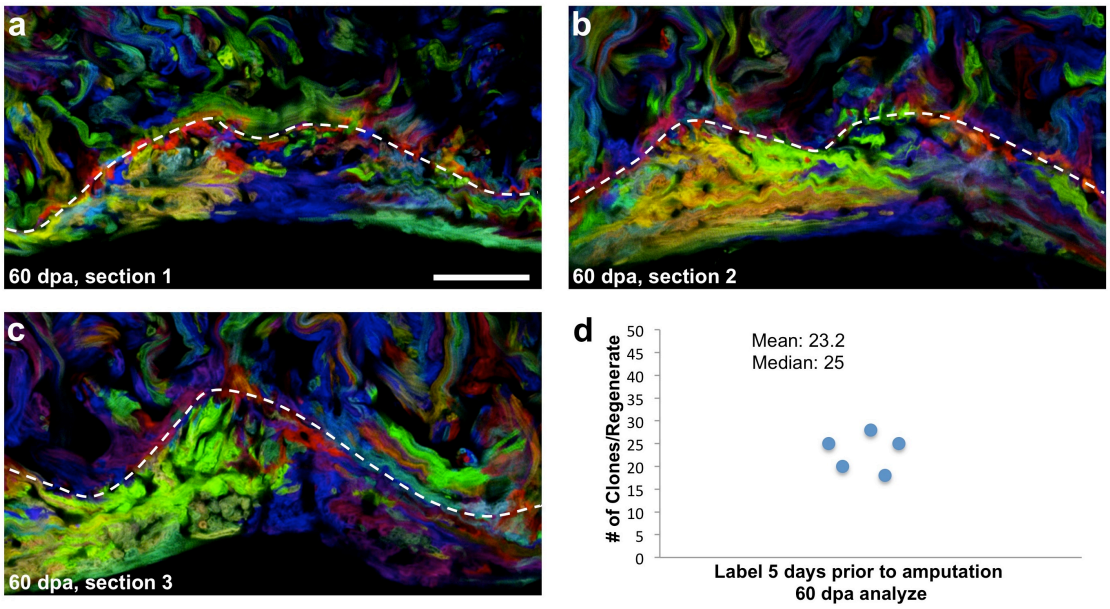


**Figure 19: Clonal analysis of regenerating cardiomyocytes by a pan-cardiomyocyte tracing method.**

**a-c,** Adult *cmlc2:CreER; priZm* animals were labeled with 4-HT 5 days prior to amputation, and ventricular apices were resected 5 days later. Three serial 30-micron sections through a 60 dpa regenerate (**a-c**), in which multiple interwoven small clones can be visualized within the regenerate. Clonal representation changes markedly between sections. Dashed lines indicate the approximate plane of resection. **d,** Number of clones counted from 3 serial sections of the regenerates in 5 different ventricles. The number of colors counted in these regenerates likely reaches the limit for this transgenic line. Scale bar, 50 μm.

### 4.3.3 Cortical Layer Formation Shares Expression of Injury and Cardiac Stress Markers that are Induced during Regeneration

We hypothesized that *gata4* induction and cortical emergence was part of a more general stress response. Stress in the form of increased afterload or stretching upon the mammalian heart is known to activate Gata4, which then transcriptionally initiates a hypertrophic program and angiogenesis, responses that serve to curb cardiac stress (Hautala et al., 2001; Hautala et al., 2002; Charron et al., 2001; Liang et al., 2001a; Liang et al., 2001b; Pikkarainen et al., 2003; Tenhunen et al., 2004; Heineke et al., 2007; van Berlo et al., 2011).

The stress-induced activation of Gata4 could be a consequence of juvenile growth that inherently increases biomechanical stress on the heart as a result of increasing organismal mass and circulatory load. To identify a more general stress-related response in myocardial cells, we assessed expression of the secreted factors Natriuretic peptide a (Nppa) and Natriuretic peptide b (Nppb) (Braunwald, 2008). Nppa and Nppb are cardiac stress markers that increase in expression within injured or failing hearts. They serve to increase vasodilation and natriuresis, which decreases stress upon the heart by reducing preload and afterload (Becker et al., 2012; Braunwald, 2008; Houweling et al., 2005; Liang and Gardner, 1999).

We found that *nppa* had low expression in the uninjured adult zebrafish ventricle, and that it increased sharply after resection injury or partial genetic ablation of cardiomyocytes (achieved through inducible Cre-mediated diphtheria toxin A expression; Fig. 20a-c) (Wang et al., 2011). *nppb* expression was binary, undetectable in uninjured adult ventricles but strongly induced by trauma (Fig. 20e-g). Interestingly, both markers were expressed in a diffuse manner in growing juvenile ventricles, suggesting comparatively higher levels of cardiac stress than uninjured adult ventricles (4-7 wpf; Fig. 20d, h).

Trauma to the adult zebrafish or mouse heart is also known to activate the epicardium, a population of mesothelial cells that envelops the ventricle (Lepilina et al., 2006; Smart et al., 2011; Zhou et al., 2011). In zebrafish, epicardial cells induce developmental markers, proliferate, and integrate into regenerating muscle in the injury site, where they ultimately contribute vascular support cells and potential mitogenic signals (Kikuchi et al., 2011b; Lepilina et al., 2006). By visualizing epicardial cells in juvenile zebrafish with a pan-epicardial reporter strain, *tcf21:DsRed2*, we saw that *gata4:EGFP*$^{+}$ cortical myocytes were surrounded on each side by a mass of epicardial cells at 6 and 8 wpf (Fig. 16b-f). The epicardium and endocardial lining also activate *raldh2* expression, an enzyme

that synthesizes retinoic acid and marks the embryonic epicardium, after apical resection to the zebrafish heart (Kikuchi et al., 2011a; Lepilina et al., 2006). We observed that *raldh2* was pronouncedly expressed within the epicardium and endocardium of growing juvenile ventricles (Fig. 21).

These studies indicate that the temporally distinct events of regeneration and juvenile cortical layer formation share a subset of induced cardiac and/or stress-responsive genes. Organ-wide *raldh2* and *nppa/b* expression at the juvenile stage are consistent with increased biomechanical stress, whereas *gata4* induction and epicardial cell augmentation in and around emerging cortical muscle identify a more localized response.

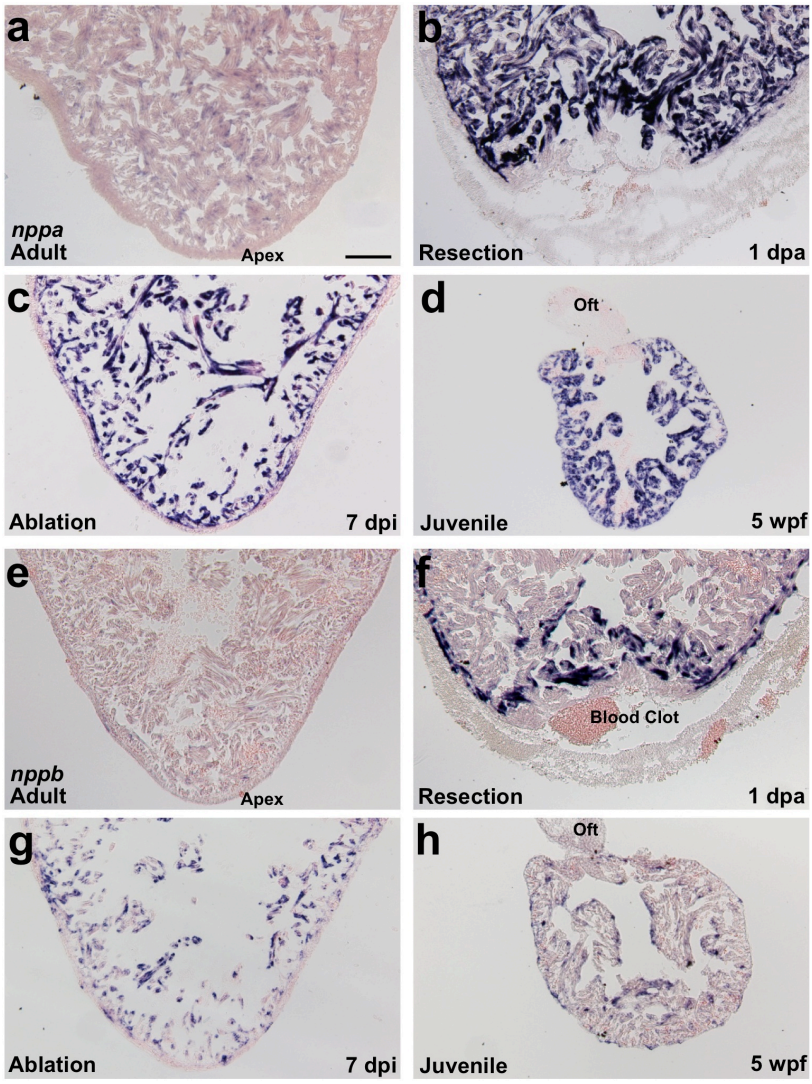


**Figure 20: *nppa/b* expression after injury and during juvenile growth.**

**a,** Section of an adult ventricle stained by *in situ* hybridization for *nppa*, indicating low but detectable expression. **b, c,** By 1 day after apical resection (**b**) (dpa) or 7 days after diffuse genetic muscle ablation (dpi) (**c**), *nppa* is strongly induced in cardiomyocytes. **d,** *nppa* expression is detected throughout the 5 weeks post-fertilization (wpf) ventricle (n = 8-14). **e,** Section of an adult ventricle stained by *in situ* hybridization for *nppb*, indicating no expression. **f, g,** By 1 day post amputation (dpa) (**f**) or 7 days after diffuse genetic muscle ablation (dpi) (**g**), *nppb* is induced in cardiomyocytes. **h,** *nppb* expression is detected throughout the 5 weeks post-fertilization (wpf) ventricle (n = 8-14). Scale bars, 100 μm.

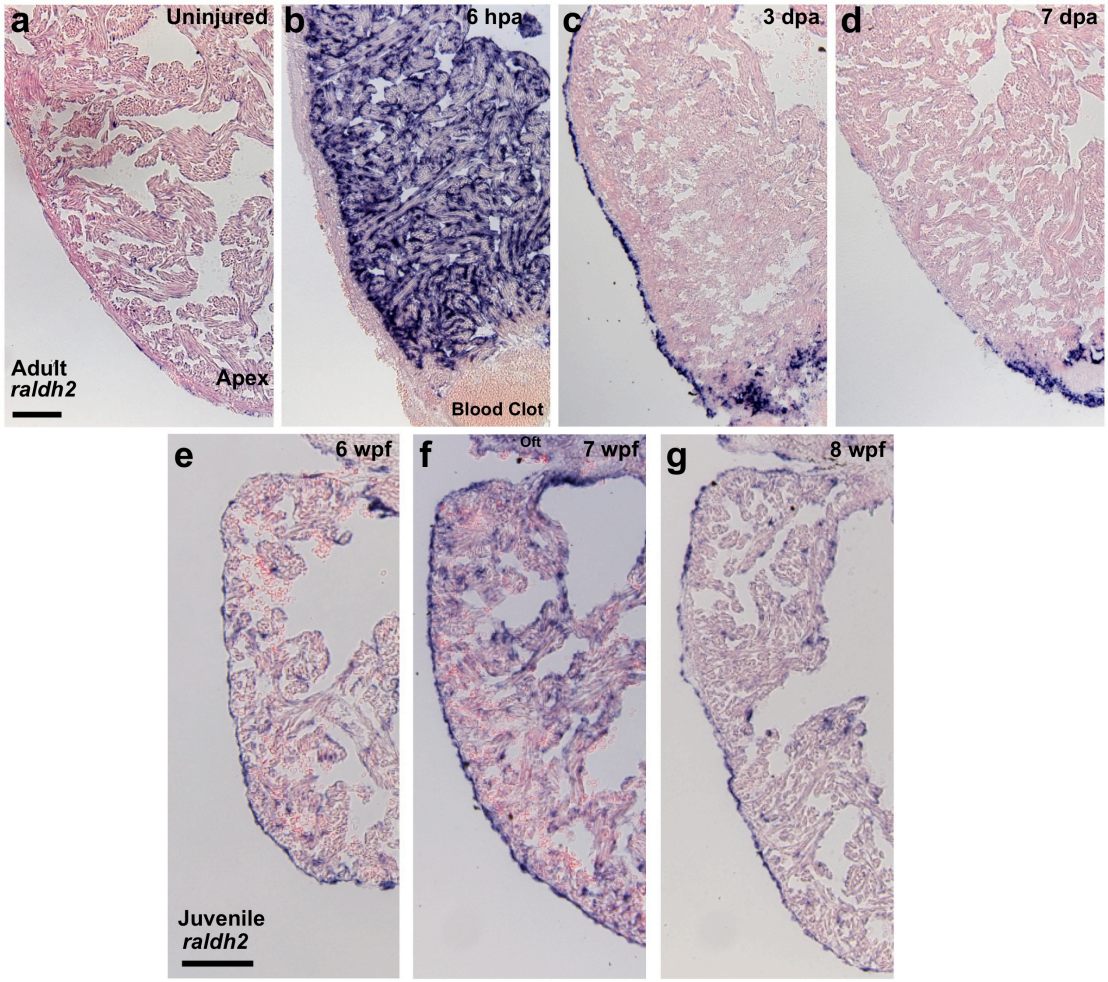


**Figure 21: *raldh2* expression after injury and during juvenile growth.**

**a-d,** Section of adult ventricles stained by *in situ* hybridization for *raldh2*. There is little or no detectable expression within an uninjured ventricle (**a**). After partial ventricular resection, *raldh2* is induced organ-wide in the endocardium by 6 hours post amputation (hpa) (**b**) and organ-wide in the epicardium by 3 dpa (**c**). Expression in these cell layers localizes to the injury site by 7 dpa (**d**). **e-f,** During juvenile growth, *raldh2* is detected in both epicardial and endocardial tissues (n = 8-20). Oft, outflow tract. Scale bars, 100 μm.

### 4.3.4 Experimental Injuries Stimulate Early and Ectopic Morphogenesis of Cortical Myocytes

Juvenile heart growth and adult regeneration are distinguished by their initiation, with the latter involving a major injury. Resection to the adult zebrafish heart triggers *gata4* expression within cortical cardiomyocytes. To examine whether the emergence of *gata4*$^{+}$ cortical myocytes in juveniles can be stimulated by injury in an analogous manner as adult regeneration, we applied a microinjury to the ventral apical surface of the 30 dpf juvenile ventricle by piercing it with a fine tungsten needle. We analyzed this site of injury for precocious cortical muscle formation 12 days later (6 wpf total growth), a time point at which no cortical muscle is present as it is covered later during juvenile growth at 8-9 wpf.

To identify whether injury stimulated the precocious emergence of cortical mycoytes, we visualized them with a multicolor labeling strategy that identifies cortical muscle clones by morphology. Cortical myocytes are easily distinguishable from primordial muscle by their external location, cell shape, and subcellular striation pattern (Fig. 7) (Gupta and Poss, 2012). In this experiment, 2 dpf *cmlc2:CreER; priZm* embryos were briefly incubated with 4-HT to label approximately half of their cardiomyocytes with various color tags as described

previously (Gupta and Poss, 2012). A microinjury was then applied at 30 dpf by piercing the heart with a fine tungsten needle. Nearly half of the ventricles acquired an ectopic surface clone of cortical cardiomyocytes in the vicinity of the pierce by 42 dpf, detectable within images of whole mount and sectioned ventricles (15 of 33 pierced, vs. 0 of 39 uninjured; Fig. 22a-c).

To confirm this result, we repeated this procedure with *gata4:EGFP* animals and examined ventricular surfaces for ectopic *gata4:EGFP*$^{+}$ cortical myocytes. Indeed, we found that *gata4:EGFP* specifically marked a small focus of ectopic cortical muscle in approximately half of the ventricles at the location of injury (12 of 23 pierced, vs. 0 of 20 uninjured; Fig. 22d-f). Although triggered by injury, it is important to note that the cortical muscle observed in these experiments was not the product of regeneration, a process that refers to the replacement of lost tissue. Rather, as cortical muscle was generated on the surface *de novo*, these events represent new morphogenesis.

Second, we used an inducible genetic ablation system to diffusely ablate cardiomyocytes at 30 dpf (Wang et al., 2011), before visualizing surface *gata4:EGFP* expression 12 days later. This injury model lesions trabecular and primordial muscle throughout the ventricle. Nearly all animals treated with the

4-HT inducer exhibited large regions of ectopic *gata4:EGFP*$^{+}$ cortical cardiomyocytes spanning both ventricular sides (15 of 16 animals, vs. 0 of 14 controls; Figures 22g-i).

These experiments revealed that injury can serve as a stimulus for cortical layer morphogenesis, suggesting that juvenile wall morphogenesis and adult heart regeneration share a triggering event.

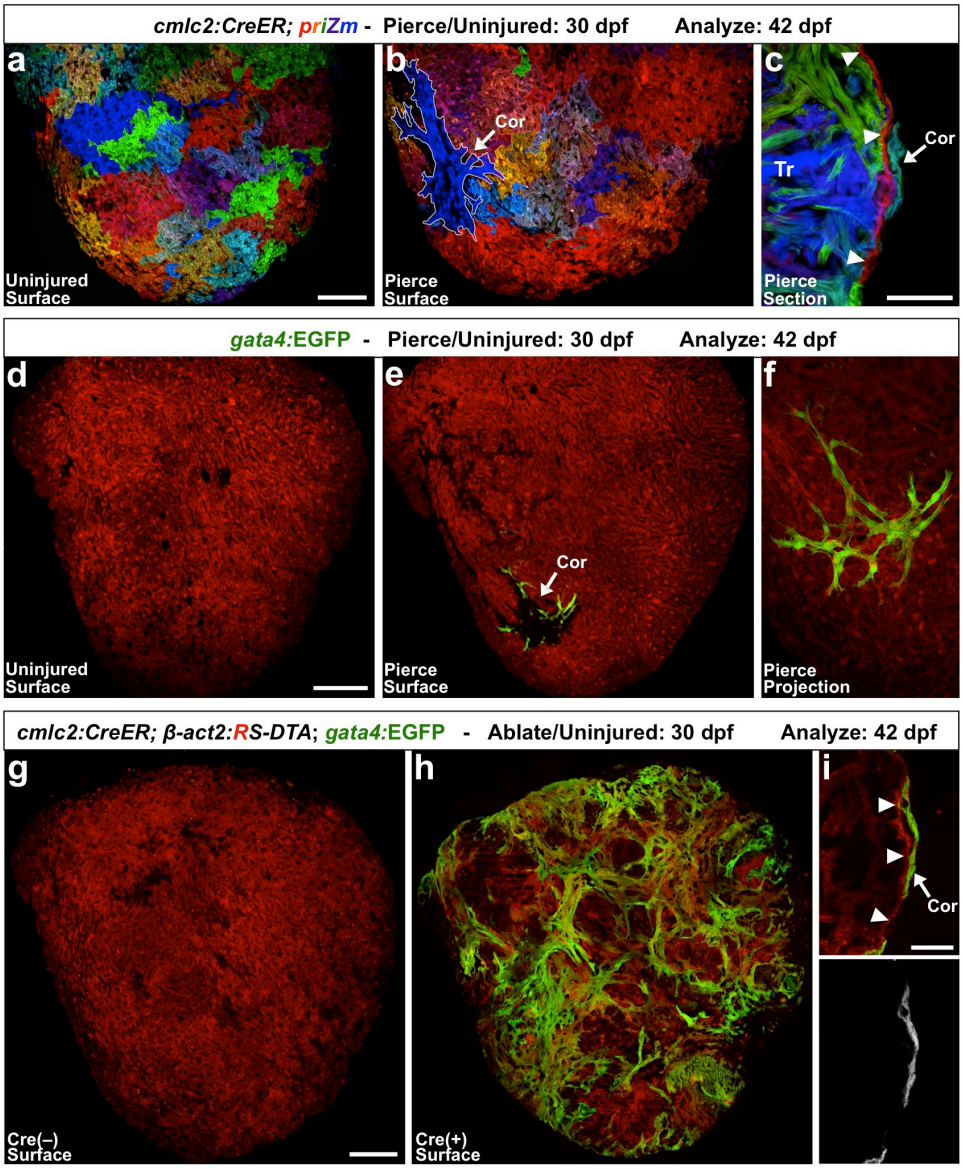


**Figure 22: Experimental injuries stimulate ectopic cortical muscle formation.**

**a,** *cmlc2:CreER; priZm* zebrafish were labeled at 2 dpf and assessed at 42 dpf, and indicate no signs of cortical cardiomyocytes on the ventral ventricular surface. **b,** When this region of the ventricle was pierced with a fine needle at 30 dpf, a small cortical clone (outlined in white) was detected at 42 dpf at the injury site in nearly half of the animals. **c,** Section indicating a cortical clone (arrow) at 42 dpf, in a ventricle that had been pierced at 30 dpf. Arrowheads indicate the single cardiomyocyte-thick primordial layer. **d, e,** 30 dpf *priZm; gata4:EGFP* ventricles

were pierced as in (**a-c**), with *β-actin2*-expressing cells indicated in red. Uninjured animals had no *gata4:EGFP*$^{+}$ cardiomyocytes on the ventral surface of the ventricle at 42 dpf (**d**). By contrast, approximately half of the animals pierced at 30 dpf displayed a focus of *gata4:EGFP*$^{+}$ cortical muscle at the site of trauma (**e**, arrow). **f,** Higher magnification confocal projection of injury site in (**e**). **g, h,** Partial genetic ablation of cardiac muscle was initiated by brief 4-HT treatment at 30 dpf and analyzed 12 days later. 4-HT-treated Cre(-) ventricles contained no *gata4:EGFP*$^{+}$ surface cardiomyocytes (**g**). By contrast, the ventricular surfaces of 4-HT-treated Cre(+) animals contained large amounts of *gata4:EGFP*$^{+}$ cortical muscle (**h**). **i,** These *gata4:EGFP*$^{+}$ cells were confirmed to be cortical myocytes (arrow) in section that were external to the primordial layer (arrowheads) Scale bars, 100 μm (**a**, **b**, **d-h**); 50 μm (**c**).

### 4.3.5 Accelerated Juvenile Growth Increases Biomechanical Stress and Stimulates Ectopic Cortical Muscle Morphogenesis

Although experimental microinjuries induced *gata4* and ectopic morphogenesis, they might not resemble endogenous influences that increase stress upon the heart. Lowering aquarium density during growth has the effect of markedly accelerating animal and cardiac growth (Wills et al., 2008). We found that raising larval zebrafish at a lower density of one animal per 2 liters (accelerated growth; AG) elevated cardiac expression of the stress marker *nbbp* at 5 wpf compared to a standard density of six animals per 2 liters (normal growth; NG; Fig. 23). This depicted that an accelerated pace of growth causes increased stress upon the heart that must perfuse added mass and pump greater circulatory volumes.

Next, to test whether this condition of increased physiologic cardiac stress stimulated ectopic breaching and cortical muscle morphogenesis, we used multicolor clonal analysis to quantify contributions to the cortical layer. Previous findings indicated that the cortical layer forms from the convergence of several expansive surface clones, each of which represents a separate event in which trabecular muscle has breached the ventricular wall. After labeling *cmlc2:CreER; priZm* animals with 4-HT at 2 dpf and subjecting them to either NG or AG conditions, we collected ventricles at juvenile and adult stages.

Histological analysis of 6 wpf revealed that NG animals had one or two detectable cortical clones at the ventricular base, whereas AG animals had more than triple the number of basal surface clones (4.1 ± 0.8 clones/heart AG vs. 1.25 ± 0.5 clones/heart NG; Fig. 24a-c). Clones were of comparable size within the two growth conditions. We then examined whole-mount images of ventricles from these two groups at 70 (AG) and 90 (NG) dpf, respectively, ages at which animal size was comparable. We calculated the areas covered by clones in ventricles with recombined (non-red) clones comprising greater than 50% of the total surface area, as previously defined (Gupta and Poss, 2012). In each group, about half met this criterion (9 of 18 ventricles, NG; 11 of 20, AG). Extrapolating for

unrecombined cortical muscle, there was an average of 8.1 ± 0.7 (mean ± standard error of the mean (s.e.m.) color clones contributing to the entire ventricular surface muscle in NG animals (Fig. 24d, f, i). Each ventricle had one or two basal clones covering more than 20% of the surface area (Fig. 24h). By contrast, AG ventricles had a much higher number of surface clones, averaging 20.4 ± 1.3 clones per animal (Fig. 24e, g, i). These clones were on average smaller (89037 $\mu m^2$ vs. 173569 $\mu m^2$) and more uniform in size, as only 4 of 11 AG ventricles contained a clone larger than 20% of the total surface area (Fig. 24h). Notably, although animals under the two tested growth conditions initiated cortical layer development with a ~2.5-fold difference in the number of source cardiomyocytes, plasticity in the system allowed each scenario to generate a grossly similar myocardial structure

These results reveal that rapid organismal growth, accompanied by a physiologic increase in biomechanical stress, stimulates new breaching events and clonal contributions to the cortical layer. Combined with the effects of experimental microinjuries on *gata4* induction and cortical morphogenesis, our findings strongly suggest that cortical layer initiation is a response to stress/injury much like adult heart regeneration.

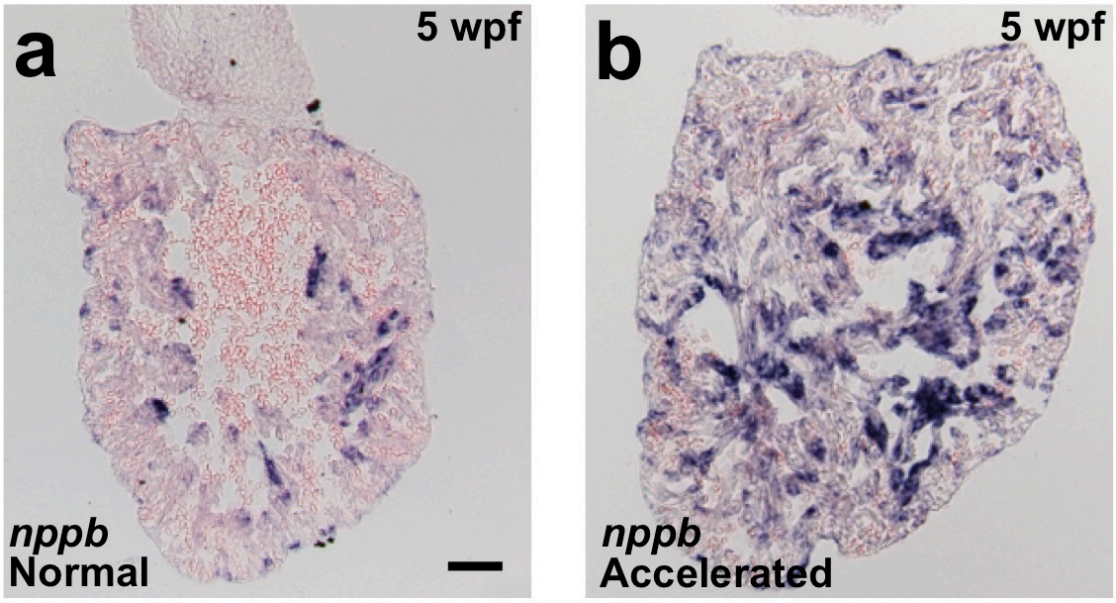


**Figure 23: *nppb* expression increases during accelerated growth.**

**a, b,** Sections of 5 wpf ventricles stained by *in situ* hybridization for *nppb*, indicating higher expression and greater cardiac stress in animals raised under low-density conditions that accelerate growth (n = 8-10). Scale bar, 50 μm.

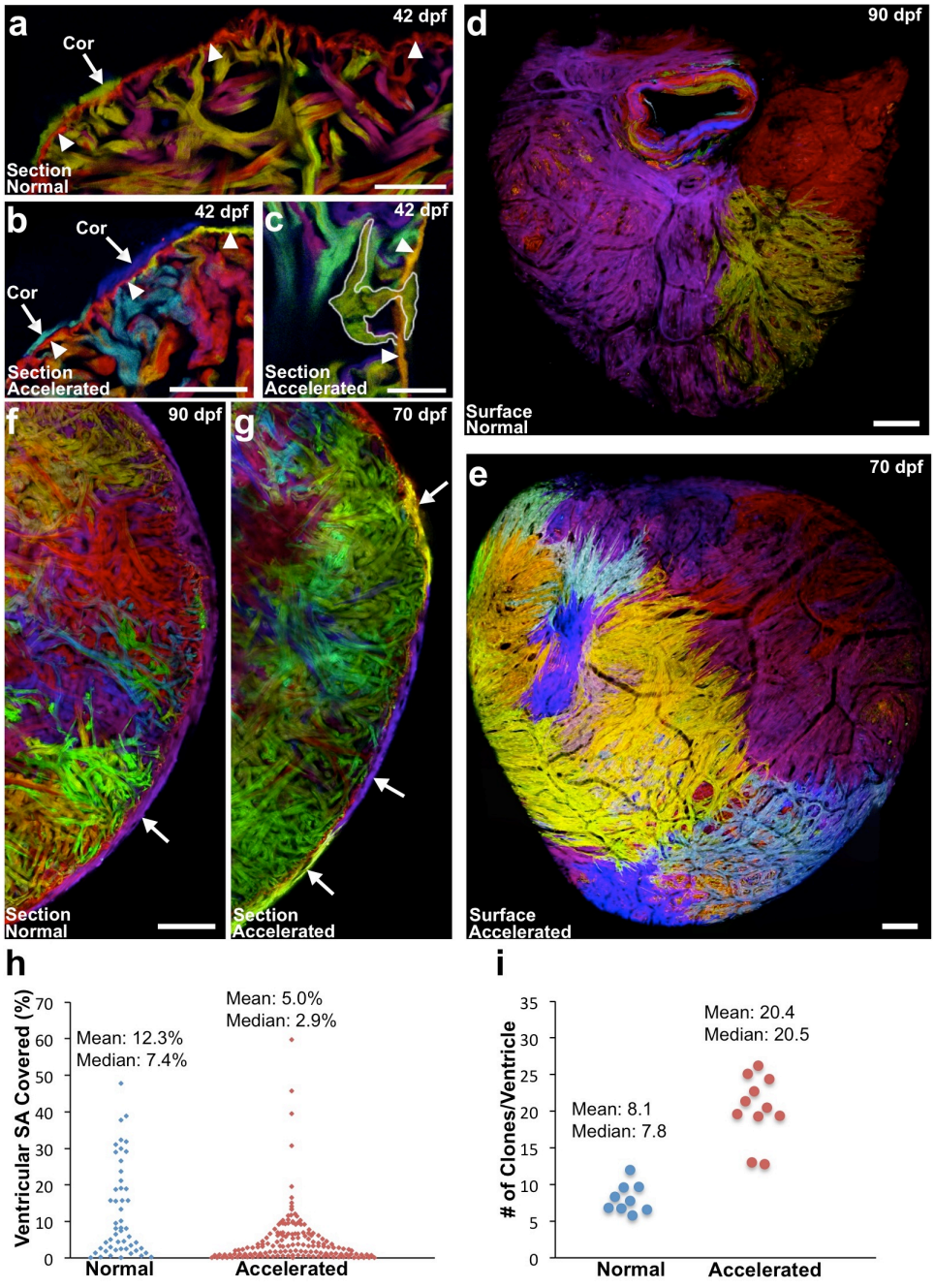


**Figure 24: Accelerating growth increase contributions to the cortical layer.**

**a-c,** Sections of 6 wpf ventricles of *cmlc2:CreER; priZm* zebrafish that were labeled at 2 dpf and grown at normal (**a**) or accelerated growth conditions (**b**, **c**). NG fish contained one or two small cortical clones at the base of the ventricle (**a**, arrow)

outside the primordial layer (arrowheads). Multiple small cortical clones were seen in AG (**b**, arrows), including those breaching (**c**, outlined) the primordial layer (**b**, **c**, arrowheads). **d, e,** Surface muscle of adult *cmlc2:CreER; priZm* ventricles of normal (**d**) or accelerated growth (**e**) conditions. More cortical clones are generated during AG. **f, g,** Confocal slices through ventricles after normal (**f**) or accelerated (**g**) growth, indicating a higher number of cortical clones (arrows) after accelerated growth. **h,** Percentage surface area (SA) occupied by clones after normal (51 clones, 9 ventricles) or accelerated growth (153 clones, 11 ventricles). **i,** Extrapolated number of surface clones per ventricle from data in (**h**). Scale bars, 100 μm (**c-g**); 50 μm (**a**, **b**); 25 μm (**c**).

### 4.3.6 Gata4 Inhibition Blocks Cortical Layer Formation and Regeneration

To determine the physiological significance of the injury-related *gata4* response in zebrafish cardiomyocytes, we constructed a new transgenic line that enabled inducible, tissue-specific expression of a dominant-negative Gata4 (g4DN) cassette (*Tg(bactin2:loxP-mTagBFP-STOP-loxP-mCherry-2a-sr-gata4)*$^{pd62}$; referred to as *β-act2:BSg4DN*). This g4DN protein blocks wild-type Gata4 from interacting with its target sequences, and its overexpression in zebrafish embryos phenocopies Gata4 loss-of-function (Torregroza et al., 2012). We crossed this line to a second line in which expression of a 4-hydroxytamoxifen (4-HT)-inducible Cre recombinase is restricted to cardiomyocytes, *cmlc2:CreER*.

To test myocardial requirements of Gata4, we pulsed with 4-HT at juvenile (30 dpf) and adult (90 dpf) stages and assessed survival. *g4DN*

expression for 30 days did not impact the survival or gross appearance of adult fish. By contrast, when *g4DN* expression was induced in 30 dpf juveniles, just prior to the first appearance of *gata4*$^{+}$ cortical cardiomyocytes, survival dropped to 73% at 7 wpf, and to just 16.3% after 30 days of *g4DN* expression (Fig. 25a). Within 2-3 weeks of 4-HT treatment, most of these animals developed overt signs of heart failure, including lethargy, gasping behavior, and edema (Fig. 25b, c).

To define the underlying cardiac pathology, we histologically assessed juvenile ventricles at 6-7 wpf. Juvenile *cmlc2:CreER; β-act2:BSg4DN* ventricles showed no evidence of cortical muscle. Instead, the ventricular wall was thinned, with many areas of discontinuity (Fig. 25d, e). Visualization of epicardial cells indicated a heightened response, with areas of penetration into gaps within the wall (Fig. 25f, g). We also observed particularly strong *nppb* expression compared to controls, consistent with increased mechanical stress (Fig. 26). These data indicate that juvenile zebrafish require myocardial Gata4 activity to form the ventricular cortical layer and sustain cardiac function during growth.

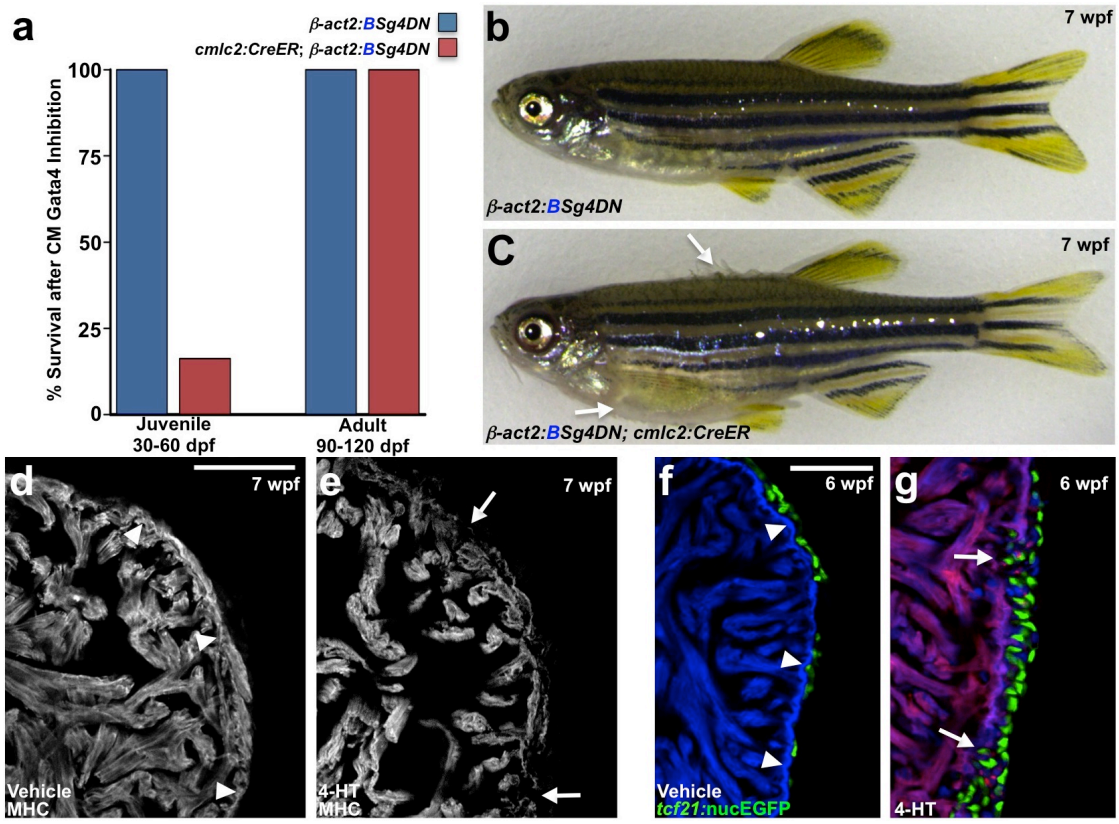


**Figure 25: Gata4 inhibition blocks juvenile cortical layer formation and causes symptoms of heart failure.**

**a,** Survival of zebrafish after induction of a dominant-negative Gata4 construct (g4DN) for 30 days in cardiomyocytes at either 30 or 90 dpf. *g4DN* induction at 30 dpf sharply reduced survival of juveniles (n = 23-43), whereas *g4DN* induction at 90 dpf did not affect survival (n = 8-16). **b,** Cre (–) control animal exposed to 4-HT at 5 wpf, appearing normal at 7 wpf. **c,** A Cre (+) clutchmate exposed to 4-HT at 5 wpf, with flared scales indicative of edema (arrows). **d, e,** Sections of the 7 wpf ventricular wall after *g4DN* induction at 5 wpf, stained for Myosin heavy chain (MHC). Control animals have cortical muscle at the base of the heart, while the wall is thinned and disrupted after *g4DN* induction (n = 4). **f , g,** Maturing juvenile ventricles visualized for *tcf21:nucEGFP*$^{+}$ epicardium (green), *g4DN* (red), and *β-actin2:BFP* (blue). The 6 wpf control ventricle (**f**) has an contiguous wall and normal epicardial cell distribution. *g4DN* induction at 5 wpf results in wall gaps (arrows) and increased epicardial cell presence at 6 wpf (**g**) (n = 6-9). Scale bars, 50 μm.

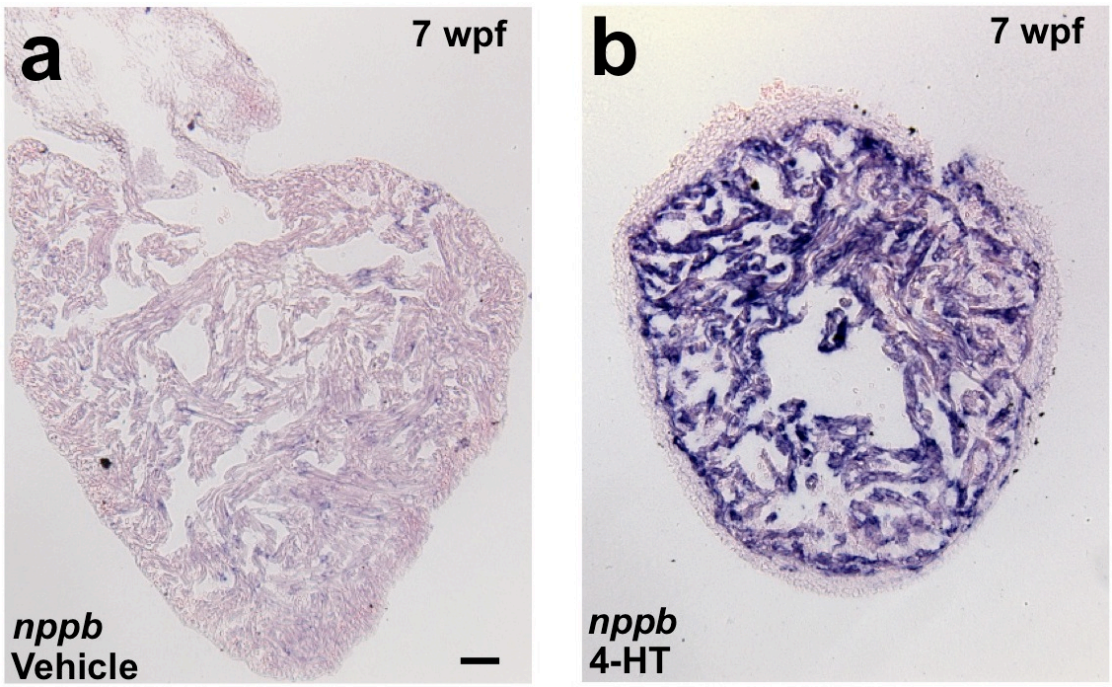


**Figure 26: *nppb* expression increases after *g4DN* induction.**

**a, b,** *β-act2:BSg4DN; cmlc2:CreER* animals were exposed to vehicle or 4-HT at juvenile stage and allowed to grow to 7 wpf. Ventricles were then stained by *in situ* hybridization for *nppb*, where ventricles expressing g4DN had higher expression of *nppb*, indicating increased cardiac stress (n= 4). Scale bar, 50 μm.

To examine Gata4 function in the injured adult zebrafish heart, we induced *g4DN* expression, partially resected ventricles, and assessed regeneration 30 days later. Strikingly, *g4DN* expression blocked muscle regeneration and caused severe scarring at the injury site (Fig. 27). The proliferation of trabecular myocytes was not significantly different between experimental groups, indicating that Gata4 is not required for cardiomyocyte hyperplasia per se. However, animals with cardiomyocyte *g4DN* expression displayed a ~73% reduction in the proliferation of cortical cardiomyocytes (Fig. 28). These data indicate that the Gata4 requirement for cardiomyocyte proliferation during regeneration is preferential or exclusive to the cortical layer.

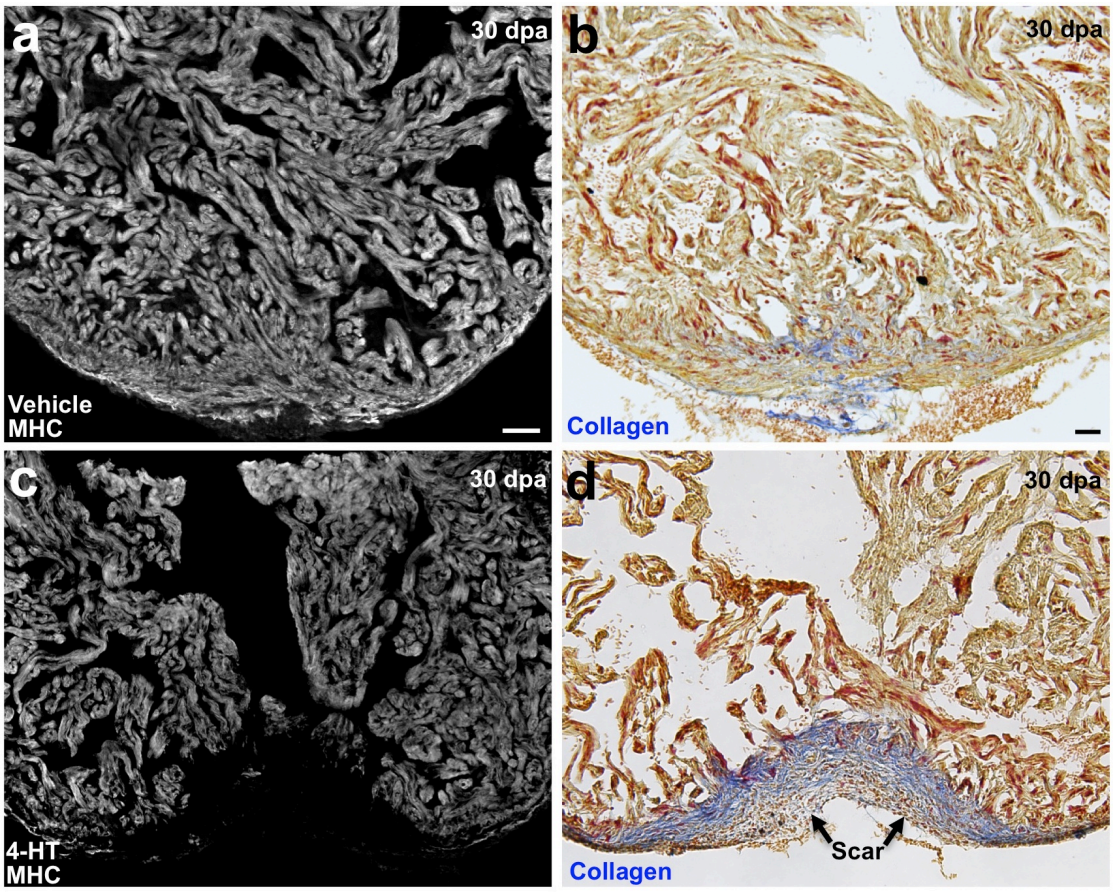


**Figure 27: Gata4 inhibition blocks adult heart regeneration.**

**a-d,** *g4DN* was induced in adults, and ventricular apices were resected, before analysis of regeneration at 30 dpf. Control animals (**a**, **b**) regenerated muscle with little or no scarring (blue indicates collagen), while *g4DN* induction blocked muscle regeneration (**c**) and induced scarring (**d**). Scale bars, 50 μm.

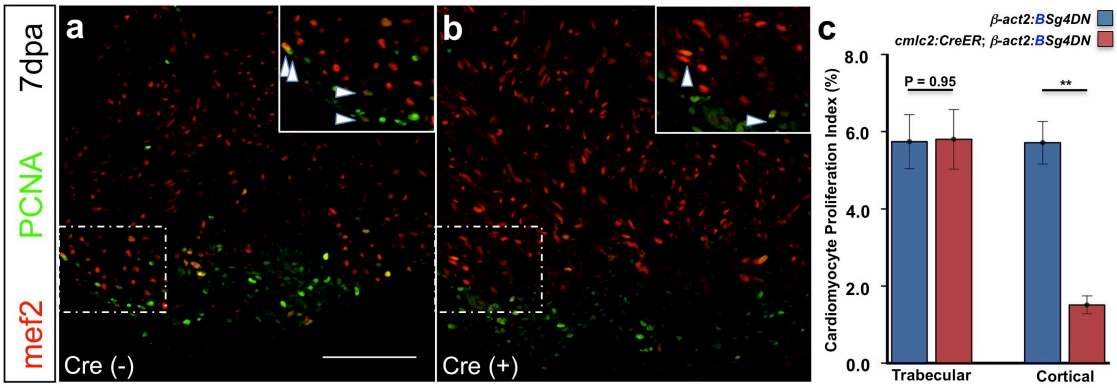


**Figure 28: *g4DN* overexpression decreases cortical myocyte proliferation.**

**a, b,** Mef2/PCNA stain of *β-act2:BSg4DN* animals with (**a**; Cre (-)) or without (**b**; Cre (+)) *cmlc2:CreER* that were exposed to 4HT, underwent ventricular amputation, and were removed at 7 dpa. Insets show high zoom of compact muscle in which a decrease can be seen within the control group. **c,** Quantification of trabecular and cortical cardiomyocyte proliferation in *g4DN* compared to control (n = 12-15). **P<0.005, Student's t-test. Scale bar, 100 μm.

## *4.4 Discussion*

Regeneration links an injury stimulus with developmental patterning programs used earlier in life. Here, we examined juvenile heart development in zebrafish to determine if gene expression and function during this phase might be recalled for adult heart regeneration. Our study identifies a Gata4-driven cardiomyocyte program that occurs in the context of mechanical stress and can be stimulated by injury, of which key aspects are repeated during adult heart regeneration. Juvenile growth programs can involve genes first used during embryogenesis, but are now being used in a physiologic context closer to adult tissue. It is possible that the reiteration of juvenile programs is a recurring strategy for adult tissue regeneration, warranting closer examination within other regenerative tissues.

Gata4 has been extensively studied in tractable *in vitro* and *in vivo* systems for transcriptional target genes, cofactor interactions, and its own regulation. Gata4 transcription factor complexes typically activate target gene transcription, which can control the presence of other cardiac transcription factors like Mef2 and Nkx2.5 (Dodou et al., 2004; Jiang et al., 1999; Lien et al., 1999), cardiomyocyte proliferation through factors like CyclinD2 and Cdk4 (Rojas et al., 2008; Yamak et al., 2012), or differentiation through regulation of

contractile genes (Oka and Molkentin, 2007; Xin et al., 2006). Mechanical stress can lead to phosphorylation of Gata4 that increases its activity (Charron et al., 2001; Liang et al., 2001; Tenhunen et al., 2004). It is likely that Gata4 acts through similar stress induced mechanisms in juvenile and adult zebrafish to regulate the cardiomyocyte program in the specialized contexts of ventricular wall morphogenesis and regeneration.

There are multiple studies that implicate patterns of organ stress in the construction of vertebrate organs. These include effects of transmural pressure during branching morphogenesis of murine lungs (Nelson and Gleghorn, 2012), and circulatory flow on kidney development and heart looping in zebrafish (Hove et al., 2003; Vasilyev et al., 2009). Our study supports a model in which myocardial breaching events in the juvenile ventricle function as a stochastic repair mechanism that reinforces possible weak points on the wall. After breaching, gata4+ cortical cardiomyocytes on the ventricular surface expand to form a muscle patch of clonally related progeny, before individual surface clones merge into a contiguous cortical layer that fortifies the wall. This process is clonally plastic, as more clones can be recruited under increasing stress. Under this model, cortical layer development is a reactionary event that provides

physiologic relief. Indeed, markers of stress normally vanish from ventricles by the adult stage. Moreover, juvenile animals under myocardial Gata4 blockade fail to form cortical muscle, a deficiency that is associated with heart failure. Thus, morphogenesis of the juvenile ventricle wall and regeneration of the resected adult ventricular apex appear to share key commonalities in triggering events, molecular responses, and protection against heart failure.

These commonalities suggest new ideas for how cardiac regenerative capacity in zebrafish may have been preserved during evolution. Heart regeneration in this species is a robust event, but as major cardiac injury is expected to be rare or occur late in life, it is unlikely to be under direct selective pressure itself. By contrast, stress-stimulated programs that enable maturation to breeding age are likely to be under strong selective pressure. From our findings, it is evident that to reach maturity, juvenile zebrafish must trigger the emergence and expansion of *gata4*$^{+}$ cortical cardiomyocytes. Thus, programmatic overlap with juvenile cortical morphogenesis, including responsiveness to stress/injury, might enable adult cardiac regenerative potential to be retained as an evolutionary byproduct.

# 5. Conclusion and Discussion

For my dissertation research, I have investigated the manner in which single cardiomyocytes proliferate during zebrafish heart morphogenesis and regeneration. By generating new transgenic tools to visualize multiple clones within a given heart, I have been able to decipher how cardiomyocyte clones construct the heart from early embryogenesis into adulthood. These initial studies revealed that the ventricular compact muscle was generated through a small number of clonally dominant cortical myocytes that encapsulated the heart in a base to apex wave of proliferation. The source of these cortical clones was trabecular myocytes that gained access to the ventricular surface through small breaches within the single cell thick primordial muscle.

During further experimentation, I found that the formation of the cortical layer shared a number of molecular expression patterns that are induced during adult zebrafish heart regeneration, including expression of the transcription factor *gata4*. This overlap was further reinforced with experiments depicting that injury, the stimulus that initiates regeneration, could induce the precocious and ectopic formation of cortical clones. Physiologically increasing biomechanical stress to the animal spurred ectopic clone formation. This resulted in an increase in the number of clones that made contributions to the cortical layer, further

implicating a stress response as a part of a trigger that initiates breaching and emergence of cortical myocytes.

## *5.1 Tools for Interrogating the Behavior of Cell Clones*

Examining how single cells divide to create an entire organism has been a focus of research for many years. Classic clonal studies employed gynandromorphs, as described by Morgan, which enabled phenotypic clonal marking in a mosaic manner within the fruit fly (Morgan and Bridges, 1919). Sturtevant and others were able to trace these marked cells and construct a morphogenetic map of *Drosophila* imaginal discs (Sturtevant, 1929; Garcia-Bellido and Merriam, 1969). In a different fashion, Sulston spent hours under a microscope watching dividing cells and meticulously noting their fates to develop a lineage tree of the worm *Caenorhabditis elegans* (Sulston et al., 1983).

A more intuitive approach would be to mark a cell of interest and chase its fate over time. One of the first markers to label individual cells was horseradish peroxidase. This was pressure injected into individual embryonic leech cells at a specific stage of development. Through subsequent staining for horseradish

peroxidase, one could assess the fates from the initial injected cell (Weisblat et al., 1978).

The advent of fluorescent protein and transgenic technologies has revolutionized our ability to probe the secrets of biology. With respect to clonal analysis, the combination of transgenics, a diverse array of fluorescent proteins, and site-specific recombinases led to the development of the Brainbow system by Lichtman's group (Livet et al., 2007). Upon Cre based recombination, a cell is given a permanent genetic tag that is represented by differential fluorescent protein expression. This cell tag, and all progeny resulting from that cell, can be decoded with fluorescent confocal microscopy. With respect to other techniques used for clonal analysis, the Brainbow offers several advantages (Buckingham and Meilhac, 2011).

Some methods that rely on rare events require the utilization of hundreds if not thousands of animals to ensure that labeled cells were derived from a single cell (Wasserstrom et al., 2008; Meilhac et al., 2004; Legué and Nicolas, 2005). The need to ascertain that progeny are in fact clonally related is overcome by the Brainbow system in two fashions. The amount of Cre activity can be modulated to ensure clonal labeling. This was evident during lineage tracing of

Lgr5$^{+}$ stem cells within the gut that utilized a four-color Brainbow reporter (Snippert et al., 2010). The authors were able to induce limited and widespread recombination with Cre recombinases of differing activity to analyze short and long term clonal dynamics. Additionally, with the combinatorial Brainbow construct, the number of genetic tags that can be given to a cell (in some lines close to 90) allows one to distinguish clones from one another, decreasing the probability that two separate clones of the same label are mixing with one another. This is a common caveat of clonal systems that utilize one or two labels.

This is the first system that allows greater than 1 or 2 labels to be examined within a given organ, which not only decreases the number of animals that one needs to look at, but also provides information as to how clones are behaving with respect to one another. This is especially pertinent during zebrafish cortical layer development, where trabecular muscle gains access to the ventricular surface through rare breaching events. To identify this rare event with a single marker, which must be induced in rare fashion, would likely have not uncovered this breaching mechanism. Applied to other tissues and model systems, it is possible that this system holds the potential to uncover other rare events that drive organ morphogenesis and general development.

Akin to other methods of clonal analysis that use site-specific recombinases, the Brainbow system obtains the benefits that come with CreER-*loxP* site-specific recombination, namely temporal control and tissue specificity. A number of *β-act2:Brainbow1.0L* or *priZm* lines were generated that have varying levels of expression that roughly correlate to the number of copies of the Brainbow cassette (Vikas Gupta, unpublished results). The *β-act2* promoter is a general promoter that drives expression within other tissues besides the heart.

As such, generating a tissue specific CreER and crossing to these *priZm* lines would allow similar multicolor clonal analyses within other tissues. Suitable cell type specific promoters exist for many of these tissues from which Cre can be expressed to analyze the clonal patterns of proliferation. It would be interesting to characterize how proliferation at the single cell level helps to generate different organs such as the spinal cord, retina, fin, or pancreas, which are organs that can also undergo adult regeneration as the zebrafish heart. Such projects are ongoing within our own lab, in addition to the multitude of labs with which we have shared this reagent.

Perhaps one of the greatest assets multicolor clonal analysis is that it allows greater ease in understanding how clonal dynamics can be changed. The

laborious nature of traditional clonal experiments is alleviated in that a relatively small number of animals can be used with Brainbow to understand how individual cells are proliferating. As such, incorporating an experimental group in which a drug is given or the environment is changed is a far less daunting task. Describing how clones proliferate normally and how their dynamics change in response to differing circumstances permits greater insight into the regulators of cellular proliferative behaviors.

## *5.2 The Formation of the Ventricular Wall and its Regulators*

### 5.2.1 Compaction Versus Envelopment

The mechanism of thickening of the compact muscle described here for the teleost zebrafish contrasts that which is thought to occur within higher vertebrates. While development of the zebrafish cortical layer takes place during juvenile growth, a comparison with higher vertebrates is most appropriate during embryonic development. At this time, the thicknesses of the ventricular walls and trabecular patterns are more closely matched, with later

developmental stages for higher vertebrates having little to no trabecular muscle (Wessels and Sedmera, 2003).

During embryonic heart development, in humans, mice, and chicks, trabecular fibers develop from the compact layer, which is a few cells thick. These trabecular myofibers are quickly lost, thought to compress against the compact layer, adding to its overall thickness (Sedmera et al., 2000). Single marker clonal analysis, during chick and mouse embryonic heart development, found wedges of clonally related cells that were seen through the thickness of the compact muscle, tapering toward the lumen. These clones did not appear to form a layer of outer cells that had another layer of clonally unrelated cells separating them (Mikawa et al., 1992; Meilhac et al., 2003).

While these results could suggest that higher vertebrates are devoid of a cortical envelopment process, seen within zebrafish, it is possible that technical limitations could make it difficult to visualize. These experiments were only able to examine a single marker; and as such, they could not appreciate how several clones were proliferating, with respect to one another other in a single organ. Furthermore, the larger number of cardiomyocytes, and thicker ventricular

structure, make it difficult to understand how these clones are proliferating in three dimensions.

To carefully examine whether the process of cortical envelopment takes place within the higher vertebrates, a large number of cardiomyocyte clones should be followed during mouse heart development. The tools for such a study are available and could be generated. The difficulty within this line of experimentation would be the method of imaging. While whole surfaces could be imaged, as performed here during zebrafish heart morphogenesis, the multiple cell layers of the mouse heart would require 3-D reconstruction to fully comprehend how the clones are proliferating to construct the heart. A simple confocal would not likely be up to the task. 2-photon microscopy would allow better depth penetration to trace clones through the embryonic myocardium and is a technique that can be combined with Brainbow system.

It is possible that cortical envelopment and compaction both take place during chick or mouse heart development. Indeed, disruptions to RA signaling cause the mouse ventricle to remain highly trabeculated, with a thinner layer of compact muscle (Kastner et al., 1994). Morphologically, the non-compacted mouse heart appears quite similar to the adult zebrafish heart. This would

suggest that a cortical envelopment process could occur prior to compaction to make the compact muscle thicker before further addition occurs. As such, one could trace a large number of clones within a non-compaction background. Since the process of compaction takes place quite rapidly, "freezing" the murine heart at this stage could make it easier to visualize whether or not cortical envelopment takes place and would allow better standardization of the hearts that are being examined.

If there does not appear to be a similar cortical envelopment process within higher vertebrates, there are many reasons as to why these two different mechanisms could exist. One explanation could deal with the lower blood pressure of the zebrafish circulatory system. An adult zebrafish has an average systolic pressure of 2 mmHg, which is more than an order of magnitude lower than higher vertebrates that have systolic blood pressures well over 100 mmHg (Hu et al., 2001). The generation of such high pressures relies upon a thick compact muscle. To keep pace with overall embryogenesis, compaction must take place quickly to maintain perfusion. Indeed, compaction takes place over 1 day for mice, 3 days for chick, and 2 weeks for humans during gestation (Sedmera and McQuinn, 2008). This compares with 6 weeks, half the amount of

time it takes to reach adulthood, for cortical muscle to encase the zebrafish ventricle.

As such, compaction may represent a more efficient and quicker means to generate a thick compact layer. The evidence that this could be the case is that trabeculae do not require coronary circulation and receive blood from diffusion as a result of their large surface area. Thus, a large amount of myocardial mass can be generated in the form of trabeculae, encompassing 80% of the total human embryonic myocardial mass at its peak, that can then add to the overall thickness of the ventricular wall by compressing into it (Blausen et al., 1990).

The amount of compact muscle within the ventricle can be quite varied amongst different species of fish. Most teleosts, such as zebrafish, have a type II ventricle that has the least amount of compact muscle. Type III belong to elasmobranches and type IV belong to endothermic sharks and active teleosts. These ventricles are different in that they have a greater coronary circulation and thicker compact muscle, with type IV having a 30% thicker compact layer than type III (Tota, 1989; Davie and Farrell, 1991). As elasmobranches, endothermic sharks, and active telosts have greater compact layers and higher blood pressures, it would be interesting to see whether they, and other species,

undergo compaction and/or cortical envelopment. This information will give us insight into how the process of compact muscle thickening has changed over the evolutionary timeline, and perhaps, how this change correlates with the evolution of higher-pressure circulatory systems and cardiac regenerative ability.

### 5.2.2 Stimulating Cortical Emergence

During further examination of compact or cortical layer formation, I show that injury can stimulate the emergence of cortical clones upon the zebrafish ventricular surface, with the clonal contribution increasing with increased physiologic stress. In the absence of experimentally induced injury that causes stress upon the heart, a more natural form of stress that the heart feels is strain. Strain in the heart is the increase in length upon a myocyte due to hemodynamic pressure stretching the heart during diastole, which can be caused by increasing preload. Additionally, increased stress upon the heart can result from increasing vascular resistance, or afterload, that the heart must pump against.

Myocytes, and other cell types, can sense various types of mechanical forces that have been shown to help mold the final shapes of many organs (Nelson and Gleghorn, 2012). There have been a number of studies that have

investigated the influence of mechanical stress in the developing vertebrate heart (Hierck et al., 2008; Hove et al., 2003; Poelmann et al., 2008; Huang et al., 2003; Taber, 1998). These studies, and results here demonstrating that injury elicits cortical emergence, provide ample evidence that stress is a likely initiator that signals to molecular sensors.

Within the heart, the stress sensors and downstream mediators of stretch and strain include TRP channels, intermediate filaments, Z-discs, and proteins such as titin (Eder and Molkentin, 2011; Buyandelger et al., 2011). Titin, named for it being the largest known protein, sits within the sarcomere from the Z-disc to the M-band, being well positioned to serve as a strain sensor. Upon stretch, muscle ankyrin repeat proteins that are bound to titin are released and translocate to the nucleus where they appear to elicit transcriptional responses (Miller et al., 2003).

As stress upon the zebrafish heart induces the emergence of cortical clones, a deeper molecular understanding of this process will benefit from looking at candidate molecules, such as titin and its effectors. If the localization of muscle ankyrin repeat proteins, or other differentially localized stress responsive factors, are important to cortical layer formation, one can examine

their localization within emerging cortical myocytes. This can be approached through antibody staining or generating transgenic animals in which the factor has been fluorescently tagged. Both of these approaches can use the far-red channel for imaging, making them compatible with the Brainbow. Titin, and other molecules that can sense strain and elicit transcriptional responses, can serve as important starting points to piece together how stress upon the heart is converted into a molecular signal that stimulates the emergence and proliferation of cortical myocyte clones.

In order to show that one of these proteins, or another stress sensor, is truly being activated and causing transcriptional responses, a number of hurdles must first be overcome to make conclusions that are more than just correlative. First, this breaching event appears to be a very rare phenomenon with the exact location of breaches being stochastic. Detecting any changes at the protein or transcriptional level that correspond to this event would be exceeding difficult given that a rare subset of cells undergo it. Isolating those breaching cardiomyocytes to perform proteomic or transcriptomic analysis requires making this process more robust. The number of breaching events needs to be increased in addition to timing it such that these breaches are all coming out at the same

time. The ablation of juvenile hearts was able to elicit such a response and could be used as a model for further investigation. However, this model does cause cell death and is not a natural form of stress. While not perfect, a different approach could be to perform a drug screen of small molecules that cause increased afterload and preload to see whether the addition of such a small molecule could be used as the inciting stimulus to cause the breaching event to be more robust. Once this hurdle is overcome, it will be far easier to detect changes at the protein or transcriptional level to screen for, or validate, those proteins and genes that are being differentially regulated in order to engage the machinery necessary for breaching. Additionally, the small molecule that is identified could further serve as another starting point to understand the molecular underpinnings that control the process of breaching and cortical layer formation.

### 5.2.3 *gata4* as a Stress Activated Factor

A likely downstream molecule from the stress signal is the transcription factor *gata4*. Stress upon the adult mammalian heart in the form of increased afterload, increased preload, or direct stretching can increase the activity of Gata4 (Hautala et al., 2001; Hautala et al., 2002). Increased Gata4 activity is

thought to occur through stress induced MAP kinase mediated phosphorylation of Gata4, which activates it (Charron et al., 2001; Liang et al., 2001a; Tenhunen et al., 2004; van Berlo et al., 2011). While *gata4* is expressed during embryonic development within the zebrafish, there appears to be little to no expression within ventricular cardiomyocytes at 5 wpf. Strong expression is then seen specifically within emerging cortical myocytes and regenerating myocytes, periods that coincide with other stress markers.

In mammals, stress upon the adult heart results in primarily hypertrophy versus the hyperplasia seen within zebrafish. *gata4*, within mammals, facilitates this stress-induced hypertrophic response in the same fashion as it appears to facilitate a stress-induced hyperplastic response in zebrafish. Murine cardiomyocyte specific knockout of *gata4* results in a reduced ability for myocytes to hypertrophy in response to pressure overload, whereas cardiomyocyte overexpression of *gata4* causes mild hypertrophy (Liang et al., 2001b; Oka et al., 2006). Thus, in both zebrafish and higher vertebrates, *gata4* appears to partially serve as a stress-activated factor that carries out a hyperplastic or hypertrophic response, respectively. Tracing the downstream targets of Gata4 could be helpful in understanding why its activation results in

two different outcomes in response to stress. Identifying these molecular targets could provide a therapeutic means to stimulate adult mammalian cardiomyocytes to proliferate.

Another response to cardiac stress that Gata4 appears to mediate is increased angiogenesis. Experiments within the murine heart found that overexpression of Gata4 within cardiomyocytes induced greater capillary density, and a cardiomyocyte specific knockout prevents pressure-induced angiogenesis. Gata4 was found to bind to the Vegf promoter, increasing its expression and secretion from cardiomyocytes (Heineke et al., 2007). The Vegf protein signals to adjacent vessels to stimulate the formation of new vessels, increasing oxygen and nutrient delivery (Giordano et al., 2001; Hsieh et al., 2006).

This angiogenic response is seen during the process of ventricular compaction within higher vertebrates. Coronary arteries begin to form within the compact muscle as trabecular myofibers are compressing into one another and the wall of the ventricle (Rychterova, 1971; Rychter and Ostadal, 1971; Vrancken Peeters et al., 1997). Within the zebrafish, the relief of coronary vessels upon the surface of the ventricle can be seen as early as 8 wpf. Interestingly, images of juvenile ventricle at 6 wpf, that had been subjugated to pierce injuries at 30 dpf,

appeared to have the relief of coronary vasculature emanating from the injury site, where *gata4*$^{+}$ cortical myocytes are emerging. Both cortical myocytes and the outline of vasculature are typically not seen at this location and time without injury. This suggests that *gata4* likely has a conserved role in being stress induced and stimulating the production of new vessels. To confirm this, our lab is looking at the development of coronary vasculature during the emergence of cortical myocytes via transgenic strains that mark the endothelium of vessels. In addition, examining the secretion and expression of Vegf, and how it relates with *gata4* expression, will be key to analyze if this angiogenic response is conserved during zebrafish cortical emergence.

## *5.3 Why does Regeneration Occur?*

The process of regenerating missing body parts and whole organs has fascinated human beings for centuries, likely as a result of our inability to undergo the significant regeneration that we observe in other species. This captivation is document as early as the time of Aristotle, who noted how tails regenerated in lizards and snakes (Aristotle, 1965). Within metazoans, regenerative abilities are widely distributed; yet, we still have not been able to

compose a full picture for why there is selection of great regenerative powers in some animals and not in others (Alvarado, 2000).

In some species that undergo asexual reproduction, such as planarians and hydra, regeneration is almost indistinguishable from reproduction. Planarians, for example, will undergo transverse fission, which results in an anterior piece and a posterior piece. The anterior piece will generate a tail and the posterior piece will generate a head, giving rise to two organisms (Curtis et al., 1902). In organisms such as these, regeneration ties in almost naturally into the organism's life cycle and reproductive success. Any injury that separates a portion of the organism from itself, in planarians as low as 1/279th of the organism, will be viewed as a reproductive event generating more offspring (Morgan, 1898).

However, mode of reproduction cannot explain the capacity for adult zebrafish heart regeneration. Additionally, it would not appear logical that the zebrafish would need to regenerate their heart in response to natural damage. Since the heart is an internal organ, it would be difficult to envision a scenario in which a predator gains access to the cardiac cavity and leaves the organism alive. A piece of the answer could derive from the fact that the zebrafish heart

undergoes proliferative homeostatic maintenance, where proliferation of cardiomyocytes can increase under favorable environmental conditions to keep pace with overall organismal growth (Poss et al., 2002; Wills et al., 2008). Thus, an injury stimulus could function in the same fashion as favorable environmental conditions to alter the homeostatic balance toward greater proliferation.

An examination of clonal behaviors under these types of accelerated growth conditions showed that the number of cortical clones that contributed to the entirety of the cortical layer increased. Looking at earlier stages of accelerated growth, more clones had emerged upon the surface of the ventricle at locations away from the base, with the size of these clones not being grossly different than what is seen under normal growth conditions. In these experiments, it is interesting to note that there were at least two other types of outcomes. The number of clones could have remained the same, depicting that each clone could individually compensate to meet the increased rate of growth. Alternatively, the initial basal clones could have increased their rate of proliferation to give rise to a smaller number of total clones. It appears that morphogenesis of the cortical layer is adaptable. In this case, a larger number of smaller sized clones

contributed to the cortical layer to meet the demands of an accelerated growth rate.

This type of adaptation is not an uncommon feature of some organs, including adult organs. For example, the stem cells within the *Drosophila* midgut will increase cell divisions, and alter resulting cell fates, to increase the number of intestinal cells in response to increased food intake (O'Brien et al., 2011). Such adaptive responses, by the gut, are exaggerated in infrequent feeders; however, this response is seen to a lesser extent in frequent feeders including humans (Carey, 1990; Secor and Diamond, 1998; Dunel-Erb et al., 2001; Drozdowski and Thomson, 2006).

Other homeostatically maintained mammalian adult organs can also undergo adaptive growth. This includes the bone marrow in response to altitude change, where erythrocyte production increases, and skeletal muscle enlargement upon weight bearing exercises (Ambrosio et al., 2009; Koury, 2005). Additionally, these same mammalian organs have the ability to regenerate to a certain extent after serious injury. If these organs grow through adaptable clonal behavior, it would suggest that adaptable clonal proliferation, either in the

juvenile stage or as an adult, would be a common feature and perhaps predictor of regenerative potential.

Such is likely true of the mammalian liver, which can regenerate after 70% surgical resection (Michalopoulos and DeFrances, 1997). After ~65% ablation to the murine liver progenitor pool, remaining cells are able to compensate for developmental cellular loss to achieve normal organ size. This would suggest that the proliferative contributions from individual clones of liver progenitors could be varied upon need. In contrast, a similar ablation to the pancreas progenitor pool resulted in a smaller sized pancreas, with lack of compensation by the remaining progenitors (Stanger et al., 2007). As the liver can regenerate at a greater capacity than the pancreas, these results suggest that the ability for adaptive and compensatory proliferation within the mammalian liver could herald its ability for great regenerative capacity even into adulthood.

The culmination of this thesis adds to this answer and further refines it. I have shown here that the process of cortical emergence shares multiple similarities with heart regeneration including: 1) activation of stress and injury markers in myocardial and epicardial cells; 2) initiation by mechanical and genetic injury; and 3) induction and requirement of Gata4 activity. In essence, it

appears as though adult heart regeneration is recapitulating this juvenile, cortical layer forming, event.

Without the emergence of cortical myocyte clones upon the surface of the ventricle, juveniles cannot reach sexual maturity. As such, evolution's selection for this process during juvenile growth would be of high value in order for zebrafish to reach appropriate breeding size to mate and give rise to offspring. However, being able to activate or not activate cortical myocytes to proliferate after reaching adult size within natural settings would likely be under neutral evolutionary pressure. As long as the zebrafish can reach mating size and give rise to offspring, there would not appear to be a clear advantage to being able to regenerate lost myocytes after large-scale injuries.

This would suggest that those species that could undergo homeostatic maintenance with or without cortical envelopment would have greater cardiac regenerative capacity. An idea such as this would be challenging to rigorously test. Initially, one could try to make a correlation between a species cardiac regenerative ability to whether it underwent homeostatic maintenance with or without cortical envelopment. The number of species looked at should be diverse and encompass those that have at least a single ventricle circulatory

system. To analyze whether the adult heart of a species underwent homeostatic maintenance, one could perform a BrdU pulse chase or PNCA staining to detect proliferation during juvenile growth and after growth has ceased in adulthood. Species could be graded by the baseline rate at which adult animals create new cardiomyocytes plotted against their capacity for heart regeneration.

Looking for cortical envelopment throughout the animal kingdom would be a rather large mountain to topple. Performing multicolored clonal lineage tracing for every species would not be a feasible approach. However, one could try to use basic histology to look for evidence of cortical myocytes. The ventricle wall thickens at the base of the heart first that moves down toward the apex. Quantifying the thickness of the ventricular wall at different locations, and at different stages of development, could provide some insight into whether that species underwent cortical encapsulation. If a specific genetic marker is found that marks this process, an *in situ* hybridization screen could be performed on ventricles from different species at different ages. Understanding the extent to which other species undergo cardiac homeostatic maintenance and whether they possess the process of cortical envelopment can perhaps help to elucidate how

regenerative capabilities have changed over the evolutionary timeline and how cardiac development has evolved.

Since it appears as though regeneration is recapitulating this juvenile process of cortical layer formation, my mentor, when he found that the fish heart could regenerate, may have in fact discovered a developmental remnant that evolution left waiting to be revealed.

## References

Alsan, B.H., and Schultheiss T.M. (2002). Regulation of avian cardiogenesis by Fgf8 signaling. Development 129, 1935-1943.

Alvarado, A.S. (2000). Regeneration in the metazoans: why does it happen? BioEssays 22, 578-590.

Ambrosio, F., Kadi, F., Lexell, J., Fitzgerald, G.K., Boninger, M.L., and Huard, J. (2009). The effect of muscle loading on skeletal muscle regenerative potential: an update of current research findings relating to aging and neuromuscular pathology. American Journal of Physical Medicine and Rehabilitation. 88, 145–155.

American Heart Association Statistics Committee and Stroke Statistics Subcommittee. (2010). Heart Disease and Stroke Statistics—2010 Update. Circulation 121, e46-e215.

Andrée, B., Duprez, D., Vorbusch, B., Arnold, H.H., and Brand, T. (1998). BMP-2 induces ectopic expression of cardiac lineage markers and interferes with somite formation in chicken embryos. Mechanisms of Development 70, 119-131.

Aristotle. (1965). Historia Animalium. In: Peck AL, translator. Vol. 1. Cambridge, Massachusetts: Harvard University Press.

Auman, H.J. Coleman, H., Riley, H.E., Olale, F., Tsai, H.J., and Yelon, D. (2007). Functional modulation of cardiac form through regionally confined cell shape changes. PLoS Biology 5, e53.

Azpiazu, N., and Frasch, M. (1993). tinman and bagpipe: two homeo box genes that determine cell fates in the dorsal mesoderm of Drosophila. Genes and Development 7, 1325-1340.

Bearzi, C., Rota, M., Hosoda, T., Tillmanns, J., Nascimbene, A., De Angelis, A., Yasuzawa-Amano, S., Trofimova, I., Siggins, R.W., Lecapitaine, N., Cascapera, S., Beltrami, A.P., D'Alessandro, D.A., Zias, E., Quaini, F., Urbanek, K., Michler, R.E., Bolli, R., Kajstura, J., Leri, A., and Anversa, P. (2007). Human cardiac stem cells. Proceedings of the National Academy of Sciences 104:14068–73.

Becker, T., Wullimann, M.F., Becker, C.G., Bernhardt, R.R., and Schachner, M. (1997). Axonal regrowth after spinal cord transection in adult zebrafish. Journal of Comparative Neurology 377, 577-595.

Becker, J.R., Robinson, T.Y., Sachidanandan, C., Kelly, A.E., Coy, S., Peterson, R.T., and MacRae, C.A. (2012). *In vivo* natriuretic peptide reporter assay identifies chemical modifiers of hypertrophic cardiomyopathy signalling. Cardiovascular Research 93, 463-470.

Beddington, R.S.P., and Robertson, E.J. (1999). Axis Development and Early Review Asymmetry in Mammals. Cell 96, 195–209.

Bellaris, R. (1986). The primitive streak. Anatomy and Embryology 174, 1-14.

Beltrami, A.P., Barlucchi, L., Torella, D., Baker, M., Limana, F., Chimenti, S., Kasahara, H., Rota, M., Musso, E., Urbanek, K., Leri, A., Kajstura, J., Nadal-Ginard, B., and Anversa, P. (2003). Adult cardiac stem cells are multipotent and support myocardial regeneration. Cell 114:763–76.

Berdugo, E., Coleman, H., Lee, D.H., Stainier, D.Y., and Yelon, D. (2003). Mutation of weak atrium/atrial myosin heavy chain disrupts atrial function and influences ventricular morphogenesis in zebrafish. Development 130, 6121-6129.

Bergmann, O., Bhardwaj, R.D., Bernard, S., Zdunek, S., Barnabé-Heider, F., Walsh, S., Zupicich, J., Alkass, K., Buchholz, B.A., Druid, H., Jovinge, S., and Frisén, J. (2009). Evidence for cardiomyocyte renewal in humans. Science 324, 98–102.

van Berlo, J.H., Elrod, J.W., Aronow, B.J., Pu, W.T., and Molkentin, J.D. (2011). Serine 105 phosphorylation of transcription factor GATA4 is necessary for stress-induced cardiac hypertrophy *in vivo*. Proceedings of the National Academy of Sciences 108:12331–6.

Bersell, K., Arab, S., Haring, B., and Kuhn, B. (2009). Neuregulin1/ErbB4 signaling induces cardiomyocyte proliferation and repair of heart injury. Cell 138, 257–270.

Biben, C., and Harvey, R.P. (1997). Homeodomain factor Nkx2-5 controls left-right asymmetric expression of bHLH gene *eHand* during murine heart development. Genes and Development 11, 1357-1369.

Blausen, B.E., Johannes, R.S., and Hutchins, G.M. (1990). Computer based reconstructions of the cardiac ventricles of human embryos. Am J Cardiovasc Pathol 3: 37–43, 1990

Bodmer, R. (1993). The gene tinman is required for specification of the heart and visceral muscles in Drosophila. Development 118, 719-729.

Braunwald, E. (2008). Biomarkers in heart failure. New England Journal of Medicine 358, 2148-2159.

Brockes, J.P., and Kumar, A. (2005). Appendage regeneration in adult vertebrates and implications for regenerative medicine. Science 310, 1919-1923.

Buckingham, M., Meilhac, S., and Zaffran, S. (2005). Building the heart from two sources of myocardial cells. Nature Reviews Genetics 6, 826-835.

Burns, C.G., Milan, D.J., Grande, E.J., Rottbauer, W., MacRae, C.A., and Fishman, M.C. (2005) High-throughput assay for small molecules that modulate zebrafish embryonic heart rate. Nature Chemical Biology 1, 263–264.

Buyandelger, B., Ng, K., Miocic, S., Gunkel, S., Piotrowska, I., Ku, C., and Knöll, R. (2011). Genetics of Mechanosensation in the Heart. Journal of Cardiovascular Translational Research 4, 238–244.

Cai, C.L., Liang, X., Shi, Y., Chu, P.H., Pfaff, S.L., Chen, J., and Evans, S. (2003). *Isl1* identifies a cardiac progenitor population that proliferates prior to differentiation and contributes a majority of cells to the heart. Developmental Cell 5, 877-889.

Cai, C.L., Martin, J.C., Sun, Y., Cui, L., Wang, L., Ouyang, K., Yang, L., Bu, L., Liang, X., Zhang, X., Stallcup, W.B., Denton, C.P., McCulloch, A., Chen, Ju., and Evans, S. (2008). A myocardial lineage derives from Tbx18 epicardial cells. Nature 454, 104-108.

Campione, M., Steinbeisser, H., Schweickert, A., Deissler, K., van Bebber, F., Lowe, L.A., Nowotschin, S., Viebahn, C., Haffter, P., Kuehn, M.R., Blum, M. (1999). The homeobox gene Pitx2: mediator of asymmetric left-right signaling in vertebrate heart and gut looping. Development 126, 1225-1234.

Carey, H.V. (1990). Seasonal changes in mucosal structure and function in ground squirrel intestine. American Journal of Physiology 259, R385–R392.

Chablais, F., Veit, J., Rainer, G., and Jaźwińska, A. (2011). The zebrafish heart regenerates after cryoinjury-induced myocardial infarction. BMC Developmental Biology 11, 21.

Charron, F., Tsimiklis, G., Arcand, M., Robitaille, L., Liang, Q., Molkentin, J.D., Meloche, S., and Nemer, M. (2001). Tissue-specific GATA factors are transcriptional effectors of the small GTPase RhoA. Genes and Development 15, 2702–2719.

Christoffels, V. M., Grieskamp, T., Norden, J., Mommersteeg, M. T., Rudat, C., and Kispert, A. (2009). Tbx18 and the fate of epicardial progenitors. Nature 458, E8-E10.

Clubb, F.J., Jr. and Bishop, S.P. (1984). Formation of binucleated myocardial cells in the neonatal rat. An index for growth hypertrophy. Laboratory Investigation 50, 571-7.

Cooper, M.S., Szeto, D.P., Sommers-Herivel, G., Topczewski, J., Solnica-Krezel, L., Kang, H.C., Johnson, I., and Kimelman, D. (2005) Visualizing morphogenesis in transgenic zebrafish embryos using BODIPY TR methyl ester dye as a vital counterstain for GFP. Developmental Dynamics 232, 359–368.

Curtis WC. (1902). The life history, the normal fission, and the reproductive organs of Planaria maculata. Proceedings of the Boston Society of Natural History 30, 515-559.

Davie, P.S., and Farrell, A.P. (1991). Cardiac performance of an isolated heart preparation from the dogfish (*Squalus acanthias*): The effects of hypoxia and coronary artery perfusion. Canadian Journal of Zoology 69, 1993-2001.

Dodou, E., Verzi, M.P., Anderson, J.P., Xu, S.M., and Black, B.L. (2004). Mef2c is a direct transcriptional target of ISL1 and GATA factors in the anterior heart field during mouse embryonic development. Development 131, 3931-3942.

Doupé, D.P., Klein, A.M., Simons, B.D., and Jones, P.H. (2010). The ordered architecture of murine ear epidermis is maintained by progenitor cells with randomfate. Developmental Cell 18, 317–323.

Drozdowski, L., and Thomson, A.B. (2006). Intestinal mucosal adaptation. World Journal of Gastroenterology. 12, 4614–4627.

Dunel-Erb, S., Chevalier, C., Laurent, P., Bach, A., Decrock, F., and Le Maho, Y. (2001). Restoration of the jejunal mucosa in rats refed after prolonged fasting. Comparative Biochemistry and Physiology Part A: Molecular and Integrative Physiology 129, 933–947.

Durocher, D., Charron, F., Warren, R., Schwartz, R.J. and Nemer, M. (1997) The cardiac transcription factors Nkx2-5 and GATA-4 are mutual cofactors. EMBO Journal 16, 5687–5696.

Eder, P., and Molkentin, J.D. (2011). TRPC Channels As Effectors of Cardiac Hypertrophy. Circulation Research 108, 265-272.

Engel, F.B., Hsieh, P.C., Lee, R.T., and Keating, M.T. (2006). FGF1/p38 MAP kinase inhibitor therapy induces cardiomyocyte mitosis, reduces scarring, and rescues function after myocardial infarction. Proceedings of the National Academy of Sciences 103, 15546–15551.

Ekker, S.C. (2000). Morphants: a new systematic vertebrate functional genomics approach. Yeast 17, 302-306.

Eyal-Giladi, H., Debby, A., and Harel, N. (1992). The posterior section of the chick's area pellucida and its involvement in hypoblast and primitive streak formation. Development 116, 819-830.

Essner, J.J., Branford, W.W., Zhang, J., Yost, H.J. (200). Mesendoderm and left-right brain, heart and gut development are differentially regulated by pitx2 isoforms. Development 127, 1081-1093.

Fu, Y., Yan, W., Mohun, T.J., and Evans, S.M. (1998). Vertebrate tinman homologues XNkx2-3 and XNkx2-5 are required for heart formation in a functionally redundant manner. Development 125, 4439–4449.

Gajewski, K., Kim, Y., Lee, Y.M., Olson, E.N. and Schulz, R.A. (1998). D-Mef2: a target for tinman activation during Drosophila heart development. EMBO Journal. 16, 515–522.

A. Garcia-Bellido, A., and Merriam, J.R. (1969). Cell Lineage of the Imaginal Discs in Drosophila Gynandromorphs. Journal of Experimental Zoology 170, 61-76.

Garcia-Martinez, V., and Schoenwolf, G.C. (1993). Primitive-streak origin of the cardiovascular system in avian embryos. Developmental Biology 159, 706–719.

Garza-Garcia, A.A., Driscoll, P.C., and Brockes, J.P. (2010). Evidence for the local evolution of mechanisms underlying limb regeneration in salamanders. Integrative and Comparative Biology 50, 528-535.

Gilbert, S. F. (2003). Developmental Biology. Sunderland, Massachusetts: Sinauer Associates.

Giordano, F.J., Gerber, H.P., Williams, S.P., VanBruggen, N., Bunting, S., Ruiz-Lozano, P., Gu, Y., Nath, A.K., Huang, Y., Hickey, R., Dalton, N., Peterson, K.L., Ross, J., Chien, K.R., and Ferrara, N. (2001). A cardiac myocyte vascular endothelial growth factor paracrine pathway is required to maintain cardiac function. Proceedings of the National Academy of Sciences 98, 5780–5785.

Glickman, N.S., and Yelon, D. (2002). Cardiac development in zebrafish: coordination of form and function. Seminars in Cell and Developmental Biology 13, 507-513.

González-Rosa, J.M., Martín, V., Peralta, M., Torres, M., and Mercader, N. (2011). Extensive scar formation and regression during heart regeneration after cryoinjury in zebrafish. Development 138, 1663–74.

Hami, D., Grimes, A.C., Tsai, H.J. and Kirby, M.L. (2011). Zebrafish cardiac development requires a conserved secondary heart field. Development 138, 2389–2398.

Harvey, R.P. (1996). NK-2 homeobox genes and heart development. Developmental Biology 178, 203–216.

Hautala, N., Tenhunen, O., Szokodi, I., and Ruskoaho, H. 2002. Direct left ventricular wall stretch activates GATA4 binding in perfused rat heart: involvement of autocrine/paracrine pathways. European Journal of Physiology 443, 362–369.

Hautala, N., Tokola, H., Luodonpää, M., Puhakka, J., Romppanen, H., Vuolteenaho, O., and Ruskoaho, H. 2001. Pressure overload increases GATA4 binding activity via endothelin-1. Circulation 103, 730–735.

Heicklen-Klein, A., and Evans, T. (2004). T-box binding sites are required for activity of a cardiac GATA-4 enhancer. Developmental Biology 267, 490–504.

Heineke, J., Auger-Messier, M., Xu, J., Oka, T., Sargent, M.A., York, A., Klevitsky, R., Vaikunth, S., Duncan, S.A., Aronow, B.J., Robbins, J., Crombleholme, T.M., and Molkentin, J.D. (2007). Cardiomyocyte GATA4 functions as a stress responsive regulator of angiogenesis in the murine heart. Journal of Clinical Investigation 117, 3198-210.

Hierck, B.P., Van der Heiden, K., Poelma, C., Westerweel, J., and Poelmann, R.E. (2008). Fluid shear stress and inner curvature remodeling of the embryonic heart. Choosing the right lane! Scientific World Journal 8, 212–222.

Hill, J.A., and Olson, E.N. (2008). Cardiac Plasticity. The New England Journal of Medicine 358, 1370-1380.

Houweling, A.C., van Borren, M.M., Moorman, A.F., and Christoffels, V.M. (2005). Expression and regulation of the atrial natriuretic factor encoding gene Nppa during development and disease. Cardiovascular Research 67, 583-593.

Hove, J.R., Köster, R.W., Forouhar, A.S., Acevedo-Bolton, G., Fraser, S.E., and Gharib, M. (2003). Intracardiac fluid forces are an essential epigenetic factor for embryonic cardiogenesis. Nature 421, 172–177.

Hsieh, P.C.H., Segers, V.F.M., Davis, M.E., MacGillivray, C., Gannon, J., Molkentin, J.D., Robbins, J., and Lee, R.T. (2007). Evidence from a genetic fate mapping study that stem cells refresh adult mammalian cardiomyocytes after injury. Nature Medicine 13:970–74.

Hsieh, P.C.H., Davis, M.E., Lisowski, L.K., and Lee, R.T. (2006). Endothelial-cardiomyocyte interactions in cardiac development and repair. Annual Review of Physiology 68, 51–66.

Hu, N., Yost, H.J., and Clark, E. B. (2001). Cardiac morphology and blood pressure in the adult zebrafish. The Anatomical Recored. 264, 1–12.

Huang, C., Sheikh, F., Hollander, M., Cai, C., Becker, D., Chu, P.H., Evans, S., and Chen, J. (2003). Embryonic atrial function is essential for mouse embryogenesis, cardiac morphogenesis and angiogenesis. Development 130, 6111–6119.

Ieda, M., Fu, J.D., Delgado-Olguin, P., Vedantham, V., Hayashi, Y., Bruneau, B.G., and Srivastava, D. (2010). Direct reprogramming of fibroblasts into functional cardiomyocytes by defined factors. Cell 142, 375–86.

Jayawardena, T.M., Egemnazarov, B., Finch, E.A., Zhang, L., Payne, J.A., Pandya, K., Zhang, Z., Rosenberg, P., Mirotsou, M., and Dzau, V.J. (2012). MicroRNA-mediated in vitro and in vivo direct reprogramming of cardiac fibroblasts to cardiomyocytes. Circulation Research 110, 1465–73.

Jiang, Y., Drysdale, T.A., and Evans, T. (1999). A role for GATA-4/5/6 in the regulation of Nkx2.5 expression with implications for patterning of the precardiac field. Developmental Biology 216, 57-71.

Johnson, S.L., and Weston, J.A. (1995). Temperature-sensitive mutations that cause stage-specific defects in Zebrafish fin regeneration. Genetics 141, 1583-1595.

Jopling, C., Sleep, E., Raya, M., Martí, M., Raya, A., and Izpisúa Belmonte, J.C. (2010). Zebrafish heart regeneration occurs by cardiomyocyte dedifferentiation and proliferation. Nature 464, 606–609.

Kastner, P., Grondona, J.M., Mark, M., Gansmuller, A., LeMueur, M., Decimo, D., Vonesch, J., Dolle, P., and Chambon, P. (1994). Genetic analysis of RXRa developmental function: convergence of RXR and RAR signalling pathways in heart and eye morphogenesis. Cell 78, 987–1003.

Kelly, R.G., Brown, N.A., and Buckingham, M.E. (2001). The arterial pole of the mouse heart forms from Fgf10-expressing cells in pharyngeal mesoderm. Developmental Cell 1, 435-440.

Kikuchi, K. Holdway, J.E., Werdich, A.A., Anderson, R.M., Fang, Y., Egnaczyk, G.F., Evans, T., Macrae, C.A., Stainier, D.Y., and Poss, K.D. (2010). Primary contribution to zebrafish heart regeneration by gata4$^{+}$ cardiomyocytes. Nature 464, 601–605.

Kikuchi, K., Holdway, J.E., Major, R.J., Blum, N., Dahn, R.D., Begemann, G., and Poss, K.D. (2011a). Retinoic acid production by endocardium and epicardium is an injury response essential for zebrafish heart regeneration. Developmental Cell 20, 397-404.

Kikuchi, K. Gupta, V., Wang, J., Holdway, J.E., Wills, A.A., Fang, Y., and Poss, K.D. (2011b). tcf211 epicardial cells adopt non-myocardial fates during zebrafish heart development and regeneration. Development 138, 2895–2902.

Kimmel, C.B., Ballard, W.W., Kimmel, S.R., Ullmann, B., and Schiling, T.F. (1995). Stages of embryonic development of the zebrafish. Developmental Dynamics 203, 253-310.

Kitajima, S., Takagi, A., Inoue, T., and Saga, Y. (2003). MesP1 and MesP2 are essential for the development of cardiac mesoderm. Development 127, 3215–3226.

Klein, A.M., Nakagawa, T., Ichikawa, R., Yoshida, S. and Simons, B.D. (2010). Mouse germline stem cells undergo rapid and stochastic turnover. Cell Stem Cell 7, 214–224.

Komuro, I., and Izumo, S. (1993). Csx: A murine homeobox-containing gene specifically expressed in the developing heart. Proceedings of the National Academy of Sciences 90, 8145-8149.

Koury, M.J. (2005). Erythropoietin: the story of hypoxia and a finely regulated hematopoietic hormone. Experimental Hematology 33, 1263–1270.

Kuhn, B. del Monte, F., Hajjar, R.J., Chang, Y.S., Lebeche, D., Arab, S., and Keating, M.T. (2007). Periostin induces proliferation of differentiated cardiomyocytes and promotes cardiac repair. Nature Medicine 13, 962–969.

Laflamme, M.A., and Murry, C.E. Heart regeneration. (2011). Nature 473, 326-335.

Laugwitz, K.L., Moretti, A., Lam, J., Gruber, P., Chen, Y., Woodard, S., Lin, L.Z., Cai, C.L., Lu, M.M., Reth, M., Platoshyn, O., Yuan, J.X., Evans, S., and Chien K.R. (2005). Postnatal isl1+ cardioblasts enter fully differentiated cardiomyocyte lineages. Nature 433:647–53.

Lawson, K.A., Meneses, J.J., and Pedersen, R.A. (1991). Clonal analysis of epiblast fate during germ layer formation in the mouse embryos. Development 113, 891-911.

Lazic, S., and Scott, I.C. (2011). Mef2cb regulates latemyocardial cell addition froma second heart field-like population of progenitors in zebrafish. Developmental Biology 354, 123–133.

Legué, E., and Nicolas, J.F. (2005). Hair follicle renewal: organization of stem cells in the matrix and the role of stereotyped lineages and behaviors. Development 132, 4143–4154.

Lepper, C., Conway, S.J., and Fan, C.M. (2009). Adult satellite cells and embryonic muscle progenitors have distinct genetic requirements. Nature 460, 627-631.

Liang, F., and Gardner, D.G. (1999). Mechanical strain activates BNP gene transcription through a p38/NF-kappaB-dependent mechanism. Journal of Clinical Investigation 104, 1603-1612.

Liang, Q., Wiese, R.J., Bueno, O.F., Dai, Y.S., Markham, B.E., and Molkentin, J.D. (2001a). The transcription factor GATA4 is activated by extracellular signal-regulated kinase 1- and 2-mediated phosphorylation of serine 105 in cardiomyocytes. Molecular and Cellular Biology 21, 7460–7469.

Liang, Q., De Windt, L.J., Witt, S.A., Kimball, T.R., Markham, B.E., and Molkentin, J.D. (2001b). The transcription factors GATA4 and GATA6 regulate cardiomyocyte hypertrophy in vitro and in vivo. Journal of Biological Chemistry. 276, 30245–30253.

Lien, C.L., Wu, C., Mercer, B., Webb, R., Richardson, J.A., and Olson, E.N. (1999). Control of early cardiac-specific transcription of Nkx2-5 by a GATA-dependent enhancer. Development 126, 75-84.

Lints, T.J., Parsons, M.L., Hartley, L., Lyons, I., and Harvey, R.P. (1993). Nkx2.5: A novel murine homeobox gene expressed in early heart progenitors cells and their myogenic descendants. Development 119, 419-431.

Liu, J., and Stainier, D.Y. (2012). Zebrafish in the study of early cardiac development. Circulation Research 110, 870-874.

Liu, J., Bressan, M., Hassel, D., Huisken, J., Staudt, D., Kikuchi, K., Poss, K.D., Mikawa, T., and Stainier, D.Y. (2010). A dual role for ErbB2 signaling in cardiac trabeculation. Development 137, 3867-75.

Livet, J., Weissman, T.A., Kang, H., Draft, R.W., Lu, J., Bennis, R.A., Sanes, J.R., and Lichtman, J.W. (2007). Transgenic strategies for combinatorial expression of fluorescent proteins in the nervous system. Nature 450, 56–62.

Loffredo, F.S., Steinhauser, M.L., Gannon, J., and Lee, R.T. (2011). Bone marrow-derived cell therapy stimulates endogenous cardiomyocyte progenitors and promotes cardiac repair. Cell Stem Cell 8:389–98.

Logan, M., Pagan-Westphal, S.M., Smith, D.M., Paganessi, L., Tabin C.J. (1998). The transcription factor Pitx2 mediates situs-specific morphogenesis in response to left-right asymmetric signals. Cell 94, 307-317.

Lopez-Garcia, C., Klein, A.M., Simons, B.D., and Winton, D.J. (2010). Intestinal stem cell replacement follows a pattern of neutral drift. Science 330, 822–825.

Marvin, M.J., Di Rocco, G., Gardiner, S., Bush, M., and Lassar A.B. (2001). Inhibition of Wnt activity induces heart formation from posterior mesoderm. Genes and Development 15, 316-327.

Matsuura, K., Nagai, T., Nishigaki, N., Oyama, T., Nishi, J., Wada, H., Sano, M., Toko, H., Akazawa, H., Sato, T., Nakaya, H., Kasanuki, H., and Komuro, I. (2004). Adult cardiac Sca-1-positive cells differentiate into beating cardiomyocytes. Journal of Biological Chemistry 279:11384–91.

Meilhac, S.M., Kelly, R.G., Rocancourt, D., Eloy-Trinquet, S., Nicolas, J.F., and Buckingham, M.E. (2003). A retrospective clonal analysis of the myocardium reveals two phases of clonal growth in the developing mouse heart. Development 130, 3877–3889.

Meilhac, S.M., Esner, M., Kelly, R.G., Nicolas, J.F., and Buckingham, M. E. (2004). The clonal origin of myocardial cells in different regions of the embryonic mouse heart. Developmental Cell 6, 685–698.

Michalopoulos, G.K., and DeFrances, M.C. (1997). Liver regeneration. Science 216, 60-6.

Mikawa, T., Borisov, A., Brown, A.M., and Fischman, D.A. (1992). Clonal analysis of cardiac morphogenesis in the chicken embryo using a replication-defective retrovirus. I. Formation of the ventricular myocardium. Developmental Dynamics. 193, 11–23.

Miller, M. K., Bang, M. L., Witt, C. C., Labeit, D., Trombitas, C., Watanabe, K., Granzier, H., McElhinny, A.S., Gregorio, C.C., and Labeit, S. (2003). The muscle ankyrin repeat proteins: CARP, ankrd2/Arpp and DARP as a family of titin filament-based stress response molecules. Journal of Molecular Biology 333, 951–964.

Mirotsou, M., Zhang, Z., Deb, A., Zhang, L., Gnecchi, M., Noiseux, N., Mu, H., Pachori, A., and Dzau, V. (2007). Secreted frizzled related protein 2 (Sfrp2) is the key Akt-mesenchymal stem cell-released paracrine factor mediating myocardial survival and repair. Proceedings of the National Academy of Sciences 104, 1643–1648.

Mjaatvedt, C.H., Nakaoka, T., Moreno-Rodriguez, R., Norris, R.A., Kern, M.J., Eisenberg, C.A., Turner, D., Markwald, R.R. (2001). The outflow tract of the heart is recruited from a novel heart-forming field. Developmental Biology 238, 97-109.

Morgan, T.H., and Bridges C.B. (1919) The origin of gynandromorphs. Carnegie Institution of Washington Publication 278, 1-122.

Morgan TH. (1898). Experimental studies of the regeneration of Planaria maculata. Development Genes and Evolution 7, 364-397.

Murry, C.E., Reinecke, H., and Pabon, L.M. (2006). Regeneration gaps: observations on stem cells and cardiac repair. Journal of American College of Cardiology 47, 1777–1785.

Nacu, E., and Tanaka, E.M. (2011). Limb regeneration: a new development? Annual Review of Cell and Developmental Biology 27, 409-440.

Nelson, C.M., and Gleghorn, J.P. (2012). Sculpting Organs: Mechanical Regulation of Tissue Development. Annual Review of Biomedical Engineering 14:129–54.

Oberpriller, J.O., and Oberpriller, J.C. (1974). Response of the adult newt ventricle to injury. Journal of Experimental Zoology 187, 249–53.

O'Brien, L.E., Soliman, S.S., Li, X., and Bilder, D. (2011). Altered modes of stem cell division drive adaptive intestinal growth. Cell 147, 603–614.

Oh, H., Bradfute, S.B., Gallardo, T.D., Nakamura, T., Gaussin, V., Mishina, Y., Pocius, J., Michael, L.H., Behringer, R.R., Garry, D.J., Entman, M.L., and Schneider, M.D. (2003). Cardiac progenitor cells from adult myocardium: Homing, differentiation, and fusion after infarction. Proceedings of the National Academy of Sciences 100:12313–18.

Oka, T., Maillet, M., Watt, A.J., Schwartz, R.J., Aronow, B.J., Duncan, S.A., and Molkentin, J.D. (2006). Cardiac-specific deletion of Gata4 reveals its requirement for hypertrophy, compensation, and myocyte viability. Circulation Research 98, 837–845.

Oka, T., and Molkentin, J.D. (2007). Developmental transcriptional pathways that also regulate heart disease states. Seminars in Cell and Developmental Biology 18, 117-31.

Orlic, D., Kajstura, J., Chimenti, S., Jakoniuk, I., Anderson, S.M., Li, B., Pickel, J., McKay, R., Nadal-Ginard, B., Bodine, D.M., Leri, A., and Anversa, P. (2001). Bone marrow cells regenerate infarcted myocardium. Nature 410, 701–705.

Pasumarthi, K.B., and Field, L.J. (2002). Cardiomyocyte cell cycle regulation. Circulation Research 90, 1044-1054.

de Pater, E. Clijsters, L., Marques, S.R., Lin, Y.F., Garavito-Aguilar, Z.V., Yelon, D., and Bakkers, J. (2009). Distinct phases of cardiomyocyte differentiation regulate growth of the zebrafish heart. Development 136, 1633–1641.

Patton, E.E., and Zon, L.I. (2001). The art and design of genetic screens: zebrafish. Nature Reviews Genetics 2, 956-966.

Pikkarainen S, Tokola H, Majalahti-Palviainen T, Kerkela R, Hautala N, Bhalla SS, Charron F, Nemer M, Vuolteenaho O, Ruskoaho H. (2003). GATA-4 is a nuclear mediator of mechanical stretch-activated hypertrophic program. Journal of Biological Chemistry 278, 23807-16.

Poelmann, R.E., Gittenberger-de Groot, A.C., and Hierck, B.P. (2008). The development of the heart and microcirculation: role of shear stress. Medical and Biological Engineering and Computing 46, 479–484.

Porrello, E.R., Mahmoud, A.I., Simpson, E., Hill, J.A., Richardson, J.A., Olson, E.N., and Sadek, H.A. (2011). Transient regenerative potential of the neonatal mouse heart. Science 331,1078–80.

Poss, K.D., Wilson, L.G., and Keating, M.T. (2002). Heart regeneration in zebrafish. Science 298, 2188–2190.

Psychoyos, D., and Stern, C.D. (1996) Fates and migratory routes of primitive streak cells in the chick embryo. Development 128, 125-135.

Qian, L., Huang, Y., Spencer, C.I., Foley, A., Vedantham, V., Liu, L., Conway, S.J., Fu, J.D., and Srivastava, D. (2012). In vivo reprogramming of murine cardiac fibroblasts into induced cardiomyocytes. Nature 485, 593–98.

Redkar, A., Montgomery, M., and Litvin, J. (2001). Fate map of the early avian cardiac progenitor cells. Development 128, 2269-2279.

Reifers, F., Walsh, E.C., Leger, S., Stainer, D.Y., and Brand, M. (2000). Induction and differentiation of the zebrafish heart requires fibroblast growth factor 8 (fgf8/acerebellar). Development 127, 225-235.

Reiter, J.F., Alexander, J., Rodawat, A., Yelon, D., Patient, R., Holder, N., and Stainer, D.Y. (1999). Gata5 is required for the development of the heart and endoderm in zebrafish. Genes and Development 13, 2983-2995.

Reiter, J.F., Verkade, H., and Stainer, D.Y. (2001). Bmp2b and Oep promote early myocardial differentiation through their regulation of gata5. Developmental Biology 234, 330-338.

Rojas, A., Kong, S.W., Agarwal, P., Gilliss, B., Pu, W.T., and Black, B.L. (2008). GATA4 is a direct transcriptional activator of cyclin D2 and Cdk4 and is required for cardiomyocyte proliferation in anterior heart field-derived myocardium. Molecular and Cellular Biology 28, 5420-5431.

Ryan, A.K., Blumberg, B., Rodriguez-Esteban, C., Yonei-Tamura, S., Tamura, K., Tsukui, T., de la Peña, J., Sabbagh, W., Greenwald, J., Choe, S., Norris, D.P., Robertson E.J., Evans R.M., Rosenfeld, M.G., and Belmonte, J.C. (1998). Pitx2 determines left-right asymmetry of internal organs in vertebrates. Nature 394, 545-551.

Rychter, Z., and Ostadal, B. 1971. Fate of "sinusoidal" intertrabecular spaces of the cardiac wall after development of the coronary vascular bed in chick embryo. Folia Morphologica 19, 31–44.

Rychterova, V. (1971). Principle of growth in thickness of the heart ventricular wall in the chick embryo. Folia Morphologica 19, 262– 272.

Saga, Y., Miyagawa-Tomita, S., Takagi, A., Kitajima, S., Miyazaki, J., and Inoue, T. (1999). MesP1 is expressed in the heart precursor cells and required for the formation of a single heart tube. Development 126, 3437–3447.

Saga, Y., Kitajima, S., and Miyagawa-Tomita, S. (2000). Mesp1 expression is the earliest sign of cardiovascular development. Trends in Cardiovascular Medicine 10, 345–352.

Schnabel, K., Wu, C.C., Kurth, T., and Weidinger, G. (2011). Regeneration of cryoinjury induced necrotic heart lesions in zebrafish is associated with epicardial activation and cardiomyocyte proliferation. PLoS ONE 6, e18503.

Schneider, V.A, and Mercola, M. (2001). Wnt antagonism initiates cardiogenesis in *Xenopus laevis*. Genes and Development 15, 304-315.

Schoenwolf, G.C., Garcia-Martinez, V., and Dias, M.S. (1992). Mesoderm movement and fate during avian gastrulation and neurulation. Developmental Dynamics 193, 235-248.

Schultheiss, T.M., Xydas, S., and Lassar A.B. (1995). Induction of avian cardiac myogenesis by anterior endoderm. Development 121, 4203-4214.

Schwartz, R.J., and Olson, E.N. (1999). Building the heart piece by piece: modularity of cis elements regulating Nkx2.5 transcription. Development 126, 4187–4192.

Secor, S.M., and Diamond, J. (1998). A vertebrate model of extreme physiological regulation. Nature 395, 659–662.

Sedmera, D., and McQuinn, T. (2008). Embryogenesis of heart muscle. Heart Failure Clinics. 4, 235–245.

Sedmera, D., Pexieder, T., Vuillemin, M., Thompson, R.P., and Anderson, R.H. (2000). Developmental patterning of the myocardium. The Anatomical Record 258, 319-337.

Senyo, S.E., Steinhauser, M.L., Pizzimenti, C.L., Yang, V.K., Cai, L., Wang, M., Wu, T.D., Guerquin-Kern, J.L., Lechene, C.P., and Lee, R.T. (2013). Mammalian heart renewal by pre-existing cardiomyocytes. Nature 493, 433–436.

Smart, N., Bollini, S., Dube, K.N., Vieira, J.M., Zhou, B., Davidson, S., Yellon, D., Riegler, J., Price, A.N., Lythgoe, M.F., Pu, W.T., and Riley, P.R. (2011). *De novo* cardiomyocytes from within the activated adult heart after injury. Nature 474, 640-644.

Snippert, H.J., van der Flier, L.G., Sato, T., van Es, J.H., van den Born, M., Kroon-Veenboer, C., Barker, N., Klein, A.M., van Rheenen, J., Simons, B.D., and Clevers, H. (2010). Intestinal crypt homeostasis results from neutral competition between symmetrically dividing Lgr5 stem cells. Cell 143, 134–144.

Song, K., Nam, Y.J., Luo, X., Qi, X., Tan, W., Huang, G.N., Acharya, A., Smith, C.L., Tallquist, M.D., Neilson, E.G., Hill, J.A., Bassel-Duby, R., and Olson, E.N. (2012). Heart repair by reprogramming non-myocytes with cardiac transcription factors. Nature 485, 599–604.

Srivastava, D., and Olson, E.N. (2000). A genetic blueprint for cardiac development. Nature 407, 221-226.

Srivastava, D., Cserjesi, P., and Olson, E.N. (1995). A subclass of bHLH proteins required for cardiac morphogenesis. Science 270, 1995-1999.

Stainier, D.Y., Lee, R.K., and Fishman, M.C. (1993). Cardiovascular development in the zebrafish. I. Myocardial fate map and heart tube formation. Development 119, 31–40.

Stanger B.Z., Tanaka, A.J., and Melton, D.A. (2007). Organ size is limited by the number of embryonic progenitor cells in the pancreas but not the liver. Nature 445, 886-891.

Stuart, G.W., McMurray, J.V., and Westerfield, M. (1988). Replication, integration and stable germ-line transmission of foreign sequences injected into early zebrafish embryos. Development 103, 403-412.

Sturtevant, A. H. (1929). The claret mutant type of Drosophila simulans, a study of chromosome elimination and cell-lineage. Zeitschrift Fur Wissenschaftliche Zoologie 135, 323-356.

Sugi, Y., and Lough, J. (1994). Anterior endoderm is a specific effector of terminal cadiac myocyte differentiation of cells from the embryonic heart forming region. Developmental Dynamics 200, 155-162.

Sulston, J.E., Schierenberg, E., White, J.G., and Thomson, J.N. (1983). The embryonic cell lineage of the nematode Caenorhabditis elegans. Developmental Biology 100, 64–119.

Taber, L.A. (1998). Mechanical aspects of cardiac development. Progress in Biophysics and Molecular Biology 69, 237–255.

Tam, P.P., Parameswaran, M., Kinder, S.J., and Weinberger, R.P. (1997). The allocation of epiblast cells to the embryonic heart and other mesodermal lineages: the role of ingression and tissue movement during gastrulation. Development 124, 1631–1642.

Tanaka, E.M. (2003). Regeneration: if they can do it, why can't we? Cell 113, 559-562.

Tenhunen O, Sármán B, Kerkelä R, Szokodi I, Papp L, Tóth M, Ruskoaho H. (2004). Mitogen-activated protein kinases p38 and ERK 1/2 mediate the wall stress-induced activation of GATA-4 binding in adult heart. Journal of Biological Chemistry 279, 24852-60.

Toma, C., Pittenger, M. F., Cahill, K.S., Byrne, B.J., and Kessler, P.D. (2002). Human mesenchymal stem cells differentiate to a cardiomyocyte phenotype in the adult murine heart. Circulation 105, 93–98.

Tota, B. (1989). Myoarchitecture and vascularization of the elasmobranch heart ventricle. Journal of Experimental Zoology 2, 122-135.

Torregroza, I., Holtzinger, A., Mendelson, K., Liu, T.C., Hla, T., and Evans, T. (2012). Regulation of a Vascular Plexus by gata4 Is Mediated in Zebrafish through the Chemokine sdf1a. PLoS One 7, e46844.

Tzahor, E., and Lassar A.B. (2001). Wnt signals from the neural tube block ectopic cardiogenesis. Genes and Development 15, 255-260.

Vakaet, L. (1984). The initiation of gastrula ingression in the chick blastoderm. American Zoologist. 24, 555-562.

Vasilyev, A., Liu, Y., Mudumana, S., Mangos, S., Lam, P.Y., Majumdar, A., Zhao, J., Poon, K.L., Kondrychyn, I., Korzh, V., and Drummond, I.A. (2009). Collective cell migration drives morphogenesis of the kidney nephron. PLoS Biology 7, e9.

Vihtelic, T.S., and Hyde, D.R. (2000). Light-induced rod and cone cell death and regeneration in the adult albino zebrafish (Danio rerio) retina. Journal of Neurobiology 44, 289-307.

Viragh, S., and Challice, C.E. (1973). Origin and differentiation of cardiac muscle cells in the mouse. Journal of Ultrastructure Research. 42, 1-24.

Vrancken Peeters, M.P.F.M., Gittenberger-de Groot, A.C., Mentink, M.M.T., Hungerford , J.E., Little, C.D., Poelmann, R.E. (1997). The development of the coronary vessels and their differentiation into arteries and veins in the embryonic quail heart. Developmental Dynamics 208, 338–348.

Waldo, K.L., Kumiski, D.H., Wallis, K.T., Stadt, H.A., Hutson, M.R., Platt, D.H., Kirby, M.L. (2001). Conotruncal myocardium arises from a secondary heart field. Development 128, 3179-3388.

Wang, J. Panáková, D., Kikuchi, K., Holdway, J.E., Gemberling, M., Burris, J.S., Singh, S.P., Dickson, A.L., Lin, Y.F., Sabeh, M.K., Werdich, A.A., Yelon, D., Macrae, C.A., and Poss, K.D. (2011). The regenerative capacity of zebrafish reverses cardiac failure caused by genetic cardiomyocyte depletion. Development 138, 3421–3430.

Warga, R.M., and Kimmel, C.B. (1990). Cell movements during epiboly and gastrulation in zebrafish. Development 108, 569-580.

Wasserstrom, A., Adar, R., Shefer, G., Frumkin, D., Itzkovitz, S., Stern, T., Shur, I., Zangi, L., Kaplan, S., Harmelin, A., Reisner, Y., Benayahu, D., Tzahor, E., Segal, E., and Shapiro E. (2008). Reconstruction of cell lineage trees in mice. PLoS ONE 3, e1939.

Weisblat, D.A., Sawyer, R.T., and Stent, G.S. (1978). Cell lineage analysis by intracellular injection of a tracer enzyme. Science 202, 1295–1298.

Wessels, A., and Sedmera, D. (2003). Developmental anatomy of the heart: a tale of mice and man. Physiologic Genomics 15, 165–176.

Whitehead, G.G., Makino, S., Lien, C.L., and Keating, M.T. (2005). fgf20 is essential for initiating zebrafish fin regeneration. Science 310, 1957-1960.

Wills, A.A., Holdway, J.E., Major, R.J., and Poss, K.D. (2008). Regulated addition of new myocardial and epicardial cells fosters homeostatic cardiac growth and maintenance in adult zebrafish. Development 135, 183–192.

Witman, N., Murtuza, B., Davis, B., Arner, A., and Morrison, J.I. (2011). Recapitulation of developmental cardiogenesis governs the morphological and functional regeneration of adult newt hearts following injury. Developmental Biology 354, 67–76.

Xin, M., Davis, C.A., Molkentin, J.D., Lien, C.L., Duncan, S.A., Richardson, J.A., and Olson, E.N. (2006). A threshold of GATA4 and GATA6 expression is required for cardiovascular development. Proceedings of the National Academy of Sciences 103, 11189-11194.

Yamak, A., Temsah, R., Maharsy, W., Caron, S., Paradis, P., Aries, A., and Nemer, M. (2012). Cyclin D2 rescues size and function of GATA4 haplo-insufficient hearts. American Journal of Physiology. Heart and Circulatory Physiology 303, H1057-1066.

Yelon, D., Horne, S.A., and Stainer, D.Y. (2000). the bHLH transcription factor hand2 plays parallel roles in zebrafish heart and pectoral fin development. Development 127, 2573-2582.

Yelon, D., Horne, S.A., and Stainer, D.Y. (1999). Restricted expression of cardiac myosin gene reveals regulated aspects of heart tube assembly in zebrafish. Developmental Biology 214, 23-37.

Yoshioka, H., Meno, C., Koshiba, K., Sugihara, M., Itoh, H., Ishimaru, Y., Inoue, T., Ohuchi, H., Semina, E.V., Murray, J.C., Hamada, H., and Noji, S. (1998). Pitx2, a bicoid-type homeobox gene, is involved in a lefty-signaling pathway in determination of left-right asymmetry. Cell 94, 299-305.

Zhou, B., Honor, L.B., He, H., Ma, Q., Oh, J.H., Butterfield, C., Lin, R.Z., Melero-Martin, J.M., Dolmatova, E., Duffy, H.S., Gise, A., Zhou, P., Hu, Y.W., Wang, G., Zhang, B., Wang, L., Hall, J.L., Moses, M.A., McGowan, F.X., and Pu, W.T. (2011). Adult mouse epicardium modulates myocardial injury by secreting paracrine factors. Journal of Clinical Investigation 121:1894–904.

Zhou, B., Ma, Q., Rajagopal, S., Wu, S.M., Domian, I., Rivera-Feliciano, J., Jiang, D., von Gise, A., Ikeda, S., Chien, K.R., and Pu, W.T. (2008). Epicardial progenitors contribute to the cardiomyocyte lineage in the developing heart. Nature 454, 109–113.

Zhou, Y., Cashman, T.J., Nevis, K.R., Obregon, P., Carney, S.A., Liu, Y., Gu, A., Mosimann, C., Sondalle, S., Peterson, R.E., Heideman, W., Burns, C.E., and Burns, C.G. (2011) Latent TGF-b binding protein 3 identifies a second heart field in zebrafish. Nature 474, 645–648.

## Biography

Vikas Gupta was born on September 16th, 1985 in Washington, District of Columbia. He attended Parkland High School in Allentown, PA. Vikas graduated from the Pennsylvania State University's Schreyer's Honors College with a BS in Biology. He matriculated into the MD/PhD program at Duke University in Durham, NC in 2007.

Publications:

**Gupta, V.,** and Poss, K.D. (2012). Clonally dominant cardiomyocytes direct heart morphogenesis. Nature 484, 479-484.

Kikuchi, K. **Gupta, V**., Wang, J., Holdway, J.E., Wills, A.A., Fang, Y., and Poss, K.D. (2011). tcf21$^{+}$ epicardial cells adopt non-myocardial fates during zebrafish heart development and regeneration. Development 138, 2895–2902.

Honors/Awards:

NHLBI supplemental award 2T32-GM007171-38 S1